

A Study of Rat Skeletal Muscle Troponin C Isoforms



Submitted by

Brett O'Connell, B. Sc. (Hons.)

A thesis submitted in the total fulfilment of the
requirements for the degree of

Doctor of Philosophy

Muscle Cell Biochemistry Laboratory
School of Biomedical Sciences
Footscray Park Campus
Victoria University
GPO Box 14428 MCMC, Victoria, 8001
Australia

May 2005

FTS THESIS
573.75419 oco
30001008599336
O'Connell, Brett
A study of rat skeletal
muscle Troponin C isoforms

Table of Contents

Summary	ix
Declaration	xii
Acknowledgments	xiii
List of publications	xiv
List of abbreviations	xvi
List of figures	xix
List of tables	xxiv
Chapter 1: Introduction	1-28
1.1 Scope	1
1.2 Skeletal muscle structure	2
1.2.1 The sarcomere	4
1.2.1.1 <i>The thick filament</i>	4
1.2.1.2 <i>The thin filament</i>	7
1.3 Models of the mechanisms of skeletal muscle contraction and of contractile activation	12

1.3.1 The sliding filament theory	12
1.3.2 The three state model of thin filament activation	14
1.4 Polymorphism of myofibrillar proteins and functional implications	16
1.4.1 Myofibrillar protein isoforms and their functional roles	17
1.4.1.1 <i>MHC isoforms</i>	17
1.4.1.2 <i>MLC isoforms</i>	19
1.4.1.3 <i>Tm isoforms</i>	20
1.4.1.4 <i>TnI isoforms</i>	20
1.4.1.5 <i>TnT isoforms</i>	21
1.4.1.6 <i>TnC isoforms</i>	21
1.4.2 Myofibrillar protein isoform composition of MHC isoform based fibre-types	23
1.4.3 The use of SDS-PAGE for studying myofibrillar protein isoform composition of single fibres	24
1.4.3.1 <i>Separation of myofibrillar proteins on polyacrylamide gels</i>	24

1.4.3.2 Identification of myofibrillar protein isoforms in single fibres with particular emphasis on TnC	24
1.5 The aims of this study	25
Chapter 2: General methods	28-41
2.1 Animals and muscles	28
2.2 Preparation of mechanically skinned single fibres	28
2.3 Composition of SDS-PAGE solubilisation buffer and electrophoretic apparatus	30
2.4 Glycine-SDS-PAGE	33
2.4.1 Preparation of glycine separating gels	33
2.4.2 Preparation of glycine stacking gels	34
2.4.3 Preparation of Glycine-SDS-PAGE running buffer	35
2.4.4 Electrophoresis of glycine gels	35
2.4.5 Silver staining of glycine gels using the Hoefer protocol	35
2.5 Alanine-SDS-PAGE	37
2.5.1 Preparation of alanine separating gels	37

2.5.2 Preparation of alanine stacking gels	38
2.5.3 Preparation of Alanine-SDS-PAGE running buffer	39
2.5.4 Electrophoresis of alanine gels	39
2.5.5 Silver staining of alanine gels using the Bio-Rad protocol	39
2.6 Scanning and densitometry of SDS gels	41
Chapter 3: Purification of fast and slow TnC isoforms from EDL and Soleus muscles of the rat	42-64
3.1 Introduction	42
3.2 Materials and methods	44
3.2.1 Muscle and proteins	44
3.2.2 Preparation of crude skeletal muscle troponin extract	44
3.2.3 Preparation of skeletal muscle ether powder	44
3.2.4 Extraction of myofibrillar proteins from skeletal muscle ether powder	49
3.2.5 Removal of tropomyosin by isoelectric precipitation	50

3.2.6 Ammonium sulfate fractionation	50
3.2.7 Preparation of crude skeletal muscle troponin extract for ion exchange chromatography	51
3.2.8 Isolation of skeletal muscle TnC by ion exchange chromatography	51
3.2.9 Analysis of chromatographic fractions by SDS-PAGE	52
3.2.10 Determination of TnC concentration in chromatographic fractions	52
3.2.11 Tryptic digestion of commercial TnC isoforms	54
3.2.12 Tryptic digestion of BSA and CaM	54
3.2.13 Tryptic digestion of rat TnC isoforms	54
3.3 Results	55
3.3.1 Purification of rat skeletal muscle TnC isoforms	55
3.3.2 Tryptic peptide mapping of rat TnC isoforms	58
3.4 Discussion	61

Chapter 4: Electrophoretic identification of TnC isoforms in single muscle fibres	65-77
4.1 Introduction	65
4.2 Methods	66
4.2.1 Identification of TnC isoform bands in single muscle fibres using EGTA	67
4.3 Results and discussion	67
4.3.1 Effect of EGTA on the electrophoretic mobility of TnC in SDS gels	67
4.3.2 Identification of TnC isoforms in single muscle fibres of the rat	70
4.3.3 Detection of TnC isoforms in single muscle fibres by silver staining	74
Chapter 5: MHC and TnC isoform composition of single skeletal muscle fibres of the rat	78-88
5.1 Introduction	78
5.2 Materials and methods	79
5.2.1 Animals, muscles and single fibre preparation	79

5.2.2 Electrophoretic analyses of myofibrillar protein isoforms in single fibres	79
5.3 Results	79
5.3.1 Classification of MHC isoform based fibre-types	79
5.3.2 TnC isoforms detected in pure and hybrid fibres	81
5.4 Discussion	85
Chapter 6: Sr²⁺-activation characteristics and TnC isoform composition of single muscle fibres of the rat diaphragm	89-118
6.1 Introduction	89
6.2 Materials and methods	92
6.2.1 Animals and muscles	92
6.2.2 Preparation of single fibres	92
6.2.3 Preparation of solutions used for force activation experiments	92
6.2.4 Protocol for isometric force activation experiments	94
6.2.5 Determination of Sr²⁺- and Ca²⁺- activation characteristics of single fibre segments	97

6.2.6 Electrophoretic analyses of myofibrillar protein isoform composition	99
6.2.6.1 Analysis of low molecular weight myofibrillar proteins (other than TnC) on SDS-PA gels	100
6.2.7 Statistics	100
6.3 Results	103
3.6.1 Myofibrillar protein isoform combinations in single fibres of rat diaphragm	103
3.6.2 Sr²⁺-activation characteristics of single fibres of rat diaphragm	106
3.6.3.1 Other contractile activation characteristics	111
6.4 Discussion	112
Concluding Remarks	119
Bibliography	121

Summary

The investigations described in this thesis were prompted by an overall interest in the phenomenon of Troponin C (TnC) polymorphism in mammalian skeletal muscle. Gaining insights into this area of inquiry has been limited, in large part due to methodological problems associated with the identification of rat (a commonly used animal model for studying mammalian skeletal muscle) TnC isoforms on SDS gels. Therefore, a method was devised for unambiguous identification of TnC isoforms in rat single muscle fibres. This method, validated using rat skeletal muscle TnC isoforms purified for the first time as part of this study, was used in conjunction with myosin heavy chain (MHC) isoform based fibre-typing and Sr^{2+} -activation measurements to explore the relationship between MHC and TnC isoform composition in mammalian skeletal muscle at the single fibre level, and to revisit the controversial issue of the relationship between TnC isoform composition and fibre-type differences with respect to Sr^{2+} -activation characteristics. More specifically, the individual studies presented in this thesis are as follows:

(1) The fast and slow TnC isoforms were isolated from rat extensor digitorum longus (EDL, 23 μ g TnC /g wet weight) and soleus (SOL, 17.6 μ g TnC /g wet weight) muscles respectively. The identity of the purified TnC isoforms was established by peptide mapping using commercial preparations of rabbit skeletal muscle fast TnC and human cardiac muscle slow TnC isoforms as reference.

(2) A novel method for unequivocal identification of TnC isoforms in single fibre segments was developed (based on the previously reported influence of Ca^{2+} on the

mobility of Ca^{2+} -binding proteins in SDS gels), which allows MHC, TnC *and* functional analyses to be carried out *on the same single fibre*. The method was validated using the purified TnC isoforms.

(3) The possibility that MHC and TnC isoforms exist in specific combinations in non-transforming rat skeletal muscle fibres was investigated by analysing the expression of these proteins in 245 single fibres from SOL (predominantly slow-twitch) and sternomastoid (SM, predominantly fast-twitch) muscles of adult rats. In this study, all fibres that contained only one MHC isoform (slow or fast) contained only the matching TnC isoform and all fibres that contained multiple fast MHC isoforms contained only the fast TnC isoform. Fibres expressing both slow and fast MHC isoforms displayed either both TnC isoforms, or only one TnC isoform of a type dependent on the relative proportion of fast/slow MHC present. These data suggest a close relationship between MHC and TnC isoform composition in non-transforming skeletal muscles of adult rat.

(4) Single fibers of rat diaphragm containing different naturally occurring combinations of myofibrillar protein isoforms were used to evaluate the contribution of TnC isoforms to fiber-type related differences with respect to sensitivity to Sr^{2+} of the contractile system. Mechanically skinned fibers were studied for their isometric force *vs.* $[\text{Sr}^{2+}]$ relationships and then analysed electrophoretically for myofibrillar protein isoform composition. The data demonstrate that fiber-type differences in Sr^{2+} -dependence of contractile activation processes are primarily determined by the TnC isoform composition, with the slow isoform conferring on average a 7 fold greater sensitivity to Sr^{2+} than the fast isoform. Moreover, the ratio of TnC isoforms determined functionally

from the force-pSr ($-\log_{10} [\text{Sr}^{2+}]$) curves is tightly ($r^2 = 0.97$) positively correlated with that estimated electrophoretically.

Together, these results validate the use of Sr^{2+} -activation characteristics to distinguish fibers containing different proportions of fast and slow TnC isoforms and to study the mechanisms by which divalent cations activate the contractile apparatus. It was also found that the functionally and electrophoretically determined ratios of TnC isoforms present in a fibre display similar, sigmoidal relationships with the ratio of MHC isoform types expressed. These relationships (i) offer further insight into the functional and molecular expression of TnC in relation to the molecular expression of MHC isoform types and (ii) may provide the basis for predicting sensitivity to Sr^{2+} , TnC and/or MHC isoforms in pure and hybrid skeletal muscle fibers.

Declaration

This thesis contains no material that has been presented for the award of any other degree or diploma in this or any other university. Except where specifically indicated in the text, the data presented herein is the result of the work of the author, and to the best of my knowledge and belief, has not been previously written or published by any other person.



Brett O'Connell

Acknowledgments

Firstly, I would like to thank my supervisor, Prof. Gabriela Stephenson, for accepting me into her lab and devoting so much time and effort to training me in scientific research.

I would also like to thank a number of other people who have been of great help to me during the course of my studies: Prof. George Stephenson and Dr. Ronnie Blazev for sharing their skills and expertise in all areas concerned with isometric force measurements of single fibres, Aida Yousef for making Ca^{2+} - and Sr^{2+} -activating solutions, Dr. Long Nguyen for mechanically skinning a great many single fibres, Dr. Greg Wilson for imparting invaluable wisdom regarding the nuances of Potter's TnC purification protocol, and Ian Sullivan for his help with equipment maintenance and in obtaining all the chemicals and proteins necessary to conduct this work.

Special thanks also go to my fellow researchers in the Muscle Cell Biochemistry Laboratory, Dr. Susie Bortolotto-Smith, Craig Goodman, Justin Kemp, Ronnie Blazev and Long Nguyen, for general help, advice and many fun times. Thanks also to Anthea Stephenson, and again to Justin and Ronnie, for proof reading this thesis, and thanks to my family and friends, particularly Peter Florey, for helping out during times of personal troubles.

List of Publications

Refereed papers:

1. **O'Connell B**, Stephenson DG, Blazeov R, and Stephenson GMM. Troponin C isoform composition determines differences in Sr^{2+} -activation characteristics between rat diaphragm fibers. *American Journal of Physiology (Cell Physiology)*. *In press*, 2004.
2. **O'Connell B**, Nguyen LT, and Stephenson GMM. A single-fibre study of the relationship between MHC and TnC isoform composition in rat skeletal muscle. *Biochemical Journal*. 378(Pt 1): 269-274, 2004.
3. **O'Connell B** and Stephenson GMM. Purification of troponin C isoforms from EDL and soleus muscles of the rat. *Journal of Muscle Research and Cell Motility*. 24(8): 555-559, 2003.

Conference presentations (non-refereed):

1. **O'Connell B**, Nguyen LT, and Stephenson GMM. A study of rat troponin C isoforms. 34th congress of the International Union of Physiological Sciences (IUPS), 2001.
2. **O'Connell B**, Nguyen LT, and Stephenson GMM. Myosin heavy chain and troponin C isoform expression in pure and hybrid skeletal muscle fibres of the rat. IUPS satellite meeting: Muscle fibre types: Development, function and regulation, 2001.

3. **O'Connell B**, Nguyen LT, and Stephenson GMM. Effect of glycerol on the electrophoretic mobility of low molecular weight myofibrillar proteins. Australian Electrophoresis Society, 6th annual conference, 1999.

List of Abbreviations

ADP	adenosine diphosphate
ATP	adenosine triphosphate
Ala	alanine
Arg	arginine
Asp	aspartic acid
BSA	bovine serum albumin
C	[N,N'-methylene-bis-acrylamide] x 100 / [acrylamide + N,N'-methylene-bis-acrylamide]
Ca ²⁺	calcium ion
Cd ²⁺	cadmium ion
CaF _{max}	maximum Ca ²⁺ -activated force
CaM	calmodulin
Cys	cysteine
DPH	diaphragm
DTT	dithiothreitol
EDL	extensor digitorum longus
Glu	glutamic acid
HEPES	N-(2-hydroxyethyl)piperazine-N'-(2-ethanesulfonic acid)
K _{Ca²⁺}	affinity for Ca ²⁺
K _{Mg²⁺}	affinity for Mg ²⁺
Leu	leucine
Lys	lysine

Met	methionine
MHC	myosin heavy chain
MLC	myosin light chain
OD	optical density
P_i	inorganic phosphate
P_t	% max force
Pb^{2+}	lead ion
Phe	phenylalanine
PA	polyacrylamide
PAGE	polyacrylamide gel electrophoresis
PMSF	phenyl methyl sulfonyl fluoride
Pro	proline
RT	room temperature
S1	subfragment S1 of myosin
SDS	sodium dodecyl sulfate
SDS-PAGE	sodium dodecyl sulfate polyacrylamide gel electrophoresis
SEM	standard error of the mean
SM	sternomastoid
SOL	soleus
Sr^{2+}	strontium ion
SrF_{max}	maximum Sr^{2+} -activated force
TEMED	N,N,N',N'-tetramethylethylenediamine
T	total concentration of monomer (acrylamide + N,N'-methylene-bis-acrylamide)

Tm	tropomyosin
Tn	troponin
TnC	troponin C
TnI	troponin I
TnT	troponin T
Tris	Tris(hydroxymethyl)methylamine
Val	valine

List of figures

<u>Figure No.</u>	<u>Figure Title</u>	<u>Page</u>
1.1	The structure of mammalian skeletal muscle.	3
1.2	Arrangement of thick and thin filaments in the sarcomere, and the structure of the thin filament.	5
1.3	The structure of myosin.	6
1.4	Schematic of myofibrillar protein interactions in the presence or absence of Ca^{2+} .	10
1.5	The cross-bridge cycle.	13
2.1	A comparison of TnC bands in skinned single fibres not incubated (lanes 1 and 2) and incubated (lanes 3 and 4) for two min in an aqueous, high Ca^{2+} , rigor solution prior to solubilisation in SDS-PAGE solubilising buffer.	31
2.2	Electrophoresis equipment.	32
2.3	Flowchart of Hoefer silver staining procedure used for glycine PA gels.	36
2.4	Flowchart of Bio-Rad silver staining procedure used for alanine PA gels.	40

3.1.1	Flowchart of steps in protocol for purification of TnC from rat skeletal muscle, day one.	45
3.1.2	Flowchart of steps in protocol for purification of TnC from rat skeletal muscle, day two.	46
3.1.3	Flowchart of steps in protocol for purification of TnC from rat skeletal muscle, days three and four.	47
3.1.4	Flowchart of steps in protocol for purification of TnC from rat skeletal muscle, day five.	48
3.2	Standard curves used to determine the amount of rat TnC in each chromatographic fraction based upon relative optical density of the silver stained bands of known concentrations of proteins resolved on 16% PA gels.	53
3.3	Electrophoretogram of the fractions produced by ion exchange chromatography of the crude troponin extract from rat EDL muscle.	56
3.4	Electrophoretogram of the fractions produced by ion exchange chromatography of the crude troponin extract from rat soleus muscle.	57

3.5	A comparison of rat EDL and reference proteins before and after limited tryptic digestion.	59
3.6	A comparison of rat SOL TnC and reference proteins before and after limited tryptic digestion.	60
4.1	Example of sample loading sequence on gels used for TnC isoform identification in single fibres.	68
4.2	The effect of different concentrations of EGTA on the migration of rat EDL TnC-f.	69
4.3	Identification of TnC isoforms in single fibres using EGTA diffusion from an adjacent lane to cause TnC bands to curve upward.	71
4.4	Variability of relative migration of TnC isoform bands in SDS gels.	73
4.5	Detection limit of silver stained TnC isoform bands (rabbit TnC-f and human cardiac TnC-s) resolved by SDS-PAGE (upper panel) and electrophoretic estimation of the TnC content of a 4 nl fibre segment using a mixture of known amounts of purified TnC isoforms as reference (lower panel).	75

5.1	Representative electrophoretograms of the thirteen MHC isoform based fibre types found in this study.	80
5.2	Examples of the MHC and TnC isoform combinations detected in the single fibres examined in this study.	82
5.3	Relationship between the proportion of fast/slow MHC isoforms present and the type of TnC isoforms detected in 'fast-slow hybrid' fibres.	84
6.1	Sample of complete data collected for a single muscle fibre.	96
6.2	Representative electrophoretograms showing the MHC and TnC isoforms detected in the single muscle fibers examined in this study.	101
6.3	Representative electrophoretograms showing typical regulatory protein isoform composition for each group.	102
6.4	Representative P_t -pSr curves of one fibre from each of the five groups	107
6.5	Graph showing the relationship between the estimated amount of TnC-s in single pure and hybrid fibre segments (n=59) and the proportion of the 'slow-type' (w_1) Sr^{2+} -sensitivity component of the force-pSr curve produced by the fibres.	110

6.6 Graph showing the relationship between the proportion of TnC-s, estimated electrophoretically (indicated by asterisks, right y-axis), the proportion of the 'slow-type' Sr^{2+} -sensitivity component (w_l) of the force-pSr curve (indicated by circles, left y-axis) and the proportion of slow MHC isoform present in each fibre (x-axis).

List of tables

<u>Table No.</u>	<u>Table Title</u>	<u>Page</u>
1.1	Reports of TnC isoform migration in single muscle fibres (or heart trabeculea) relative to MLC2 isoforms	26
2.1	Composition of Glycine SDS-PA separating gels	34
2.2	Composition of Glycine SDS-PA stacking gels	34
2.3	Composition of Alanine SDS-PA separating gels	38
2.4	Composition of Alanine SDS-PA stacking gels	38
5.1	TnC isoform composition of the pure and hybrid MHC-based fibre types obtained from the soleus and sternomastoid muscles of adult rat	81
5.2	Theoretically possible MHC-TnC isoform combinations	88
6.1	Composition of stock solutions used to make force activation solutions	93
6.2	MLC, TnI, TnT+Tm isoform composition and Sr ²⁺ -activation characteristics of fibres classified by MHC and TnC isoform composition	104

Chapter 1: Introduction

1.1 Scope

Skeletal muscle contraction is a finely regulated process such that mechanical outcome matches physiological need. The best understood regulatory mechanism in mammalian skeletal muscle (often referred to as 'thin filament activation' or 'contractile activation') involves the reversible binding of myoplasmic Ca^{2+} to the thin filament protein TnC; this triggers a sequence of reversible structural/positional changes in several myofibrillar proteins, some associated with the thin filament (actin, TnC, troponin I, TnI, troponin T, TnT and tropomyosin, Tm) and one (myosin) associated with the thick filament (Squire and Morris, 1998). The exact mechanisms by which the contractile activation process regulates the interaction between myosin (the molecular motor) and actin that results in the development of active force are only partly understood. The quest for furthering our knowledge in this field of inquiry is made even more challenging by the fact that, except for actin, all the proteins mentioned above exist in different molecular forms (isoforms), with the number of isoforms varying markedly between different myofibrillar proteins (*cf.* two for TnC and nine for MHC).

Much of the current knowledge about key players and events involved in the Ca^{2+} -dependent regulation of mammalian skeletal muscle contraction has been derived from studies using various preparations (whole muscles, bundles of fibres, intact or skinned single fibres) of rat skeletal muscles. A survey of the relevant literature carried out at the beginning of this investigation revealed substantial gaps in the information available (some of which are listed in section 1.5) on rat skeletal muscle isoforms. Accordingly, the

work described in this thesis focused on (i) purification of rat skeletal TnC isoforms, (ii) the development of a protocol for unambiguous identification of TnC isoform bands on polyacrylamide (PA) gels of single muscle fibres, (iii) the patterns of co-expression of TnC and MHC isoforms in single muscle fibres containing one or several MHC isoforms and (iv) the relationship between TnC isoform composition and fibre type differences with respect to the Sr^{2+} -sensitivity of the contractile apparatus. To place this work in perspective, brief background information relevant to these topics will be presented in this chapter.

1.2 Skeletal muscle structure

Vertebrate skeletal muscle is a tissue functionally specialised for producing force and movement. Skeletal muscle cells (also referred to as fibres; see Fig 1.1) are characteristically long and thin in shape, parallel in arrangement, independent in operation, multinucleated, and show transverse striations along their length when viewed under a light microscope. Running the length of each muscle fibre are many thread-like anatomical structures called myofibrils that can shorten, causing the fibre to contract by as much as a third of its original length (Hochachka, 1994). The myofibrils are linear chains of highly organized structures known as sarcomeres, which represent the basic functional units responsible for muscle contraction.

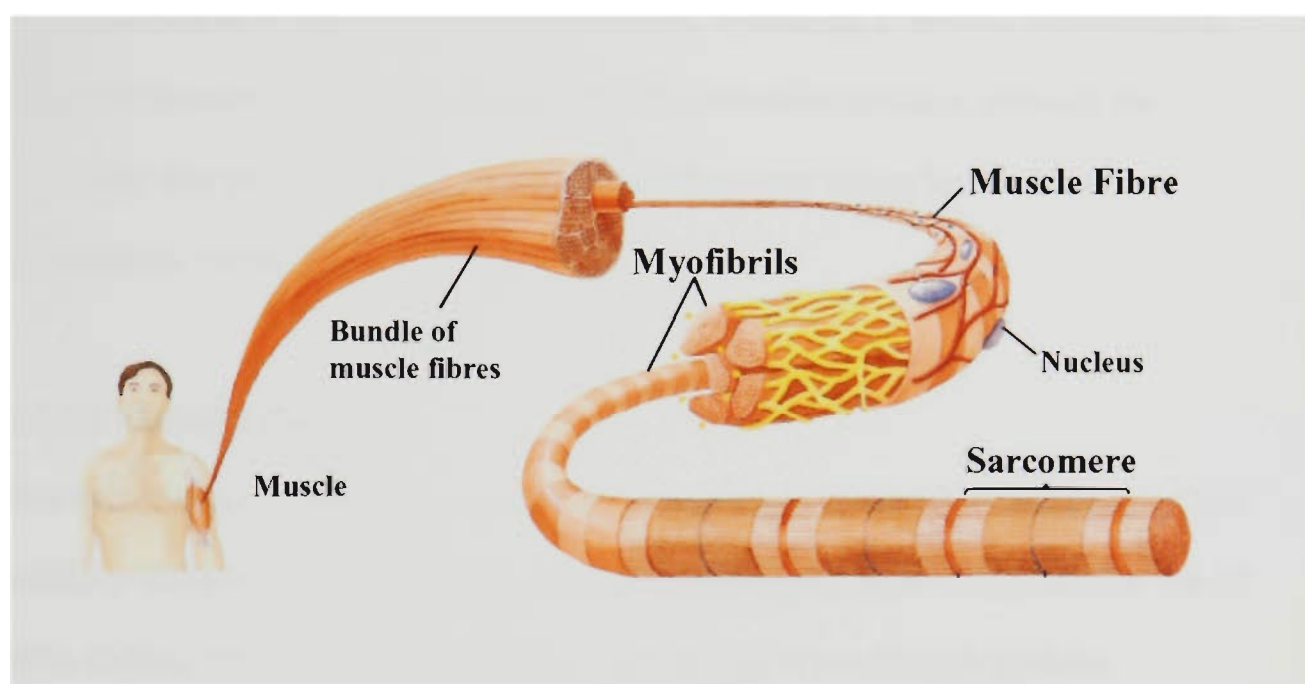


Fig. 1.1. The structure of mammalian skeletal muscle.
Modified from Nelson and Cox, 2000.

1.2.1 The sarcomere

The two major structures of the sarcomere in all skeletal muscles are the thick and thin filaments, which are inter-digitated and regularly spaced as shown in Fig 1.2; the alternating regions of overlap and non-overlap between the thick and thin filaments account for the striated appearance of skeletal muscle fibres. Some of the sarcomeric proteins (eg. the contractile proteins myosin and actin, and the regulatory proteins Tm and Troponin, Tn) have well defined functional roles. Others (eg. C protein, tropomodulin) appear to be entirely devoted to maintaining the sarcomere structure, although the possibility that they play minor roles in contractile events cannot be ruled out (Hochachka, 1994).

1.2.1.1 *The thick filament*

The thick filament consists primarily of the protein myosin, a hexamer composed of two MHCs (~220 kDa each; Maita *et al.*, 1991) and four myosin light chains (MLCs, ~16-27 kDa; Collins, 1991). The myosin molecule is made up of two flexible globular protrusions, or myosin heads, each connected by a 'neck' region to a long, straight tail formed by the α -helical arrangement of the two MHC polypeptides (see Fig 1.3). Each myosin head-neck region (also referred to as the myosin subfragment S1) comprises two myosin light chains and a ~50 kDa globular domain of one of the myosin heavy chains (Burke and Kamalakannan, 1985). It is important to note that the S1 domain of each MHC contains two structural components essential for muscle contraction, *viz.* the ATP binding/hydrolysis site and the actin-binding site. Based on their location at the 'neck' region of the S1 subfragment, MLCs are believed to be involved in the movement of the

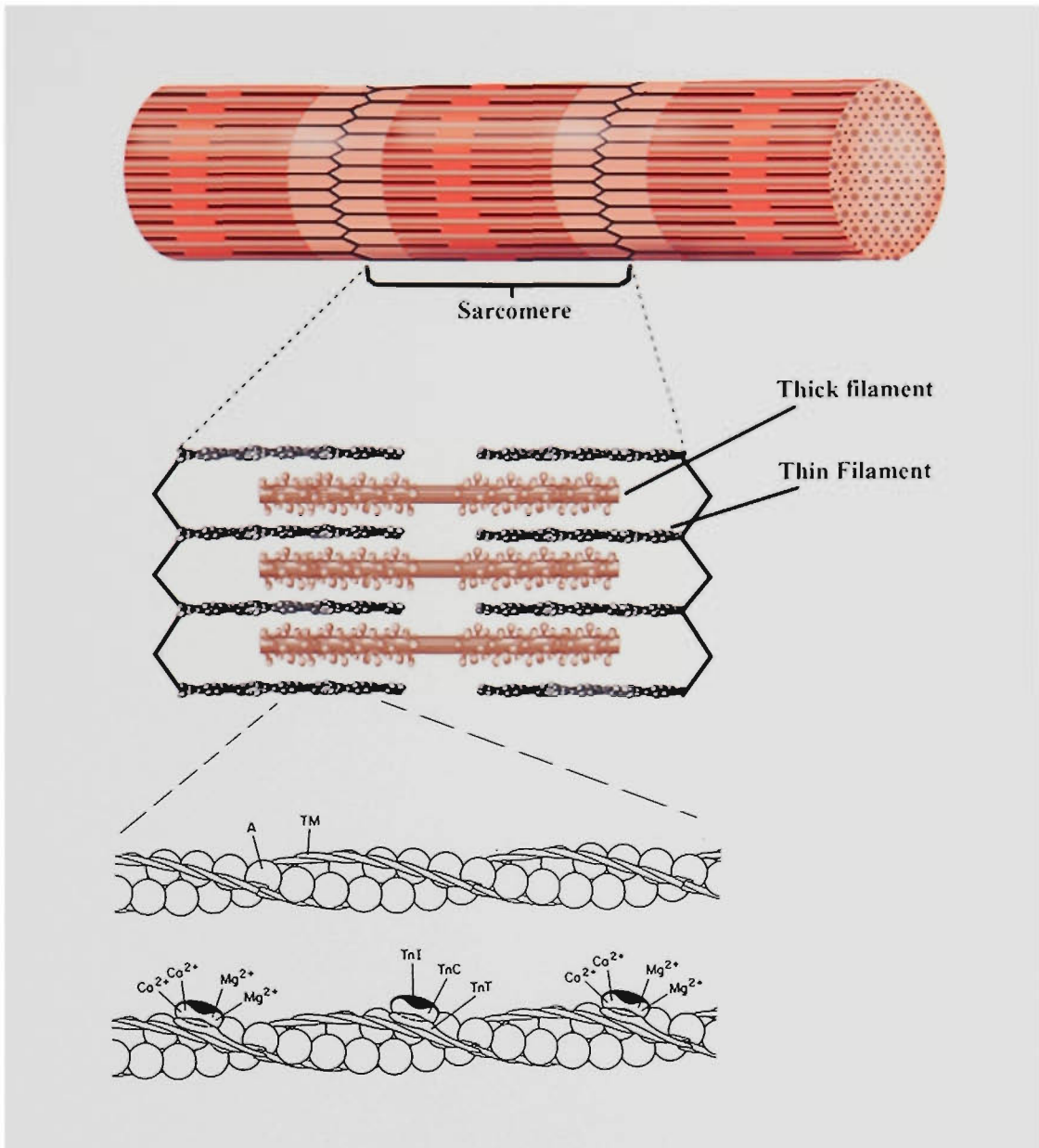


Fig. 1.2. Arrangement of the thick and thin filaments in the sarcomere, and the structure of the thin filament. Modified from Marieb, 2001 and Moss et al., 1995. A, actin; TM, tropomyosin; TnI, troponin I; TnC, troponin C; TnT, troponin T. Note the Ca²⁺/Mg²⁺ binding sites on troponin C.

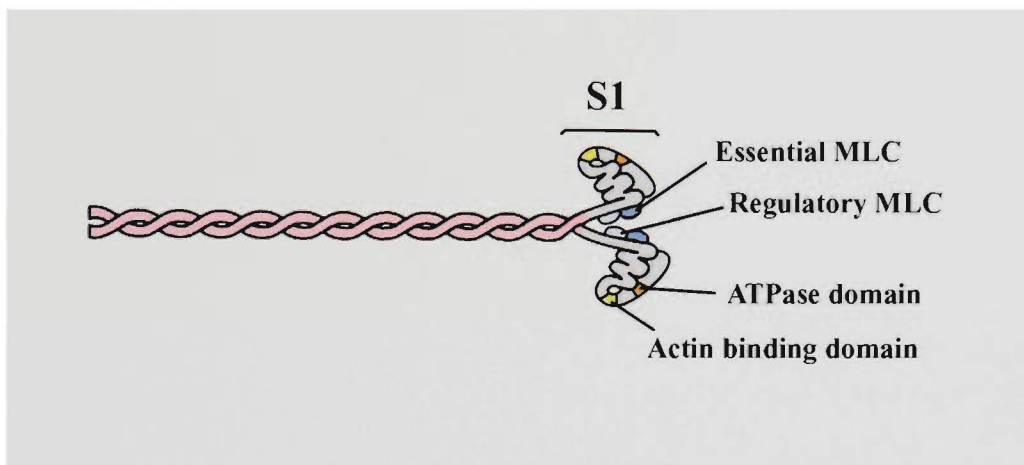


Fig. 1.3. The structure of myosin. Modified from Nelson and Cox, 2000.

myosin head that occurs during ATP hydrolysis. The thick filament is formed by the intertwining of the tails of many myosin molecules such that the myosin heads protrude regularly from the thick filament shaft in alignment with surrounding thin filaments (see Fig. 1.2), allowing for optimal actin binding opportunities (Hochachka, 1994).

1.2.1.2 *The thin filament*

The thin filament (see Fig 1.2) contains a number of proteins whose role in the process of muscle contraction is relatively well established. These include the contractile protein actin and the regulatory proteins Tm and Tn. In skeletal muscle, actin exists as polymers of globular G-actin monomers (~42 kDa; Uyemura *et al.*, 1978) that form long F-actin strands. Each G-actin monomer contains four subdomains (1, 2, 3 and 4), at least one of which (subdomain 1) appears to be involved in actin-S1 interactions (for review see Squire and Morris, 1998). The backbone of a single thin filament is formed by a double helix of F-actin strands (Lorenz *et al.*, 1995).

Winding around the actin helix is a Tm filament, composed of head-to-tail, non-covalently linked molecules, where each Tm molecule (a parallel, two stranded, α -helical coiled-coil structure of ~70 kDa; Hitchcock-DeGregori *et al.*, 1985) spans ~7 G-actin monomers, and is associated with one Tn complex (see review by Gordon *et al.*, 2000). The Tn complex consists of three subunits: (i) TnI (~ 24 kDa; Simpson, 2002), a basic protein (pI ~9.6 for the rat protein, as reviewed by Reggiani and Kronnie, 2004) which binds to actin in the absence of Ca^{2+} , thereby preventing myosin heads from binding strongly to actin, (ii) TnT (~ 37 kDa; Briggs *et al.*, 1984), a relatively basic protein (pI ~ 8-9 in the chicken, Ogut and Jin, 1998) which is involved in the binding of the Tn

complex to Tm at the overlap region of adjacent Tm molecules (Heeley *et al.*, 1987), and (iii) TnC (~18 kDa; Collins *et al.*, 1977) an acidic (pI ~4 for the mouse protein, as reviewed by Reggiani and Kronnie, 2004) Ca²⁺-binding protein that confers Ca²⁺-sensitivity to the interaction between actin and myosin. The charge differences between TnI, TnT and TnC have been exploited by Greaser and Gergely (1971) when developing the ion-exchange chromatography step in the protocol for purification of Tn subunits.

TnC is a member of the EF-hand family of calcium binding proteins, which also includes the non-filament bound muscle proteins parvalbumin (~ 12 kDa, Potter *et al.*, 1977) and calmodulin (CaM, ~ 17 kDa, Cohen *et al.*, 1980). Characteristically, these proteins (i) contain regions known as EF-hand Ca²⁺/Mg²⁺-binding sites that are formed from a common helix-loop-helix peptide motif in which negatively charged amino acid residues (Asp and Glu) are strategically positioned to chelate divalent cations (da Silva and Reinach, 1991), and (ii) undergo a functionally significant conformational change upon binding Ca²⁺. The four EF-hand binding sites of TnC have been named I to IV, counting from the N-terminal of the protein (Collins *et al.*, 1977).

Sites I and II bind Ca²⁺ ($K_{Ca^{2+}} = 3 \times 10^5 \text{ M}^{-1}$) but not Mg²⁺ *in vivo* (Potter and Gergely, 1975), and since they are considered to be directly involved in regulating thin filament activation, are referred to as the 'regulatory sites'. More specifically, Ca²⁺ binding to these sites induces a conformational change in TnC (causing exposure of a hydrophobic pocket in the N-terminus region) which enhances the interaction of TnC and TnI, weakens the interaction between actin and TnI (thereby releasing TnI inhibition of myosin-ATPase) and alters the position of the associated Tm molecule on the thin filament (thereby

exposing the myosin binding sites on actin, see reviews by Gordon *et al.*, 2000; Gomez *et al.*, 2002). Although Ca^{2+} is the physiological activator of muscle contraction, it has been shown that the binding of other divalent cations such as Sr^{2+} (Ebashi *et al.*, 1968), Cd^{2+} , or Pb^{2+} (Chao *et al.*, 1990) to the regulatory sites of TnC can also lead to contraction.

Ca^{2+} -binding sites III and IV are situated at the carboxyl end of the protein and have a higher affinity for Ca^{2+} than the regulatory sites. The affinity of these sites for Ca^{2+} and Mg^{2+} ($K_{\text{Ca}^{2+}} = 2 \times 10^7 \text{ M}^{-1}$ and $K_{\text{Mg}^{2+}} = 2 \times 10^3 \text{ M}^{-1}$, Potter and Gergely, 1975) is such that they are considered to be filled with Ca^{2+} or Mg^{2+} *in vivo* at all times (Robertson *et al.*, 1981). These sites are considered to be primarily involved in maintaining the structural integrity of the Tn complex (Zot and Potter, 1982; Morimoto, 1991; Gomez *et al.*, 2002).

According to current knowledge, TnC interacts with TnI and TnT, TnI interacts with TnC, TnT and actin, TnT interacts with TnC, TnI and Tm, and Tm interacts with TnT and actin (see Fig 1.4) While details regarding the chemical nature of the interactions between thin filament proteins are largely unknown, it is clear that the strength of some of these interactions, particularly those between TnI and actin and between TnI and TnC, is dependent on Ca^{2+} being bound to TnC (for recent review see Gordon *et al.*, 2000). Thus, it has been shown that the Tn complex can maintain its integrity even in highly denaturing conditions (8 M urea) as long as Ca^{2+} is present (Head and Perry, 1974). By

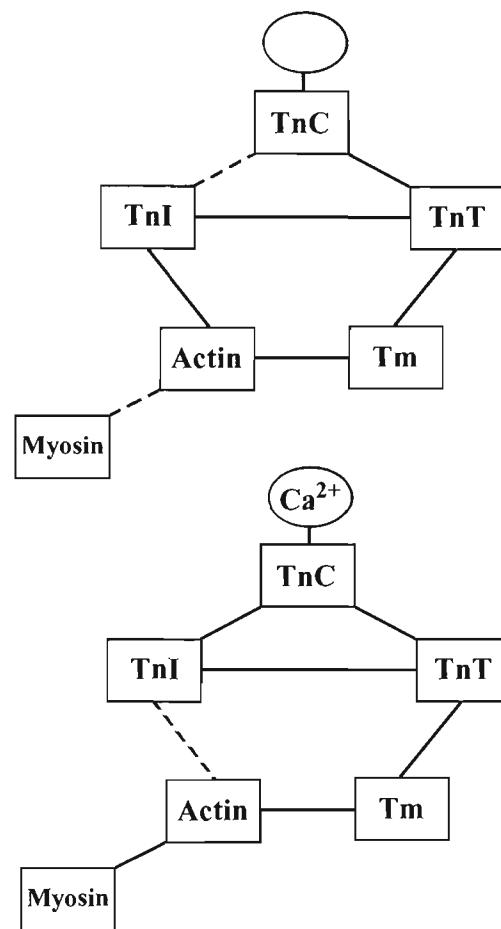


Fig. 1.4. Schematic of myofibrillar protein interactions in the presence or absence of Ca^{2+} . Shown are the strong interactions (solid lines) and weak interactions (dashed lines) observed between contractile proteins when Ca^{2+} is absent (upper panel) or bound to TnC (lower panel).

comparison, divalent cation chelators such as EDTA have been found to dissociate the Tn complex (Cox *et al.*, 1981). On this basis, EDTA has been used in protocols for TnC extraction from single muscle fibres (for review see Moss, 1992) and for TnC purification (see below).

The three subunits of the Tn complex were first isolated by Greaser and Gergely (1971) using a procedure that spawned several variations in the following years (Greaser and Gergely, 1973; Perry and Cole, 1974; Head and Perry, 1974; Potter and Gergely, 1974). Elements of these purification methods were later combined by Potter (1982) into a protocol which has since been used widely as a basis for purifying TnC. The major steps involved in this protocol include (i) the preparation of an ether powder containing myofibrillar proteins, (ii) extraction of the ether powder with a low ionic strength solution, (iii) removal of Tm by isoelectric precipitation, (iv) isolation of the Tn complex by ammonium sulfate fractionation, (v) dissociation of the Tn subunits by urea and EDTA, and (vi) isolation of the TnC by anion-exchange chromatography. In the study described in Chapter 3, the method of Potter (1982) was used, with minor modifications, to purify the TnC isoforms from small amounts of rat hindlimb muscles.

1.3 Models of the mechanisms of skeletal muscle contraction and of contractile activation

1.3.1 The sliding filament theory

The sliding filament theory of muscle contraction, which was formulated simultaneously by two independent groups, namely Huxley and Niedergerke (1954) and Huxley and Hanson (1954), is the basis on which rests all the current knowledge regarding the details of the molecular mechanisms involved in muscle contraction.

According to this theory, the thick and thin filaments do not change length during muscle contraction, but rather cause the sarcomere to shorten as they slide past one another due to the cyclical interaction of myosin heads with actin. This process, known as the cross-bridge cycle (shown diagrammatically in Fig. 1.5), involves ATP hydrolysis by the ATPase associated with the myosin heads, which is dramatically activated by the binding of S1 to F-actin (for review see Gordon *et al.*, 2000). Note that it is the release of inorganic phosphate from the ATPase site on the MHCs which appears to be associated with the swinging movement of all or part of the myosin head on actin that acts as a 'power-stroke'.

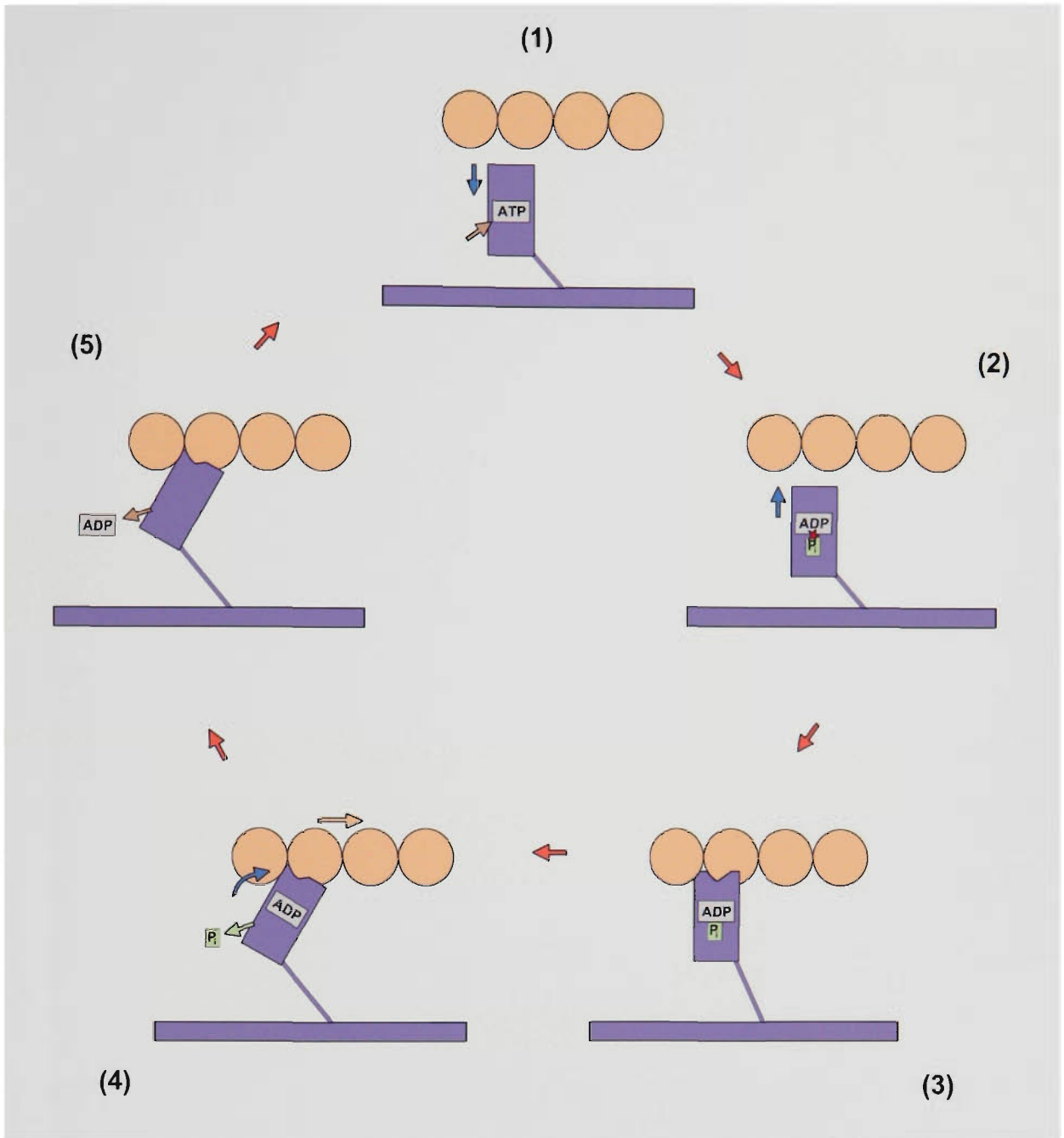


Fig. 1.5. The Cross-Bridge Cycle. Upon the binding of ATP to S1, the myosin head detaches from F-actin (step 1). Cleavage of the ATP to form ADP and P_i (step 2) causes S1 to bind to F-actin (step 3). Ejection of P_i from S1 is associated with the "power stroke" (step 4) whereby a movement in the myosin head slides the F-actin (toward the right in this diagram). Following the power stroke, ADP is ejected from S1 (step 5), and the cycle continues with the binding of another molecule of ATP to S1 (step 1).

1.3.2 The three state model of thin filament activation

As first demonstrated by Ebashi (1963, 1964), the formation of cycling cross-bridges is $[Ca^{2+}]$ dependent, where the sensitivity to Ca^{2+} is conferred by the thin filament via allosteric interactions between Tm and the Tn subunit proteins (Ebashi *et al.*, 1968).

The binding of Ca^{2+} to TnC initiates the highly complex process of *thin filament activation* in which actin, myosin, Tm and Tn subunits all contribute to inducing a movement of Tm around the thin filament to expose the myosin binding sites on actin (for reviews see Squire and Morris, 1998; Gordon *et al.*, 2000). Ongoing investigations into the mechanism underlying this process continue to produce evidence which supports *the three-state model* of thin filament activation first proposed by McKillop and Geeves (1993). According to this model, the thin filament can exist in three 'activation states', which differ with respect to the extent/nature of S1 binding to actin. The three state model replaces the well known *steric-blocking model* of cross-bridge regulation proposed by Huxley (1972), in which Tm and Tn physically block S1 access to binding sites on actin in the absence of Ca^{2+} , while S1 is free to bind actin (and thus produce force) when the positions of Tm and Tn are shifted following Ca^{2+} binding to TnC.

According to the three-state model, the thin filament can exist in the following forms (for review see Gordon *et al.*, 2000):

(i) *The blocked state* (S1 bound to actin only by very weak electrostatic forces). This is the default state of the thin filament in the absence of Ca^{2+} . In this state TnI is strongly bound to actin, hindering the ability of S1 to form the stronger, hydrophobic interactions

with actin necessary for force production. Additionally, the position of Tm on the thin filament in this state prevents S1 access to many of the binding sites on the seven G-actin monomers spanned by it. Upon Ca^{2+} binding to TnC, the thin filament shifts to the 'closed' state.

(i) *The closed state* (S1 associated weakly with actin via hydrophobic interactions). In this state Ca^{2+} binding to TnC has produced a movement of the Tn complex such that TnI no longer interferes with S1 binding to the G-actin monomer with which it is associated, and the position of Tm has shifted 25-30° around the F-actin strand (Lorenz *et al.*, 1995) exposing more potential S1 binding sites on propinquent G-actin monomers.

(ii) *The open state* (strong binding of S1 in a force producing manner). In the open state strongly bound myosin heads have pushed Tm a further 10° around the actin strand, thereby exposing even more potential myosin binding sites along the actin strand and enabling maximum myosin ATPase activity; in this state, the thin filament is considered 'fully activated' (Gordon *et al.*, 2000). Note also that when the thin filament is in this state, the presence of strongly bound S1 on actin displaces Tm to a greater degree than is possible by Ca^{2+} -induced movement alone (Moraczewska, 2002; Tobacman, 2002).

Recent findings from X-ray diffraction and fluorescence resonance energy transfer studies (Li and Fajer, 1998; Morris *et al.*, 2001; Hai *et al.*, 2002; Moraczewska, 2002) indicate that the equilibrium between the blocked and closed states is regulated by Ca^{2+} binding to TnC, while the transition from the closed to the open states is affected by the conformational position of the myosin heads bound to actin at certain stages of the actomyosin-ATP hydrolysis cycle. Furthermore, it appears that there are mutual influences between the binding of Ca^{2+} to TnC and the transition of myosin heads

between conformational states associated with specific steps in the ATP hydrolysis reaction (for a comprehensive review see Gordon *et al.*, 2000). Thus there is evidence that S1 strongly attached to actin causes an increase in the affinity of TnC for Ca^{2+} during conditions of rigor (Bremel and Weber, 1972; Greene and Eisenberg, 1980; Guth and Potter, 1987) and cross-bridge cycling (Guth and Potter, 1987; Fuchs and Wang 1991, Martyn *et al.*, 1999).

Taken together these findings suggest that the process of contractile activation in skeletal muscle may be modulated by a subtle functional interplay between myosin and TnC, the nature of which is influenced by the degree of thin filament activation (Adhikari and Wang, 2004). However, due to the extremely complex nature of the myofibrillar protein interactions involved in the process of thin filament activation, many details about the exact contributions made by the MHC and TnC proteins remain to be elucidated.

1.4 Polymorphism of myofibrillar proteins and functional implications

In mammals, MHC, MLC, the subunits of the Tn complex and Tm are polymorphic proteins, whose expression is influenced by several factors including (but not limited to) age, substrate availability, neuromuscular activity and hormones (Pette and Staron, 2001). The polymorphism of myofibrillar proteins is widely regarded as an evolutionary adaptation that allows a fibre to fine-tune its contractile performance to mechanical demand within the strictly conserved structure of the sarcomere. Increased awareness of inter-fibre differences with respect to molecular composition and functional phenotype has led to the preferential use of single fibres over whole muscle preparations in

physiological and/or biochemical investigations of the molecular mechanisms involved in muscle contraction. This approach was also used in the studies described in Chapters 4, 5 and 6 of this thesis.

1.4.1 Myofibrillar protein isoforms and their functional roles

1.4.1.1 MHC isoforms

Myosin proteins are coded for by a multi-gene superfamily comprising 18 classes, with MHC expressed in striated muscle belonging to Class II (Berg *et al.*, 2001). In mammals there exist 4 gene families of Class II myosin (including fast skeletal, cardiac, smooth muscle and non-muscle), from which at least 9 MHC isoform types have been detected at both the protein level and mRNA level (ie. β /slow, α , IIa, IIb, IId, embryonic, neonatal, extraocular and mandibular, Schiaffino and Reggiani, 1996); the number and identity of these isoforms in skeletal muscle appears to be species, muscle and age specific (Pette and Staron, 2001). In the trunk and limb muscles of small adult mammals such as the rat, only four MHC isoforms have been commonly detected. In the present study, these isoforms are designated MHC IIb, MHC IId (also known as MHC IIx), MHC IIa and MHC I.

There appear to be four regions of significant amino acid sequence divergence among the isoforms, two located in the MHC tail, one in the neck region and one in the myosin head near the ATP and actin binding sites (Schiaffino and Reggiani, 1996). In agreement with the location of isoform specific sequences in the functional domain of the MHC molecule, a number of contractile characteristics of a muscle cell have been shown to be closely related to the type of MHC isoform it contains. These include maximum

shortening velocity, peak mechanical power and optimal velocity of shortening (Bottinelli *et al.*, 1996), stretch activation properties (Galler *et al.*, 1994), ATP consumption rate during isometric contraction, and tension cost (Stienen *et al.*, 1996). Based on the maximum shortening velocity and ATP hydrolysis rate conferred to a fibre, the four MHC isoforms have been ranked fastest to slowest MHC IId>IIa>IIb>I (Bottinelli *et al.*, 1991).

It is important to note that due to the relatively high abundance of the MHC protein in muscle fibres (~50% total myofibrillar protein content, Pearson and Young, 1989) and to its fundamental role in the contractile process, the composition of MHC isoforms is currently the most commonly used basis for fibre-type classification. Based on this criterion, it has been found that skeletal muscles of adult rats contain fibres that express only one MHC isoform ('pure' fibres; designated here as type **I**, type **IIA**, type **IID** or type **IIB** fibres), and fibres that express more than one MHC isoform ('hybrid' fibres; designated here as type **IIA + IID**, type **I + IIA**, type **I + IIA + IID**, etc).

A remarkable feature of mammalian skeletal muscle, commonly referred to as *plasticity*, is that its fibre type composition can be modified in response to changes in the functional demands (Pette and Staron, 2001). The muscles undergoing fibre type changes are referred to as transforming muscles (as opposed to 'non-transforming' or 'normal' muscles). It is important to point out that transforming muscles appear to differ from normal muscles with respect to both the proportion of hybrid fibres (higher in transforming muscles) and to the variety of MHC isoform combinations that occur in the hybrid fibres (greater in transforming muscles). Thus, hybrid fibres from normal muscles have been found to contain mostly specific MHC combinations predicted by the 'nearest

neighbour rule' (Pette *et al.*, 1999), such that in each fibre a given MHC isoform coexists only with the next fastest (or slowest) MHC isoform. In contrast, many hybrid fibres from transforming muscles were found to contain MHC isoform combinations which do not follow this nearest neighbour rule (for review see Stephenson, 2001).

1.4.1.2 MLC isoforms

As previously mentioned, associated with each myosin head in rat skeletal muscle are one each of two classes of MLCs; the essential/alkali light chains (which exist in two molecular forms designated MLC1 and MLC3) and the regulatory/phosphorylatable light chains (named MLC2). Rat skeletal muscle contains two MLC1 isoforms (MLC1-s and MLC1-f), two MLC2 isoforms (MLC2-s and MLC2-f) and one MLC3 (sometimes referred to as MLC3-f). These five isoforms appear to be coded for by four genes, with MLC1-f and MLC3 being splice variants from the same gene (Periasamy *et al.*, 1984). It is thought that MLC2 can alter myofibrillar Ca^{2+} -sensitivity according to its state of phosphorylation (Stephenson and Stephenson, 1993), while the essential light chains are thought to be involved in activities which influence cross-bridge cycling rates (Niezanska *et al.*, 2002). To date no clear functional differences related to these functions have been established between fibres containing different MLC isoforms.

1.4.1.3 *Tm isoforms*

There are two types of polypeptide chains that make up the Tm molecule, known as α -Tm and β -Tm. These two polypeptides can assemble to produce $\alpha\alpha$ or $\beta\beta$ homodimers, or $\alpha\beta$ heterodimers (Cummins and Perry, 1973). There are two α -Tm isoforms, fast and slow, but only one β isoform; in skeletal muscle, these three proteins are coded for by different genes (Schiaffino and Reggiani, 1996). It is worth noting that some fibre types have been found to differ with respect to the type of α -Tm isoform present, and/or by the ratio of the α and β subunits in the dimer, in a species and muscle specific manner (Schiaffino and Reggiani, 1996). Since α -Tm and β -Tm are considered to be physiologically identical (Cummins and Perry, 1973), and since there is no information on the functional differences between the fast and slow α -Tm isoforms, the physiological impact of structural differences between the Tm isoforms on contractile activation processes remains unclear.

1.4.1.4 *Troponin I isoforms*

TnI exists in rat skeletal muscle as fast and slow isoforms, each coded for by a separate gene. Amino acid sequence analyses indicate that the two TnI isoforms are highly homologous, particularly in the region believed to be responsible for the inhibitory action of TnI on actin-myosin interaction. In humans, for example, the two sequences differ only by three amino acid residues (Glu, Leu, Phe in TnI-f; Leu, Val, Met in TnI-s, Gomez *et al.*, 2002). To date there are no reports on the functional significance of these structural differences.

1.4.1.5 Troponin T isoforms

Mammalian skeletal muscle appears to contain a multitude of TnT isoforms (eg. at least 6 fast and 2 slow isoforms have been found in rabbit skeletal muscle, Pette and Staron, 1990). These isoforms are generated from two genes by alternative RNA splicing and various post-translational modifications, and appear to differ structurally with respect to the size and charge of the N-terminal region (Ogut and Jin, 1998). According to current evidence, muscle type and age specific differences with respect to TnT isoforms are related to several aspects of the contractile activation process including Ca^{2+} -sensitivity, the level of activation of ATPase and the degree of co-operativity of the contractile activation process (for review see Gordon *et al.*, 2000).

1.4.1.6 Troponin C isoforms

Mammalian skeletal muscle TnC is known to exist only as two isoforms; one fast (TnC-f) and one slow/cardiac (TnC-s), which are coded for by separate genes, and do not undergo post-transcriptional modifications (Schiaffino and Reggiani, 1996). In terms of functional significance, the most important structural difference between the isoforms occurs in the amino acid sequence of Ca^{2+} -binding site I (insertion of Val-28 in TnC-s sequence which is not present in TnC-f; substitutions of the key ligands for Ca^{2+} -chelating: Asp-28, Asp-30 and Asp-34 of TnC-f for Leu-29, Ala-31 and Cys-34, respectively in TnC-s, Gomez *et al.*, 2002). Consequently, site I of TnC-s is inactive, and only site II is available for regulation. Nuclear magnetic resonance spectroscopy of TnC isoforms in the Ca^{2+} -bound/free states has shown that because of the inactivation of site I, Ca^{2+} binding to site II in TnC-s does not produce a steric movement analogous to that of TnC-f (Sia *et al.*, 1997).

Structural differences between the TnC isoforms have been shown to affect such properties of the contractile apparatus as pH sensitivity of contraction (Metzger, 1996), sarcomere length sensing (Akella *et al.*, 1997) and rigor cross-bridge activated optimal tension (Brandt and Schachat, 1997). Furthermore, there is evidence to suggest that TnC isoforms may play a key role in fibre type differences with respect to the sensitivity to Sr^{2+} of the contractile activation process (eg. Morimoto and Ohtsuki, 1987). Such a role has been challenged, however, by the findings of other laboratories (eg. Kerrick *et al.*, 1980), as discussed in detail in the Introduction to Chapter 6. A close examination of the studies concerned with this issue reveals two kinds of methodological problems that may account for the conflicting data. One kind relates to the inherent shortcomings of the method used for the functional testing of TnC isoforms (ie. TnC extraction/replacement in single muscle fibres; detailed in a review by Moss, 1992), and the other to the effectiveness of the protocols used for the separation, visualisation and identification of TnC isoform bands on SDS gels (discussed below in section 1.4.3.2). The study described in Chapter 6 revisits the issue of the role of TnC isoforms in determining fibre-type differences with respect to the sensitivity to Sr^{2+} of the contractile activation processes using an experimental strategy that avoids the two kinds of problems. This strategy involves (i) the use of a novel method for definitive identification of TnC isoforms in single fibres (described in Chapter 4 and validated using the rat skeletal TnC isoforms purified as described in Chapter 3), and (ii) measurement of the Sr^{2+} -activation characteristics of pure and hybrid fibres that contain different *naturally occurring* combinations of myofibrillar protein isoforms.

1.4.2 Myofibrillar protein isoform composition of MHC isoform based fibre-types

The use of the MHC isoform composition of a fibre as a basis for fibre-typing in studies concerned with the mechanisms of skeletal muscle contraction implies that in a given fibre there is a close relationship between the MHC isoforms expressed and other biochemical and physiological characteristics relevant to the contractile process.

Following this line of argument, one might expect, for example, that fibres expressing one type of MHC isoform would contain only the corresponding type of MLC and regulatory protein isoforms. This appears to be the case for some, but not all, myofibrillar proteins. Thus in rat skeletal muscle, the fast MLC3 isoform has never been reported to be present in type **I** fibres while it and/or the MLC1-f isoform are always detected in type **II** fibres. In contrast, a number of laboratories have frequently reported the presence of both the fast and slow MLC1 and MLC2 isoform types in some pure type **II** fibres (for review see Pette and Staron, 2001). Cases of 'mis-matched' fast/slow MHC and TnC isoform types have also been reported for both pure type **I** and pure type **II** fibres of the adult rat (Danieli-Betto *et al.*, 1990; Geiger *et al.*, 1999). Taken together, these findings suggest that the tightness of the relationship between the types of MHC isoforms and the types of other myofibrillar protein isoforms expressed in a fibre is protein specific. Of course, one cannot exclude the possibility that some of the reported myofibrillar protein mis-matches could be experimental artefacts due to methodological limitations (discussed below). This possibility is supported by the data obtained from the study described in Chapter 5, in which the relationship between the MHC and TnC isoform content in rat single fibres was examined using a method that avoids common methodological pitfalls (described in Chapter 4).

1.4.3 The use of SDS-PAGE for studying myofibrillar protein isoform composition of single fibres

1.4.3.1 Separation of myofibrillar proteins on polyacrylamide gels

SDS-PAGE has proven to be an extremely useful device for studying myofibrillar protein isoforms in various muscle preparations. Moreover, SDS-PAGE analysis of MHC isoform composition in single fibres has become the method of choice for fibre-typing. In this context, it is important to note that due to the nature of SDS-PAGE, which separates proteins based on their molecular size, and to the wide range of sizes of myofibrillar proteins (~200 for MHC and ~16 for MLC3), one cannot use the same gel for analysis of all myofibrillar protein isoforms involved in muscle contraction. This can become a problem when the sample size is very small, as is the case for rat skeletal muscle fibres, particularly in studies where both myofibrillar protein isoform composition analysis and functional testing are carried out on the same single fibre segment. For example, in the study by Kischel *et al.* (2001), the use of immunoblotting for identification of TnC isoforms in rat single fibres precluded electrophoretic analysis of the MHC isoform composition of the same single fibres due to the small sample size.

1.4.3.2 Identification of myofibrillar protein isoforms in single fibres with particular emphasis on TnC

In most studies the identification of myofibrillar proteins separated by SDS-PAGE has been carried out using purified proteins as markers, or by using specific antibodies. However, these options remain unavailable for identification of TnC isoforms in rat skeletal muscles due to the lack of purified rat TnC isoforms. As a result, in studies that

required knowledge of TnC isoform composition in single fibres, the identification of TnC isoforms has been based primarily on their electrophoretic mobility relative to that of other myofibrillar protein isoforms, such as the MLC2 isoforms. However, as illustrated by the examples given in Table 1.1, there is a large inter-study variability with respect to the relative electrophoretic mobilities of TnC and MLC2 isoforms of a given species, which challenges the reliability of this approach. This point is discussed further in Chapter 4, where a novel method that allows definitive identification of TnC isoform bands on SDS gels of single rat fibres is described.

1.5 The aims of this study

As emphasised in this introduction, TnC is a key player in the Ca^{2+} -dependent regulation of skeletal muscle contraction. At the time work on this thesis began it was noted that information regarding the relationship between TnC and MHC isoform composition in rat skeletal muscle fibres was unclear, and that there was a controversy regarding the contribution of TnC isoforms to the inter-fibre type differences with respect to Sr^{2+} -activation of contraction. These cognitive gaps were attributed to limitations associated with the methods used in the relevant studies for identification of TnC isoforms in single fibres. Following this line of reasoning it was hypothesised that if a method was established for unequivocal identification of TnC isoforms in single rat skeletal muscle fibres, which could be used in conjunction with established methods for MHC isoform analysis and for determining Sr^{2+} -activation characteristics, then issues regarding TnC mentioned above could be clarified. In this context, the main aims of this study were as follows:

Table 1.1 Reports of TnC isoform migration in single muscle fibres (or heart trabeculae) relative to MLC2 isoforms

* Non-endogenous TnC. ** After hindlimb unloading.

TnC isoform	Relative migration	Species and fibre source	Reference
<i>Hamster</i>			
fast*	above MLC2s	Syrian hamster trabeculae	Babu, <i>et al.</i> , 1987
fast*	above MLC2s	Syrian hamster trabeculae	Gulati, <i>et al.</i> , 1988
slow	co-migrates with MLC2s		
<i>Rabbit</i>			
fast	below MLC2f	Rabbit psoas	Babu, <i>et al.</i> , 1992
slow*	below MLC2f		
fast	above MLC2f	Rabbit psoas	Swartz, <i>et al.</i> , 1997, Zot & Potter, 1982, Yates & Greaser, 1983, Shiraishi, <i>et al.</i> , 1992.
fast	below MLC2f	Rabbit psoas	Babu, <i>et al.</i> , 1986.
slow*	above MLC2f	Rabbit psoas	Morris, <i>et al.</i> , 2001
fast	above MLC2f	Rabbit psoas	Hannon, <i>et al.</i> , 1993, Moss, <i>et al.</i> , 1986
slow*	above MLC2f		
fast	above MLC2f	Rabbit adductor magnus	Kerrick, <i>et al.</i> , 1985
slow*	above MLC2f		
fast	above MLC2f, below MLC2s	Rabbit (various fast skeletal)	Schachat, <i>et al.</i> , 1985
slow	above MLC2f, below MLC2s	Rabbit (soleus and diaphragm)	
fast	above MLC2f	Rabbit (various fast skeletal)	Morimoto, 1991
slow	below MLC2s	Rabbit soleus	Sweeney, <i>et al.</i> , 1990
<i>Rat</i>			
fast	above MLC2f and MLC2s	Rat diaphragm and psoas	Eddinger & Moss, 1987
fast*	above MLC2s	Rat cardiac	Hoar, <i>et al.</i> , 1988
slow	above MLC2s		
fast**	above MLC2f, below MLC2s	Rat soleus	Kischel, <i>et al.</i> , 2001
slow	below MLC2f		
fast	above MLC2f, below MLC2s	Rat diaphragm	Geiger, <i>et al.</i> , 1999
slow	above MLC2f, below MLC2s		
fast	below MLC2f	Rat diaphragm	Danielli-Betto, <i>et al.</i> 1990.
slow	below MLC2f		

Aim 1. *To establish a method that allows the definitive determination of TnC isoforms in electrophoretically typed (based on MHC isoform composition) single fibre segments, which have undergone testing for contractile activation characteristics. And related to this:*

Aim 2. *To validate the method for TnC isoform determination in rat skeletal muscle fibres using purified rat TnC isoforms.* It is important to note that at the time that this investigation was started, there was no report of rat TnC isoform purification despite rat being a frequently used animal in mammalian muscle studies. This raised the question whether the basic method established by Potter (1982) for purifying rabbit Tn subunits would be applicable to rat skeletal muscle TnC. Therefore the next aim of the study was:

Aim 3. *To purify the rat fast and slow TnC isoforms using predominantly fast (extensor digitorum longus) and slow (soleus) muscles respectively.* Once a reliable method for TnC isoform identification in single fibres was established, it was used:

Aim 4. *To examine the possibility that TnC and MHC isoforms combine according to a defined pattern in non-transforming skeletal muscle fibres of the rat, and*

Aim 5. *To evaluate the contribution made by TnC isoforms to the inter-fibre-type differences with respect to Sr^{2+} -activation in rat skeletal muscle.*

Chapter 2: General methods

Note that unless otherwise stated, all procedures used in the studies described in this thesis were carried out at room temperature (RT; $21\pm 1^\circ\text{C}$).

2.1 Animals and muscles

The animals used in this investigation were male Sprague Dawley rats, aged 13 weeks. The rats were kept in a temperature controlled environment (21°C) with *ad libitum* access to food and water. The extensor digitorum longus (EDL), soleus (SOL), sternomastoid (SM) or diaphragm (DPH) muscles were dissected as required immediately after killing the animal by deep halothane inhalation in accordance with the permits granted by the Animal Ethics Committee at Victoria University. Muscles to be used for TnC purification (EDL and SOL) were immediately stored at -20°C until required (see Chapter 3). Muscles used for preparing single fibres (SOL, SM or DPH, see Chapters 4, 5 and 6) were blotted on filter paper, then immediately pinned in a Petri dish, on a Sylgard 184 base (Dow Corning, USA) under paraffin oil (AJAX).

2.2 Preparation of mechanically skinned single fibres

All operations described in this section were carried out at RT, under paraffin oil. The single muscle fibres used in the study concerned with the development of a TnC isoform identification protocol (Chapter 4), the study concerned with the relationship between MHC and TnC isoform composition in rat skeletal muscle (Chapter 5), and the study concerned with the role of TnC isoforms in Sr^{2+} -activation differences between different fibre types (Chapter 6) were mechanically skinned. The fibres, randomly isolated from

the muscle, were mechanically skinned with a pair of fine jewellers forceps (Inox no. 5, Switzerland) with the aid of a dissecting microscope (Olympus, magnification range 6.4-40, Japan) attached to a video monitor set up and a fibre optic light source (Euromex, Holland). The volume of each skinned fibre segment, assumed to be cylindrical, was determined using the width (mean of five values) and length of the segment. The dimensions of the fibre segment were measured on the video monitor using a pair of precision calipers (Mitutoyo, Japan). The volume of the fibre segment was calculated according to the following equation:

$$V = d^2 \times L \times \pi / 4 \times (136.5)^2 \times (23.25) \quad (\text{Eq. 2.1})$$

where V is the volume of the fibre segment in picolitres, d and L are the average diameter and length of the fibre segment measured in millimeters on the video screen, and the values $(136.5)^2$ and (23.25) are magnification conversion factors for the diameter and length measurements respectively.

Fibres subjected to both isometric force measurements and MHC and TnC isoform analyses were first mounted on the force measurement apparatus as described in Chapter 6, and then following the force experiments, were placed into a small volume (1 μ l per 4 nl fibre segment) of SDS-PAGE solubilisation buffer (see section 2.3 for composition). Fibres which were used exclusively for SDS-PAGE analysis of MHC and TnC isoform composition (in Chapters 4 and 5) were first incubated for 2 min in a solution of similar composition to the Ca^{2+} *Maximally Activating Solution*, (see Chapter 6, page 93), but without the ATP and creatine phosphate, prior to being placed into SDS-PAGE solubilisation buffer (1 μ l of per 4 nl fibre segment volume). The aqueous, high $[Ca^{2+}]$.

rigor solution was intended to remove the diffusible Ca^{2+} -binding proteins which could interfere with the detection of TnC, with minimum loss of TnC, and to maximise the difference in $[\text{Ca}^{2+}]$ between the sample well and the adjacent EGTA well in the TnC isoform identification protocol (see Chapter 4 for a full description of the protocol). However, a series of control experiments carried out prior to the study described in Chapter 6 showed no obvious difference (either in intensity or in migration) between the TnC bands in fibres not incubated (Fig. 2.1, lanes 1 and 2) and fibres incubated (Fig. 2.1, lanes 3 and 4) in the high $[\text{Ca}^{2+}]$ rigor solution. Therefore this solution was not used further in the study described in Chapter 6.

2.3 Composition of SDS-PAGE solubilisation buffer and electrophoretic apparatus

For all electrophoretic analyses performed in this thesis, including Alanine-SDS-PAGE analysis of single muscle fibres for MHC isoforms (required in Chapters 5 and 6), Glycine-SDS-PAGE analyses of single muscle fibres for TnC isoforms (required in Chapters 4, 5 and 6) and for other low molecular weight protein isoforms (required in Chapter 6) or for analyses of chromatographic fractions and tryptic digests (required in Chapter 3), the samples were solubilised in a buffer containing 80 mM Tris-HCl, pH 6.8, 2.3% w/v SDS, 5% w/v β -mercaptoethanol, 10 mM DTT, 12.5% v/v glycerol, 13.6% w/v sucrose, 0.01% w/v bromophenyl blue, 0.1 mM PMSF, 0.002 mM leupeptin and 0.001 mM pepstatin. All gels were run using the Hoefer Mighty Small electrophoresis equipment (see Fig. 2.2).

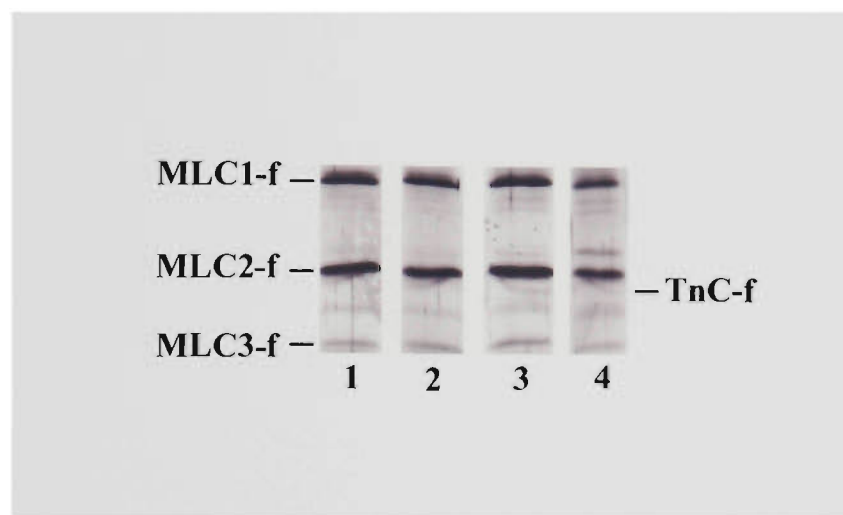


Fig. 2.1. A comparison of TnC bands in skinned single fibres not incubated (lanes 1 and 2) and incubated (lanes 3 and 4) for two min in an aqueous, high Ca²⁺, rigor solution prior to solubilisation in SDS-PAGE solubilising buffer. All fibres were pure fast fibres from the SM. The TnC-f isoform band in each lane can be identified by its upward curve as described in Chapter 4. Note that incubation of the fibre in the aqueous solution affected neither the intensity nor the migration of the TnC band.

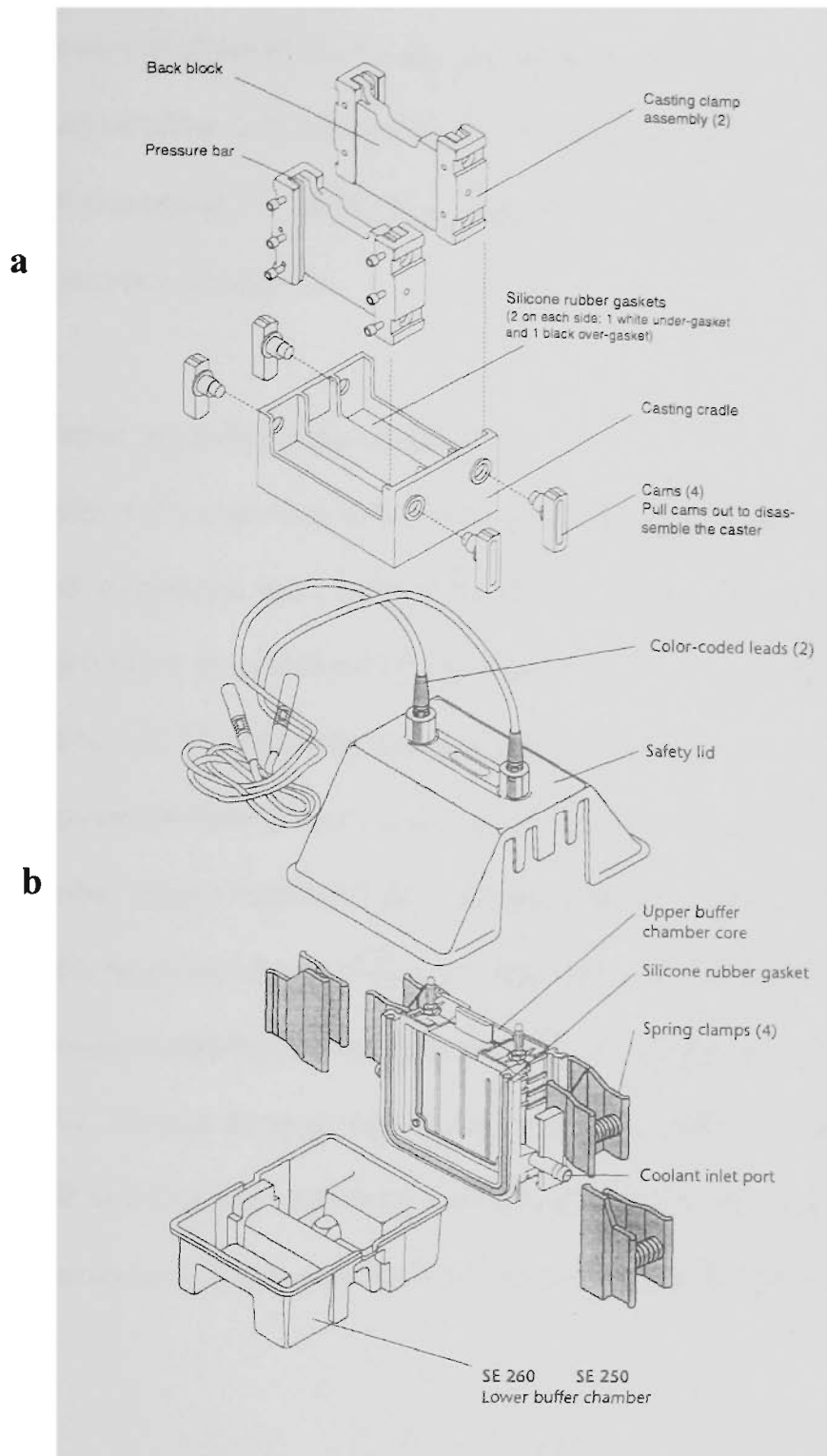


Fig. 2.2. Electrophoresis equipment. (modified from Hoefer Gel Electrophoresis Unit Instructions). (a) Hoefer SE 235 multiple gel caster. (b) Hoefer SE 260 electrophoresis setup.

2.4 Glycine-SDS-PAGE

All electrophoretic analyses of low molecular weight (< ~45 kDa) myofibrillar proteins were performed on either 16% PA glycine gels for single muscle fibres (see Chapters 4, 5 and 6) and chromatography fractions (see Chapter 3) or 18% PA Glycine gels for peptide mapping analysis (see Chapter 3).

2.4.1 Preparation of glycine separating gels

The components of the separating gels were added to a conical flask in the order listed in Table 2.1. Each component was swirled fully into solution before adding the next. Immediately following the addition of the polymerisation initiators (ammonium persulfate and N,N,N',N'-tetramethylethylenediamine; TEMED), the separating gel solution was poured between two 10 x 10.5 cm glass plates separated by 0.75 mm spacers (clamped together using a Hoefer SE 235 multiple gel caster, see Fig. 2.2a) to a height of 7.5 cm. The setting gel was then covered by a thin layer (~0.5 cm) of Milli-Q water to minimise exposure to atmospheric oxygen, an inhibitor of polymerisation (Hepworth, *et al.*, 1999). After ~10 min the space between the plates was filled up to the top with the Glycine-SDS-PAGE running buffer (see section 2.4.3) to minimise diffusion induced losses of gel components (such as SDS) to the covering solution. The gel was left to set at RT overnight.

Table 2.1. Composition of Glycine SDS-PA separating gels.

Chemical Stock Solution	16% Gels		18% Gels	
	Volume (ml)	Final Concentration	Volume (ml)	Final Concentration
T=36%, C=2.6% Acrylamide-Bis Acrylamide	5.340	T=16%, C=2.6%	6.000	T=18%, C=2.6%
3M Tris-HCl, pH 9.3	3.000	0.75M	3.000	0.75 M
Milli-Q Water	2.278	n/a	1.618	n/a
Glycerol	1.200	10% v/v	1.200	10% v/v
10% w/v SDS	0.120	0.1% w/v	0.120	0.1% w/v
10% w/v Ammonium persulfate	0.048	0.04% w/v	0.048	0.04% w/v
T.E.M.E.D.	0.014	0.116% v/v	0.014	0.116% w/v
TOTAL	12.000		12.000	

2.4.2 Preparation of glycine stacking gels

After the separating gel had set, the running buffer was removed and replaced with the stacking gel solution (comprising the chemicals listed in Table 2.2), which was prepared as described above for the separating gel. Immediately after pouring the gel solution, a 15-pronged comb was inserted to form the sample loading wells. The stacking gel was allowed to set for 25 minutes, after which the comb was removed. Strips of filter paper were used to absorb any unpolymerised acrylamide left in the wells, which were then filled with the Glycine-SDS-PAGE running buffer (see section 2.4.3).

Table 2.2. Composition of Glycine SDS-PA stacking gels.

Chemical Stock Solution	16% Gels	
	Volume (ml)	Final Concentration
T=10%, C=4.76% Acrylamide-Bis Acrylamide	2.400	T=4%, C=4.76%
0.5M Tris-HCl, pH 9.3	1.500	0.125M
Milli-Q Water	1.374	n/a
Glycerol	6.000	10% v/v
10% w/v SDS	0.060	0.1% w/v
10% w/v Ammonium persulfate	0.060	0.1% w/v
T.E.M.E.D.	0.006	0.1% v/v
TOTAL	6.000	

2.4.3 Preparation of Glycine-SDS-PAGE running buffer

The running buffer used for Glycine-SDS-PAGE (0.4 L per electrophoretic set up) contained 50 mM Tris, 380 mM Glycine and 0.1% w/v SDS, freshly prepared from a 5 x concentrated stock solution containing 0.25 M Tris (no pH adjustment), 1.9 M Glycine and 0.5% SDS.

2.4.4 Electrophoresis of glycine gels

Each pair of gels was clamped to a Hoefer SE 260 electrophoresis setup (see Fig. 2.2b) forming upper and lower buffer chambers, both of which were filled with the running buffer (described in section 2.4.3). Samples (up to 15 μ l) were applied to the wells using a 20 μ l pipette and electrophoretic gel loading tips. After sample application, the electrophoresis unit was connected to a power supply. Electrophoresis was carried out at RT with a constant current of 10 mA per gel (ie. 20 mA per set up) for 4.25 hours, during which the voltage typically increased from 90-100 V to 200-210 V. Once the electrophoresis was complete, the gels were immediately removed from the electrophoresis setup and placed in 250 ml of a fixing solution containing 40% ethanol and 10% acetic acid. The gels were agitated on an automatic rocker for at least 15 min, and then left overnight at RT before being stained with silver the following day (see section 2.4.5).

2.4.5 Silver staining of glycine gels using the Hoefer protocol

The silver staining procedure used for glycine gels was the Hoefer protocol outlined in the flowchart shown in Fig. 2.3. The gels were taken from the fixing solution and placed

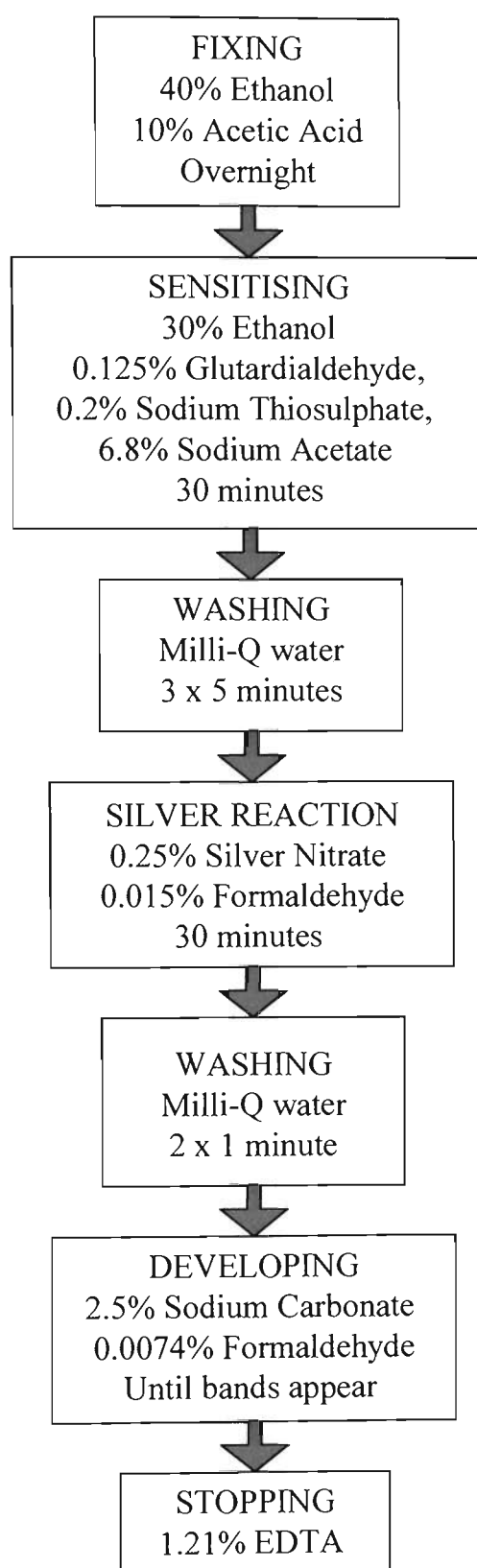


Fig. 2.3. Flowchart of Hoefer silver staining procedure used for glycine PA gels.

into 250 ml of a sensitising solution (30% v/v ethanol, 0.125% w/v glutaraldehyde, 0.2% w/v sodium thiosulphate, 6.8% w/v sodium acetate) in which they were shaken on the automatic rocker for 30 minutes. Following the sensitising step, the gels underwent three 5 minute washes in 250 ml Milli-Q water, after which they were shaken for 20 minutes in 250 ml of a silver reaction solution containing 0.25% w/v silver nitrate and 0.015% w/v formaldehyde. The gels were then washed twice for 1 minute in 250 ml Milli-Q water before being placed in a developing solution (2.5% w/v sodium carbonate and 0.0074% w/v formaldehyde) until the protein bands began to appear. Once the bands were sufficiently resolved from the background, the gels were transferred to the stopping solution (1.21% w/v EDTA), where they remained for up to a week before being scanned as described in section 2.6.

2.5 Alanine-SDS-PAGE

Alanine-SDS-PAGE was employed for all analyses of MHC isoforms in single fibres (see Chapters 5 and 6).

2.5.1 Preparation of alanine separating gels

The alanine separating gels were prepared exactly as described for glycine gels in section 2.4.1, except that the gel components used were those listed in Table 2.3, and the gels were covered with Alanine-SDS-PAGE running buffer (see section 2.5.3) and left to set (RT) for 4 hours prior to the addition of the stacking gel (see section 2.5.2).

Table 2.3. Composition of Alanine SDS-PA separating gels.

Chemical Stock Solution	Volume (ml)	Final Concentration
T=30%, C=1.2% Acrylamide-Bis Acrylamide	3.040	T=7.6%, C=1.2%
3M Tris-HCl, pH 8.8	1.700	425mM
1M L-Alanine	0.900	4mM
Milli-Q Water	2.331	n/a
Glycerol	3.600	30% v/v
10% w/v SDS	0.360	0.3% w/v
10% w/v Ammonium persulfate	0.060	0.05% w/v
T.E.M.E.D.	0.009	0.075% v/v
TOTAL	12.000	

2.5.2 Preparation of alanine stacking gels

The alanine stacking gels were prepared exactly as described for glycine stacking gels (see section 2.4.2), except that (i) the chemical composition of the gel was that shown in Table 2.4, (ii) the gel was allowed to set for 60 minutes, and (iii) the cleaned electrophoretic wells were covered with Alanine-SDS-PAGE running buffer (see section 2.5.3).

Table 2.4. Composition of Alanine SDS-PA stacking gels.

Chemical Stock Solution	Volume (ml)	Final Concentration
T=30%, C=2.6% Acrylamide-Bis Acrylamide	0.800	T=4%, C=2.6%
0.5M Tris-HCl, pH 6.8	1.500	0.125M
80mM EDTA	0.300	4mM
Milli-Q Water	0.757	n/a
Glycerol	2.400	40% v/v
10% w/v SDS	0.180	0.3% w/v
10% w/v Ammonium persulfate	0.060	0.1% w/v
T.E.M.E.D.	0.003	0.05% v/v
TOTAL	6.000	

2.5.3 Preparation of Alanine-SDS-PAGE running buffer

The running buffer used for Alanine-SDS-PAGE (0.4 L per set up) contained 25 mM Tris, 175 mM Alanine and 0.1% w/v SDS. The buffer was freshly prepared on the morning of electrophoresis and kept at 4°C until required.

2.5.4 Electrophoresis of alanine gels

Electrophoresis was carried out for 28 hours at 4°C with a constant voltage of 150 V, during which the current typically ranged from ~30 mA at the start of the electrophoresis to ~4 mA at the end. Once the electrophoresis was complete, the gels were immediately removed from the electrophoresis set up and placed in 250 ml of a fixing solution containing 50% methanol, 10% acetic acid and 5% glycerol. The gels were agitated on an automatic rocker for at least 15 min, and then left overnight at RT before being stained with silver the following day (see section 2.5.5).

2.5.5 Silver staining of alanine gels using the Bio-Rad protocol

The Bio-Rad silver staining procedure used for alanine gels, outlined by the flowchart shown in Fig. 2.4, was carried out as follows. The gels were taken from the fixing solution and washed twice (with shaking) for 10 minutes in ~200 ml Milli-Q water. While the second wash was being performed, the Silver/Development Solution for the next staining step was prepared as follows; to 35 ml of Milli-Q water was sequentially added (i) 5 ml of silver complexing solution (5% w/v sodium carbonate), (ii) 5 ml of reduction modifying solution (10% w/v tungstosilicic acid), (iii) 5 ml of image development solution (2.8% w/v formaldehyde), then (iv) 50 ml of development accelerating solution (5% w/v sodium carbonate). Upon completion of the second wash,

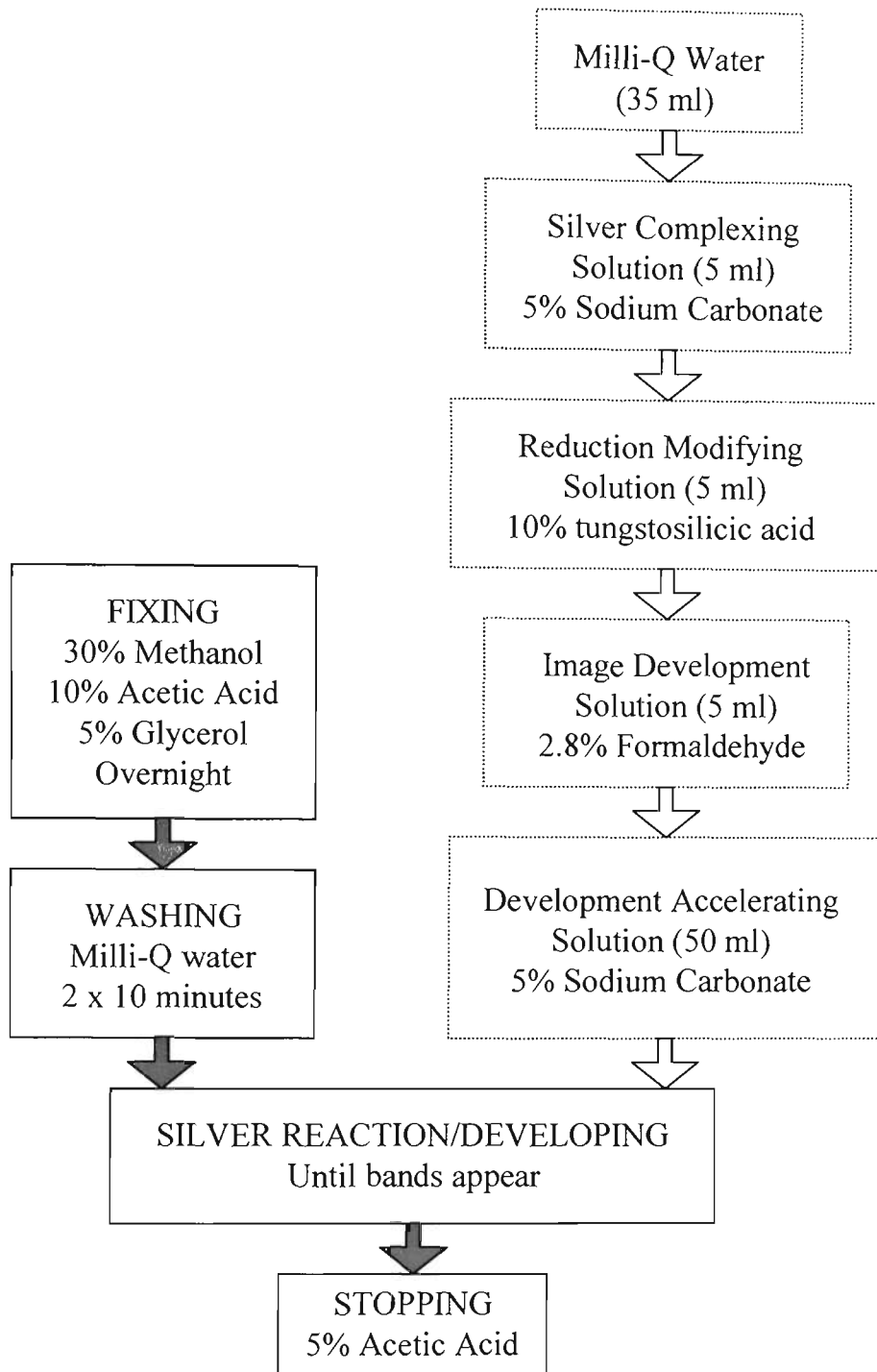


Fig. 2.4. Flowchart of Bio-Rad silver staining procedure used for alanine PA gels. The dashed boxes and open arrows indicate the order in which the respective components are added when preparing the Silver Reaction/Developing solution.

the Milli-Q water was replaced with the freshly prepared Silver/Development Solution in which the gels were gently shaken for ~15-20 minutes until the bands appeared. Once the bands were deemed to be sufficiently resolved from the background, the gels were placed in a stopping solution of 5% acetic acid where they remained for up to a week before being scanned as described in section 2.6.

2.6 Scanning and densitometry of SDS gels

The gels were scanned with a Molecular Dynamics Personal Densitometer using ImageQuant software (version 5.2) set to a 12 bit, 100 micron pixel resolution. Whenever required, densitometry was performed on protein bands providing that they were sufficiently well resolved from neighbouring bands such that an *object average background correction* could successfully be applied using the ImageQuant software. In such cases, equally sized boxes were drawn around each of the protein bands to be analysed (*band boxes*), as well as an area of the gel that contained only gel background (*background box*). For each box, the degree of darkness of every pixel was calculated, added together and the average taken. The average optical density for each band was calculated by subtracting the average pixel darkness of the *background box* from the average pixel darkness of the *band box*.

Chapter 3: Purification of fast and slow TnC isoforms from EDL and Soleus muscles of the rat

3.1 Introduction

As stated in Chapter 1 (see page 21), mammalian skeletal muscle TnC exists as two types; TnC-f and TnC-s. To date, these isoforms have been purified from a diverse range of species including rabbit TnC-f (Collins *et al.*, 1977) and TnC-s (Wilkinson, 1980), cow TnC-s (Van Eerd and Takahashi, 1976), African lizard and python TnC-f (Demaille *et al.*, 1974), dogfish TnC-f (Malencik *et al.*, 1975), human TnC-f (Romero-Herrera *et al.*, 1976) and chicken TnC-f (Wilkinson, 1976). Notably, there has been no report of rat TnC isoform purification, despite the rat being an animal commonly used in physiological studies of mammalian muscle contractility. Purified rat TnC isoforms would be of obvious benefit in functional studies of TnC using rat skeletal muscle and the TnC extraction/replacement strategy (eg. Kishel *et al.*, 2000). Furthermore, the purified proteins are essential for the production of specific rat anti-fast and anti-slow TnC antibodies, which would be of great benefit in studies aiming to unequivocally identify and quantify TnC isoforms in whole muscle or single fibre preparations (eg. Kishel *et al.*, 2001; Stevens *et al.*, 2002).

This study was concerned with the purification of the fast and slow TnC isoforms of rat skeletal muscle using EDL, a predominantly fast-twitch muscle and SOL, a predominantly slow-twitch muscle, respectively.

The identities of the purified TnC proteins were established using proteolytic peptide mapping, a method that has proven to be both widely accessible (compared with amino acid sequencing) and reliable for identifying or 'fingerprinting' proteins (Cleveland *et al.*, 1977). The proteolytic enzyme used was trypsin, which cleaves proteins specifically at Arg and Lys residues. As shown by Grabarek (Grabarek *et al.*, 1981), the extent of tryptic digestion of rabbit TnC-f isoform (which contains 7 Arg and 9 Lys residues) is affected by the presence/absence of Ca^{2+} . In the presence of Ca^{2+} , the TnC molecule takes a conformation which exposes one of the Arg and two of the Lys residues to tryptic attack, causing the protein to split into three main peptides, which do not cleave further. In the absence of Ca^{2+} /presence of EDTA, the tryptic digestion of TnC is far more rapid and produces a different peptide pattern as the splitting takes place at residues that are presumably inaccessible to trypsin when TnC is in the Ca^{2+} -bound conformation (Grabarek *et al.*, 1981).

The identification of the rat TnC isoforms purified in this study involved the comparison of their tryptic peptide maps with those of two commercially purified reference proteins, the rabbit TnC-f and the human TnC-s (from cardiac muscle) isoforms. The use of these proteins as references was based on compelling evidence that the amino acid sequences of TnC isoforms are remarkably well conserved between species (eg. rabbit TnC-f and human TnC-f differ by one amino acid residue, Pro in human and Ala in rabbit Gomez *et al.*, 2002).

3.2 Materials and methods

3.2.1 Muscle and proteins

The EDL and SOL muscles from ~30 male Sprague Dawley rats (aged 13 weeks) were collected over a period of ~5 months as described in Chapter 2, and stored at -20°C until further processed. TnC from rabbit skeletal muscle (rabbit TnC-f) was obtained from TriChem Resources, Inc. (PA, USA) and TnC from human cardiac muscle (human TnC-s) from Life Diagnostics, Inc (PA, USA). Molecular weight standards, bovine serum albumin (BSA) and CaM were purchased from Sigma (MO, USA).

3.2.2 Preparation of crude skeletal muscle troponin extract

Troponin was prepared from EDL muscles (5-6 g wet weight) and SOL muscles (5-6 g wet weight) essentially according to the method for fast skeletal muscle described by Potter (Potter, 1982), with slight modifications. The entire process, which took five days, is outlined in the flowchart in Figs. 3.1.1-3.1.4 and detailed below. Except where stated otherwise, the operations described below were performed at 4°C , and all centrifugations were done in a Hettich Universal 32R refrigerated centrifuge.

3.2.3 Preparation of skeletal muscle ether powder

Small portions of frozen muscle were removed from storage in the freezer and diced at RT with a scalpel into cubes roughly $1\text{-}2\text{ mm}^3$, which were returned to the freezer as soon as possible (having spent no more than 1 minute at RT). Once 5-6 g of chopped muscle was acquired, it was equally divided into 10 ml centrifuge tubes and suspended in 5 volumes of a chilled wash solution containing 1% Triton X-100, 50 mM KCl and 5 mM

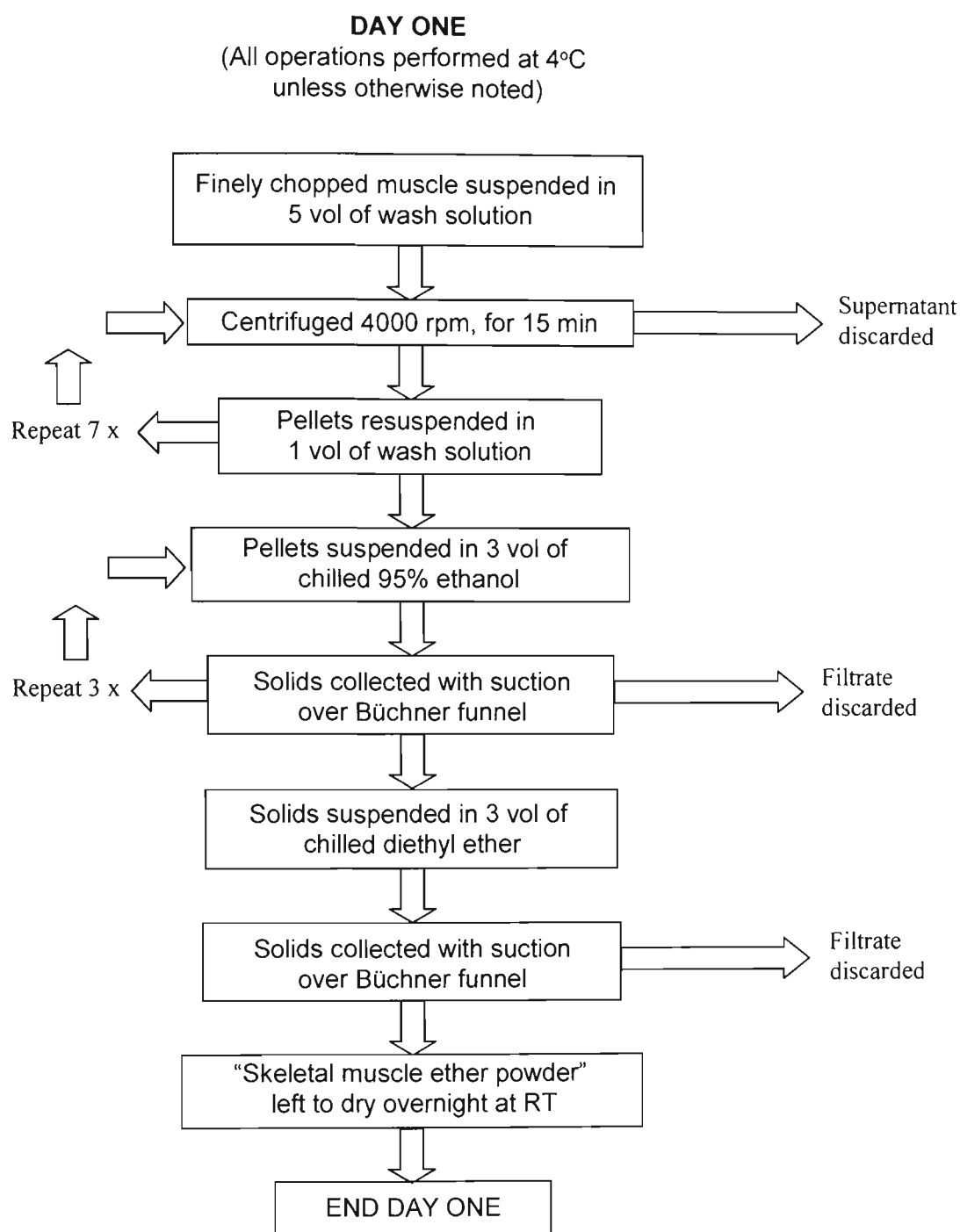


Fig. 3.1.1. Flowchart of steps in protocol for purification of TnC from rat skeletal muscle, day one. Modified from: Potter, J.D. (1982). Preparation of troponin and its subunits *Methods in Enzymology* **85**, 241-263.

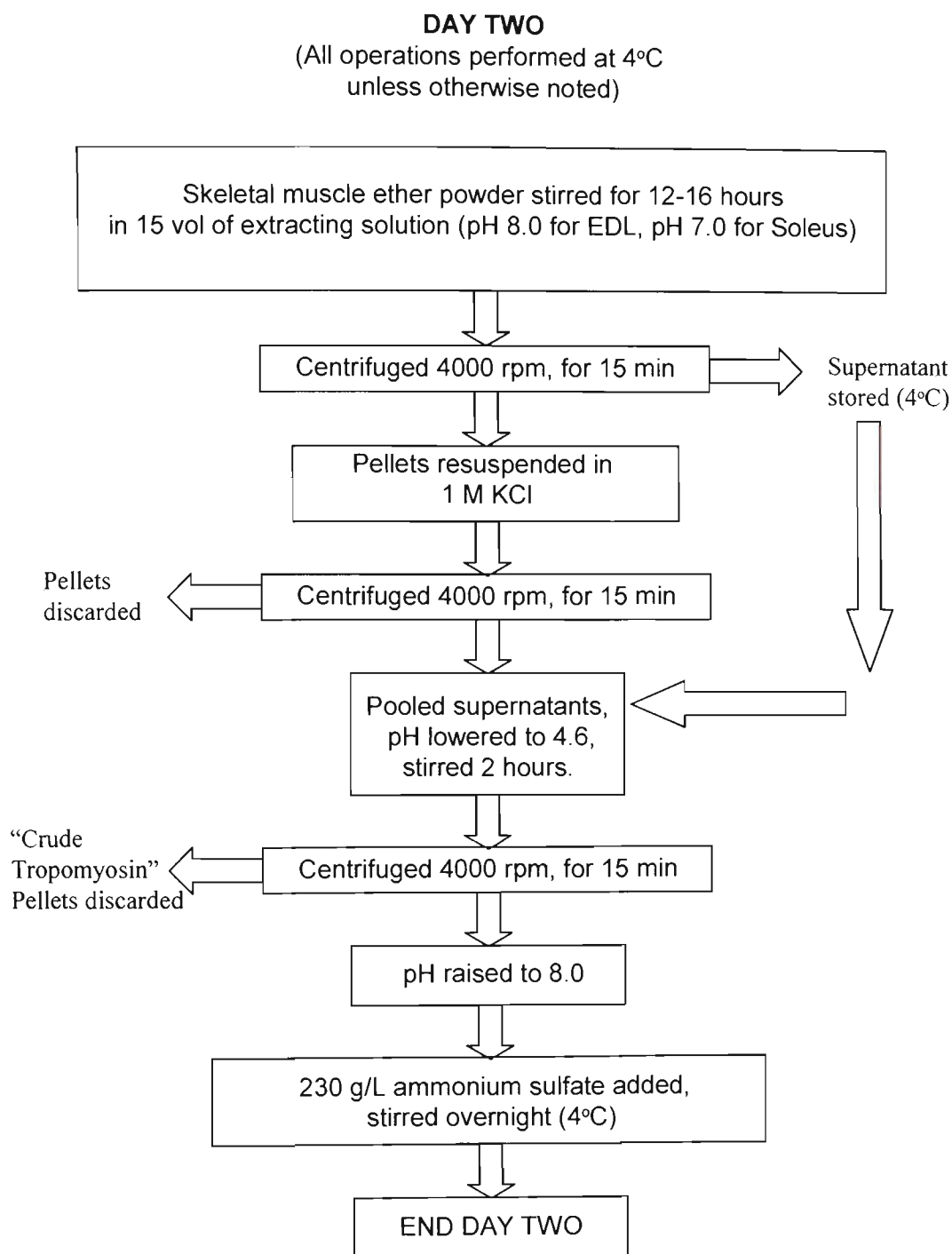


Fig. 3.1.2. Flowchart of steps in protocol for purification of TnC from rat skeletal muscle, day two. Modified from: Potter, J.D. (1982). Preparation of troponin and its subunits *Methods in Enzymology* **85**, 241-263.

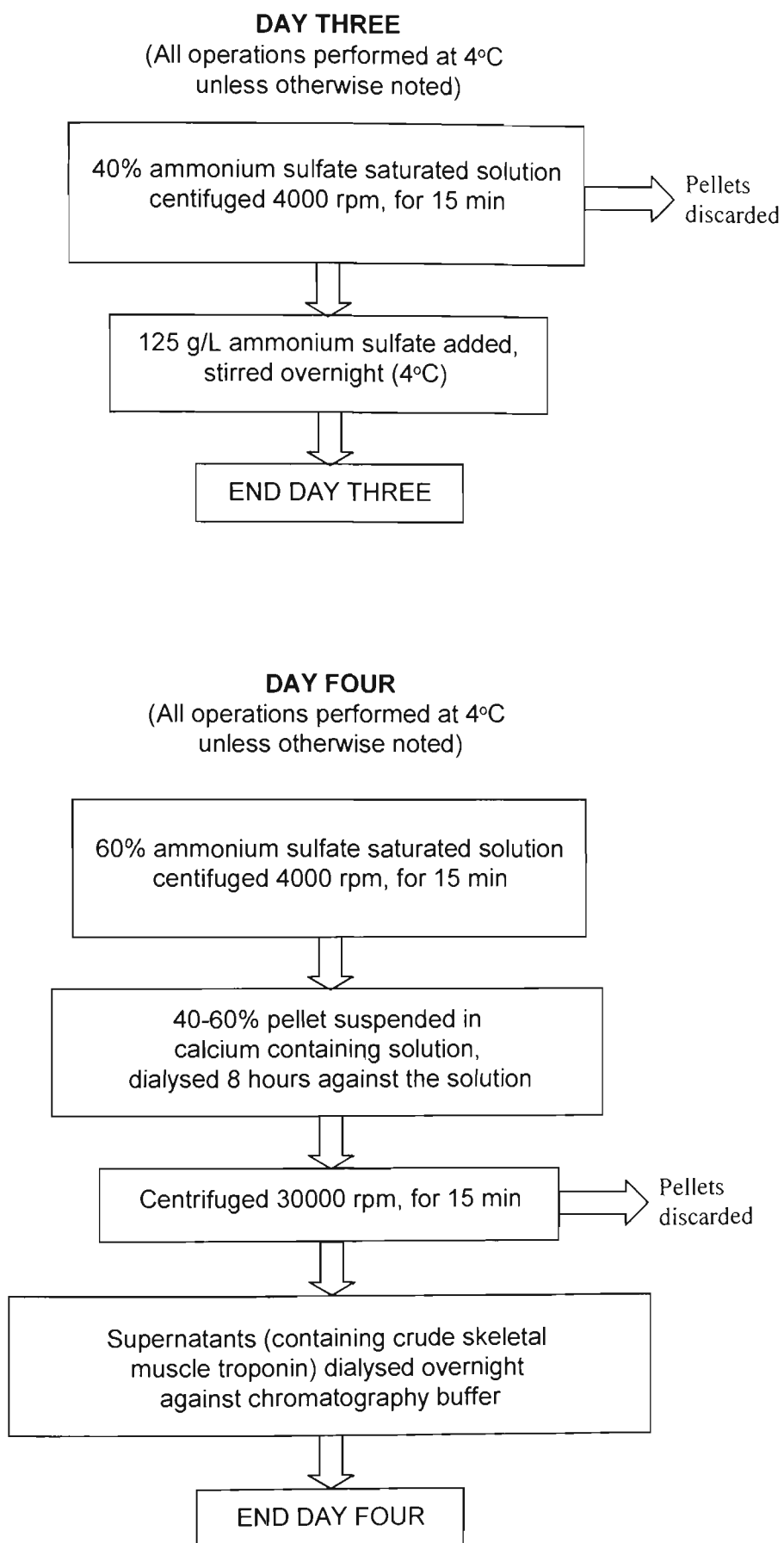


Fig. 3.1.3. Flowchart of steps in protocol for purification of TnC from rat skeletal muscle, days three and four.

Modified from: Potter, J.D. (1982). Preparation of troponin and its subunits *Methods in Enzymology* **85**, 241-263.

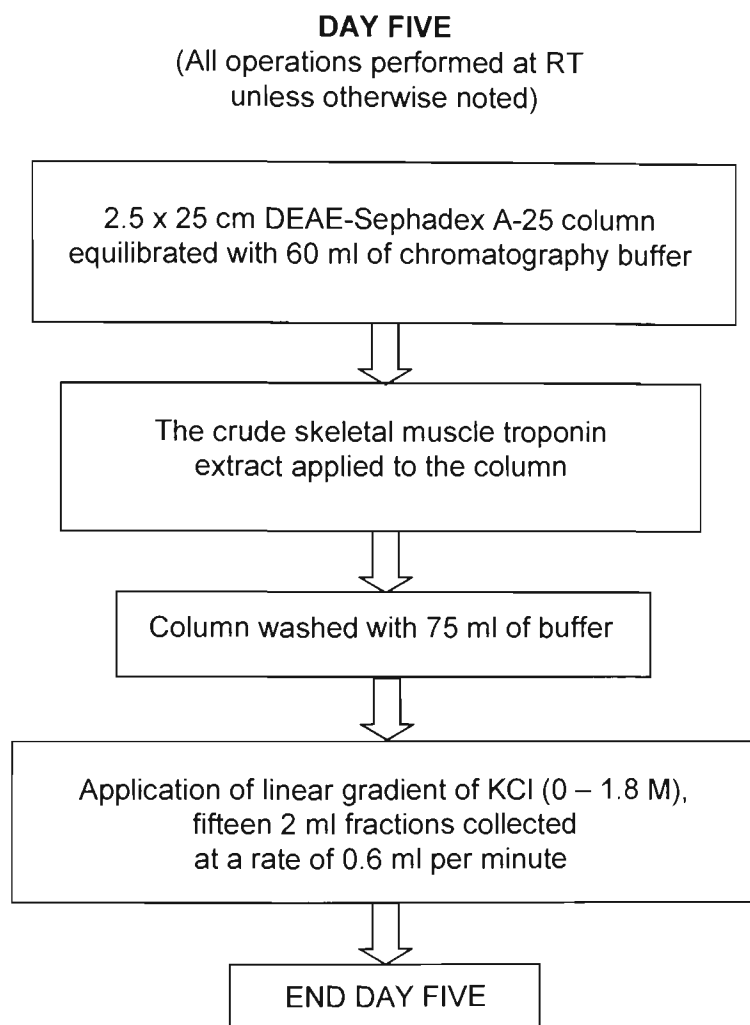


Fig. 3.1.4. Flowchart of steps in protocol for purification of TnC from rat skeletal muscle, day five. Modified from: Potter, J.D. (1982). Preparation of troponin and its subunits *Methods in Enzymology* **85**, 241-263.

Tris, pH 8.0 in order to break open the muscle membrane systems and remove soluble proteases (Potter, 1982). After the chopped tissue was suspended in the wash solution, the tubes were centrifuged at 4000 rpm for 15 minutes. The pinky-red supernatant was discarded, and the pellets were resuspended in 1 volume of the washing solution and centrifuged as described above. This washing process was repeated a further six times in this way (for a total of eight washes), until the supernatant had become almost colourless and pellets were a dull tan. The washed pellets were then suspended in a beaker containing three volumes of pre-chilled 95% ethanol and collected with suction over a Büchner funnel three times, then once again using diethyl-ether instead of ethanol. After the ether wash, the resulting *skeletal muscle ether powder* was left to dry at RT overnight before being weighed.

3.2.4 Extraction of myofibrillar proteins from skeletal muscle ether powder

The ether powder from the EDL muscle (~2.1 g) or the SOL muscle (~1.4 g) was placed in a beaker and stirred for 12-16 hours in 15 volumes of an extracting solution containing 1 M KCl, 25 mM Tris, 0.1 mM CaCl₂ and 0.1 mM DTT, pH 8.0 for EDL, or pH 7.0 for SOL, as recommended by Hartner *et al.* (1989), to increase the yield of slow troponin.

The ether powder extract was then centrifuged at 4000 rpm for 15 minutes. The supernatants were collected and stored in a beaker at 4°C while the pellets were re-suspended in 7 volumes of 1M KCl, then immediately centrifuged as above. The supernatants from this centrifugation were pooled with the previous, and the pellets were discarded.

3.2.5 Removal of tropomyosin by isoelectric precipitation

The combined supernatants were maintained at 4°C on ice as the pH (which measured 7.9 for the EDL extract, and 6.9 for the SOL extract) was gradually lowered to 4.6 by the drop-wise addition of HCl (0.4 M). The solution was stirred gently for 2 hours to allow the precipitation of tropomyosin before being centrifuged (4000 rpm for 15 minutes). The *crude tropomyosin* pellets were discarded, and the pH of the supernatant was adjusted to 8.0 by the addition of KOH.

3.2.6 Ammonium sulfate fractionation

Following the pH adjustment, the volume of the solution was measured. The solution was then brought to 40% saturation with 230 g/L ammonium sulfate, which was slowly added to the gently stirring solution while maintaining the pH between 7.6 and 8.0 with KOH. The solution was stirred overnight at 4°C and centrifuged (4000 rpm for 15 minutes) the next day. The pellets were discarded and the supernatants retained. The supernatant volume was measured before being brought to 60% ammonium sulfate saturation with 125 g/L ammonium sulfate, which was added slowly to the gently stirring solution, whilst ensuring the pH remained between 7.6 and 8.0 with KOH. After being left to stir overnight, the solution was centrifuged (4000 rpm for 15 minutes) and supernatant discarded. The remaining 40-60% pellets containing *crude skeletal muscle troponin* were suspended in 1 ml of a solution containing 0.2 mM Tris, 0.1 mM CaCl₂, pH 8.0.

3.2.7 Preparation of crude skeletal muscle troponin extract for ion exchange chromatography

The crude skeletal muscle troponin suspension was placed in a dialysis tube (Membrane Filtration Products, Inc, Nominal molecular weight cut off 6000-8000) and dialysed for 8 hours against 1 x 200 ml of a solution containing 0.2 mM Tris, 0.1 mM CaCl₂, pH 8.0. After dialysis, the solution was spun at high speed (30000 rpm) for 15 min at 4°C in a Beckman Optima TLX refrigerated ultracentrifuge. The pellets, which consisted of insoluble material that was not suitable for passing through the chromatographic column, were discarded. The supernatants, containing a *crude skeletal muscle troponin extract*, were returned to a dialysis tube and dialysed for 8 hours against 3 x 200 ml of the chromatography buffer (6 M Urea, 50 mM Tris, 1 mM EDTA and 0.1 mM DTT, pH 8.0) in preparation for application to the column (see section 3.2.8).

3.2.8 Isolation of skeletal muscle TnC by ion exchange chromatography

The following steps were performed at RT unless otherwise stated. A 2.5 x 25 cm DEAE-Sephadex A-25 column was equilibrated with at least 60 ml of the chromatography buffer containing 6 M urea, 50 mM Tris, 1 mM EDTA and 0.1 mM DTT (pH 8.0). The crude skeletal muscle troponin extract was applied to the column, which was then immediately washed with 75 ml of buffer before being eluted with a linear gradient of KCl (0 – 1.8 M). Fifteen 2 ml fractions were collected at a rate of 0.6 ml per minute and dialyzed overnight (4°C) against 1 L of 10 mM imidazole, 50 mM NaCl and 0.02% NaN₃ (pH 8.0) before being analysed for proteins by Glycine-SDS-PAGE (see section 3.2.9).

3.2.9 Analysis of chromatographic fractions by SDS-PAGE

A 50 μl aliquot of each fraction was added to an equal volume of solubilising buffer (see section 3.2 for composition), and left to stand at RT overnight before being boiled for 3 minutes the following day. The samples were electrophoresed on 16% PA glycine gels as described in Chapter 2.

3.2.10 Determination of TnC concentration in chromatographic fractions

The protein concentration in the chromatographic fractions was under the detection limit of the conventional Bio-Rad method ($1\mu\text{g}/\text{ml}$). To overcome this problem, the TnC isoform concentrations in the chromatographic fractions were determined using standard curves of commercial TnC isoforms and scanning densitometry. This method was validated using the following strategy. Firstly, the optical densities (ODs) of protein bands on silver-stained 16% PA gels of samples containing known concentrations of BSA were used to construct standard curves for the range of 0-3 $\mu\text{g}/\mu\text{l}$ (see example graph shown in Fig. 3.2a). These standard curves were then used to measure the protein concentrations of the commercial TnC preparations (rabbit TnC-f and human TnC-s). After finding that these values were in agreement with those given by the manufacturers (based upon the Bio-Rad Protein Assay, also using BSA as a standard), standard curves were constructed, using the commercial rabbit TnC-f and human TnC-s preparations (range 0-0.08 $\mu\text{g}/\mu\text{l}$ protein; see Figs. 3.2b and 3.2c), to determine the protein concentration in each of the chromatographic fractions from the EDL and SOL muscles respectively (using an average OD values obtained from three different sample lanes).

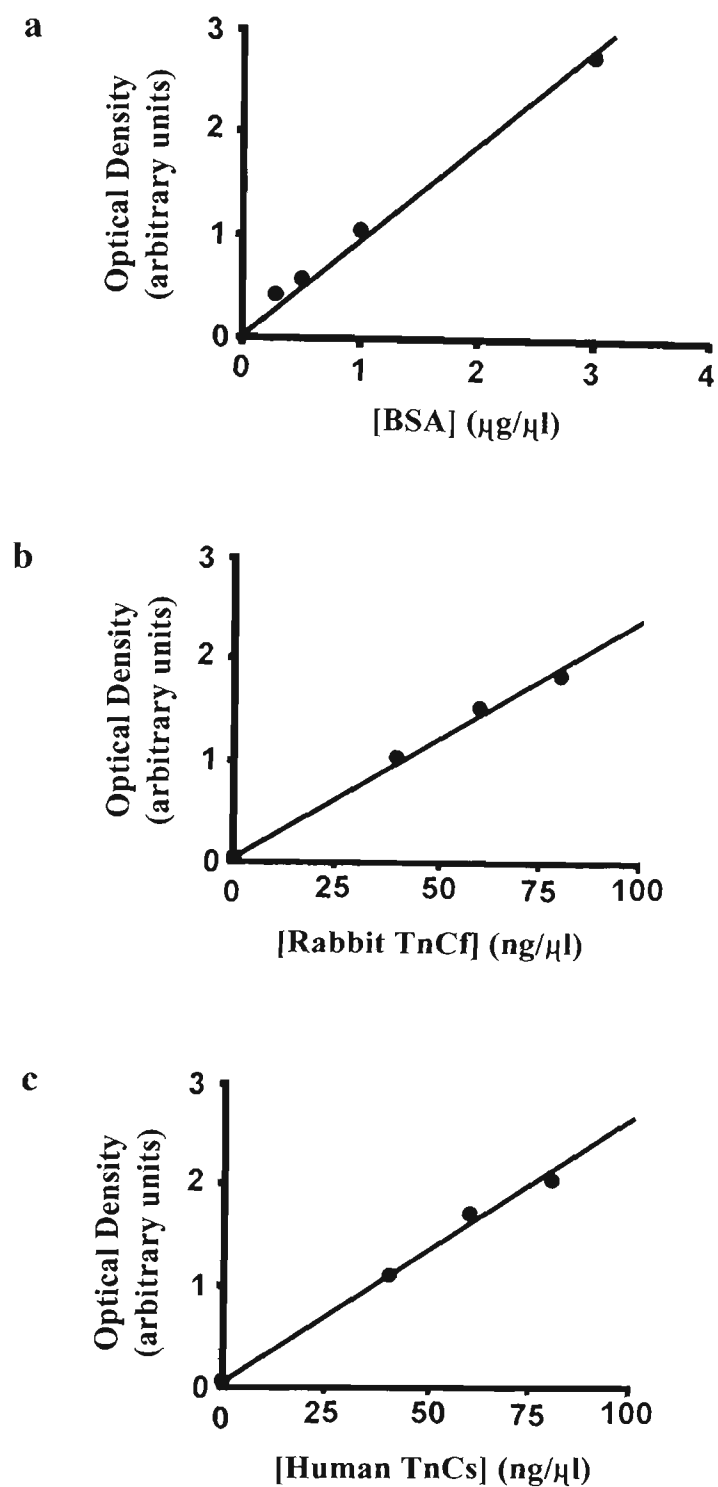


Fig. 3.2. Standard curves used to determine the amount of rat TnC in each chromatographic fraction based upon relative optical density of the silver stained bands of known concentrations of proteins resolved on 16% PA gels.

3.2.11 Tryptic digestion of commercial TnC isoforms

The procedure used for limited digestion of commercial TnC with trypsin, based on the study by Grabarek *et al.* (1981), was carried out as follows. Ten micrograms of rabbit TnC-f or human TnC-s was incubated in 70 μ l of a solution containing 100 mM NH_4HCO_3 , 1 mM EDTA, and 0.02 μ g trypsin, pH 7.9, at RT for up to 12 hrs. At selected times (1, 10, 20, 30, 60, and 180 min, and after 12 hours), 10 μ l aliquots of the solution (each containing \sim 1.4 μ g TnC) were transferred to 30 μ l solubilisation buffer containing protease inhibitors (leupeptin/trypsin ratio $>10:1$ w/w) to stop the digestion. After SDS-PAGE analysis of the samples (on 18% glycine PA gels; see Chapter 2), the time point which showed the highest number of peptides of approximately equal intensity was chosen as the optimum for comparing to the analogous rat TnC isoform. Under these conditions this time was 30 minutes for both rabbit TnC-f and human TnC-s.

3.2.12 Tryptic digestion of BSA and CaM

Both BSA (a non calcium binding protein used as a negative control) and CaM, a calcium binding protein with 52% homology to TnC (Grant *et al.*, 1981) used as a positive control, were digested with trypsin as described above.

3.2.13 Tryptic digestion of rat TnC isoforms

One microgram of TnC purified from rat EDL or SOL muscle was incubated in a solution containing 10 mM imidazole, 50 mM NaCl, 0.02% NaN_3 , 1 mM EDTA and 0.002 μ g trypsin, pH 8.0 (in a total of 70 μ l for EDL and 140 μ l for SOL), at RT for up to 12 hours. Samples (10 μ l for EDL or 20 μ l for SOL) were taken at regular time points (20, 30, and 60 minutes, and 3, 4, 5 and 12 hours), stopped with 10 μ l solubilisation buffer

(leupeptin/trypsin ratio >10:1 w/w), and analysed by SDS-PAGE on 18% glycine PA gels as described in Chapter 2. Under these conditions, the digestion time for producing similar peptide patterns to those optimized for rabbit TnC-f and human TnC-s was 5 hours for rat TnC from both the EDL and SOL muscles.

3.3 Results

3.3.1 Purification of rat skeletal muscle TnC isoforms

Ion exchange chromatography of the crude troponin extract from rat EDL muscles produced five fractions that contained a predominant protein species of apparent molecular weight 19.1 kDa (Fig. 3.3, lanes 4-8). The majority of this protein species eluted at 600-900 μ S conductivity, with negligible amounts appearing in later fractions. The only contaminant in this preparation appeared as a faint band with an apparent molecular weight of 18.1 kDa (indicated in Fig. 3.3, lanes 4 and 5, by an arrowhead). The 19.1 kDa (Fig. 3.5, lane 2) protein displayed identical electrophoretic mobility to rabbit TnC-f (Fig. 3.5, lane 3). Note that after prolonged storage at -20°C a second minor band (indicated by the arrowhead in Fig. 3.5, lane 2) was detected in the rat EDL TnC preparation.

Electrophoretic analysis of the chromatographic fractions obtained from the SOL muscle showed five fractions containing a protein species of apparent molecular weight 18.1 kDa, eluting at 580-900 μ S (shown in Fig. 3.4, lanes 5-9), with negligible amounts appearing in subsequent fractions. This protein (Fig. 3.6, lane 2) exhibited the same

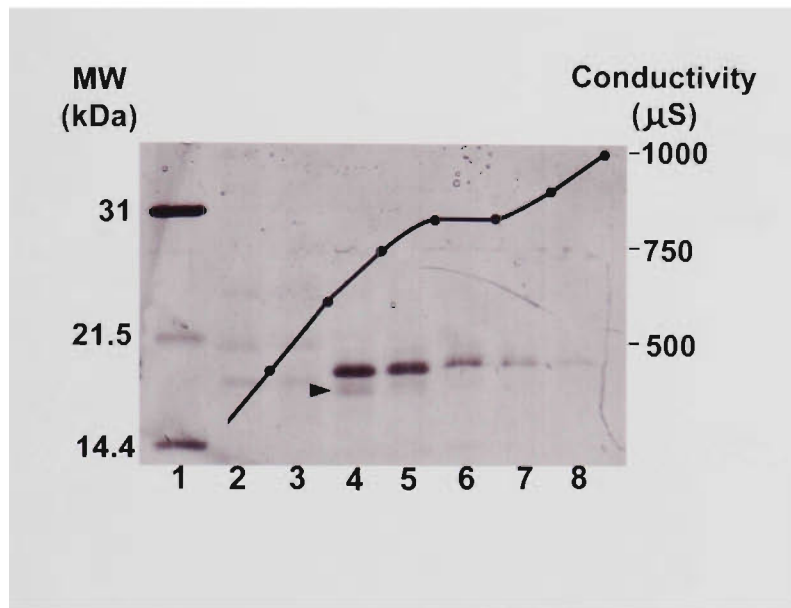


Fig. 3.3. Electrophoretogram of the fractions produced by ion exchange chromatography of the crude troponin extract from rat EDL muscle. (Lane 1) molecular weight standards; (lanes 2-8) fractions 7-13. The conductivity in μS , as measured after the elution of each 2 ml fraction, is shown (\bullet). The arrowhead indicates the minor contaminating protein species.

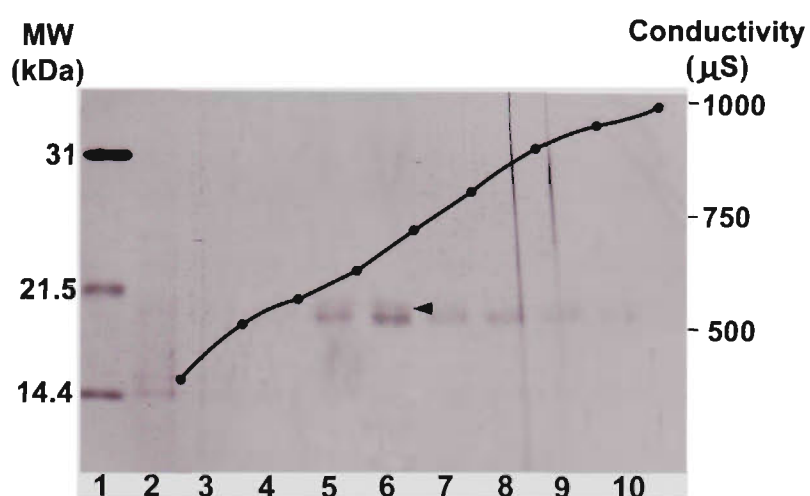


Fig. 3.4. Electrophoretogram of the fractions produced by ion exchange chromatography of the crude troponin extract from rat soleus muscle. (Lane 1) molecular weight standards; (lanes 2-10) fractions 4-12. The conductivity in μS , as measured after the elution of each 2 ml fraction, is shown (●). The arrowhead indicates the minor contaminating protein species.

electrophoretic mobility as that of human TnC-s (Fig. 3.6, lane 3). A minor contaminant (visualized as a faint band with an apparent molecular weight 19.0 kDa marked by an arrowhead, Fig. 3.4, lanes 5 and 6) was observed in two fractions.

The estimated yields were 23 μg TnC-f/g wet muscle weight for the 19.1 kDa protein purified from rat EDL muscle and 17.6 μg TnC-s/g wet muscle weight for the 18.1 kDa protein purified from rat SOL muscle.

3.3.2 Tryptic peptide mapping of rat TnC isoforms

Figure 3.5 (lanes 4-7) shows a comparison of the tryptic peptide patterns produced by the 19.1 kDa protein purified from rat EDL (lane 4), rabbit TnC-f (lane 5), the negative control protein (BSA; lane 6), and CaM, a Ca^{2+} -binding protein of similar size and structure to TnC (lane 7). The 19.1 kDa protein purified from rat EDL muscle (lane 4) shares all peptides with rabbit TnC-f (lane 5). Note that three of the bands (indicated by asterisks) in these samples that were clearly visualized on the original gel were poorly resolved from the background after computer scanning. The presence of these bands is better observed in the inset, which shows the samples of lanes 4 and 5 from a different gel after manipulation of the image contrast and tonal scaling. The tryptic peptide pattern of the 19.1 kDa protein purified from rat EDL (lane 4) matches neither that of BSA (lane 6) nor that of the Ca^{2+} -binding protein CaM (lane 7). Similarly, the peptide pattern of the 18.1 kDa protein purified rat SOL muscle (Fig. 3.6, lane 4) matches that of human TnC-s (lane 5), but shares no common peptides with the BSA or CaM tryptic digests. Thus, by comparing the tryptic digests of the proteins purified from rat EDL and SOL muscles

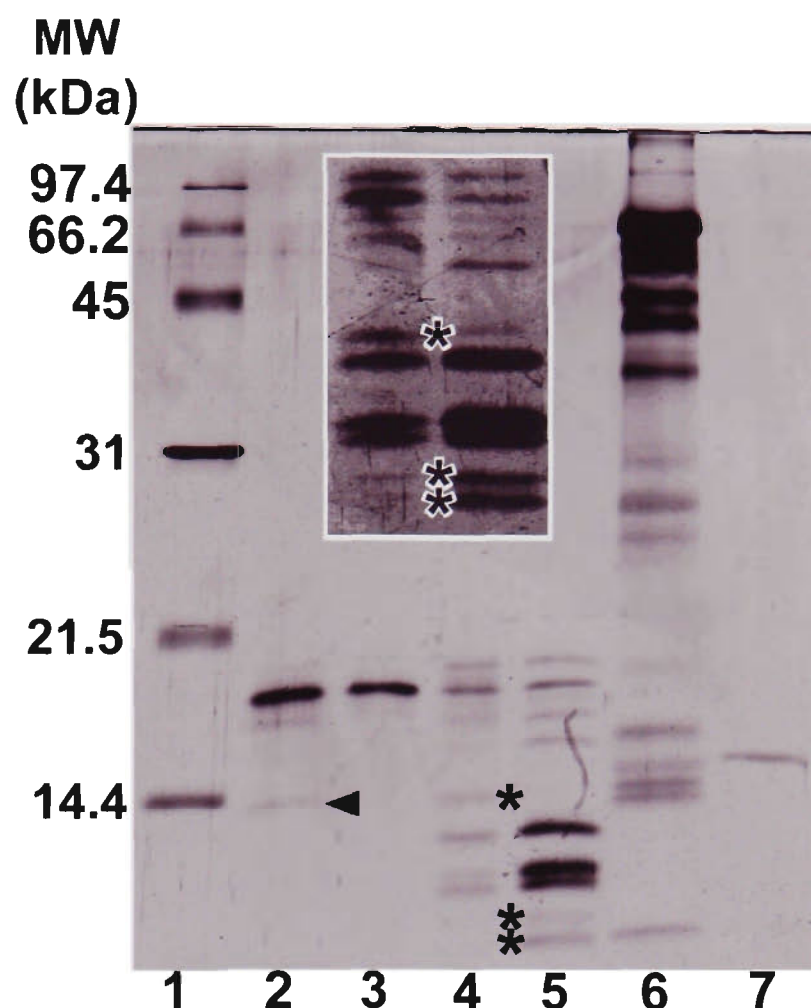


Fig. 3.5. A comparison of rat EDL and reference proteins before and after limited tryptic digestion. (Lane 1) molecular weight standards; (lane 2) rat EDL TnC (0.04 μg) before tryptic digestion; (lane 3) commercially purified rabbit TnC-f (0.04 μg) before tryptic digestion; (lane 4) rat EDL TnC (0.07 μg) after 5 hours incubation with trypsin; (lane 5) commercially purified rabbit TnC-f (0.43 μg) after 30 min incubation with trypsin; (lane 6) BSA (0.356 μg) after 12 hours incubation with trypsin; (lane 7) CaM (0.356 μg) after 30 min incubation with trypsin. Note that CaM produced no peptide bands of a sufficient size to be retained on 18% gels when subjected to identical tryptic digestion conditions as the rabbit TnC-f. The arrow head indicates a proteolytic product generated after long term storage of rat EDL TnC at -20°C without protease inhibitors. The asterisks (in both the main figure and inset) indicate the positions of peptide bands which are visible on the original gel, yet too faint to be resolved well from the background after computer scanning. Inset: Contrast and tone manipulated computer image of rat EDL TnC (as in lane 4) and rabbit TnC-f (as in lane 5) tryptic digests taken from another gel, in which the bands not visible in the main figure (indicated by asterisks) can be seen.

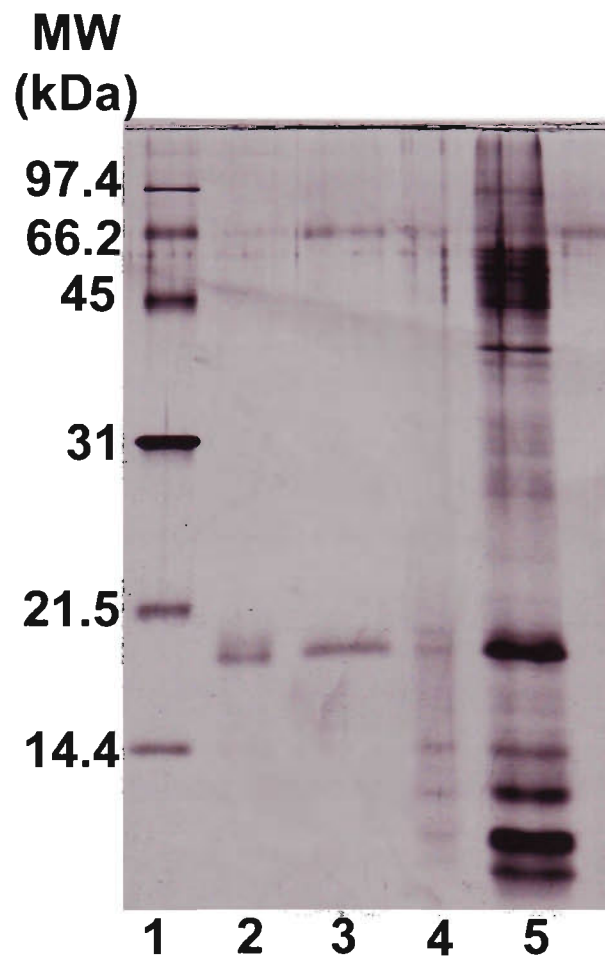


Fig. 3.6. A comparison of rat SOL TnC and reference proteins before and after limited tryptic digestion. (Lane 1) molecular weight standards; (lane 2) rat SOL TnC (0.015 μg) before tryptic digestion; (lane 3) commercially purified human TnC-s (0.016 μg) before tryptic digestion, (lane 4) rat SOL TnC (0.0625 μg) after 5 hours incubation with trypsin; (lane 5) commercially purified human TnC-s (0.118 μg) after 30 min incubation with trypsin.

with those of commercial TnC isoforms and of negative controls, the identity of the purified rat proteins were confirmed as the rat TnC isoforms. As seen in Figs. 3.5 and 3.6, all minor contaminants from the rat EDL and SOL TnC preparations display identical electrophoretic mobilities to peptides produced by the tryptic digestions of the two preparations.

3.4 Discussion

This is the first report of purification of the fast and slow TnC isoforms from rat skeletal muscle. The finding that the protein species isolated from the fast-twitch rat EDL muscle displayed identical characteristics in terms of electrophoretic mobility and tryptic digestion to the commercial preparation of rabbit skeletal (fast) TnC strongly suggests that the purification procedure used in this study was successful in isolating the fast rat TnC isoform. Likewise, the identical electrophoretic and tryptic digestion properties displayed by the commercially available human cardiac (slow) TnC and the protein species isolated from the slow-twitch rat SOL muscle indicates that the slow rat TnC isoform was also successfully purified.

It is difficult to judge the relative effectiveness of the TnC purification protocol for rat muscle described here since Potter (1982) reported no yield, and other reports of TnC purification yields are very rare. However, from what has been reported it is clear that the rat TnC yields produced by this study (ie. 23 μg fast TnC /g EDL wet weight and 17.6 μg slow TnC /g SOL wet weight) are markedly lower than those previously reported for TnC purified from other species (eg. 325 μg TnC /g skeletal frog muscle (Van Eerd *et al.*,

1978), 600 μg TnC /g slow rabbit muscle (Wilkinson, 1980)). This is not surprising given the small size of rat EDL and SOL muscles (less than 0.15 g wet weight), which make it difficult to acquire sufficient starting material and related to this, the higher impact of the losses inherent within a multi-stage procedure, such as Potter's troponin extraction protocol (Potter, 1982), on the TnC yield.

Notwithstanding the low yield, Potter's procedure for isolating fast TnC from skeletal muscle worked reasonably well (after modifications to the chromatographic step as described) with a small volume of material (about 5 g from 40-50 EDL muscles) to produce 23 μg fast TnC /g EDL wet weight. Purifying the slow isoform was considerably more difficult. However, Potter's purification procedure (with the mentioned modifications) for TnC from skeletal muscle performed on about 5 g SOL muscle (50-60 muscles) generated enough pure slow TnC from SOL muscle (17.6 $\mu\text{g}/\text{g}$ wet weight) for peptide mapping.

The possibility was considered that the minor contaminant which eluted in the first two fractions containing EDL TnC could be the slow TnC isoform, since this contaminant and slow rat TnC isoform share an apparent molecular weight of 18.1 kDa. Such a high amount of slow TnC co-purifying from the EDL muscle is highly unlikely however, as the EDL is known to contain almost exclusively fast myofibrillar proteins (Stephenson, 2001). This was confirmed by SDS-PAGE analysis of an EDL homogenate (not shown), which displayed no evidence of the slow TnC isoform. The same purification procedure performed on SOL muscle also produced a minor contaminant eluting in the first two fractions containing the slow TnC, however the apparent molecular weight of this

contaminant (19 kDa) did not suggest co-purification of the fast TnC isoform (apparent molecular weight 19.1 kDa). Rather, it appears that the contaminants of both the EDL and SOL TnC preparations are highly likely to be degradation products of TnC. In each of the two preparations, the contaminating species correspond to peptides which appear early in the tryptic digest (see Figs. 3.5 and 3.6). It is probable that some degradation would have occurred during the purification procedure, since the extracted proteins were incubated up to five days (at 4°C) in solutions with no protease inhibitors (as the product obtained was to be subsequently subjected to tryptic digestion). Further proteolytic degradation could be observed in the EDL TnC preparation (the peptide band indicated by an arrow head in Fig. 3.5, lane 2) after being kept at -20°C without protease inhibitors for twelve months, while the SOL TnC preparation showed no further evidence of degradation after nine months of identical storage conditions.

Chapter 4: Electrophoretic identification of TnC isoforms in single muscle fibres

4.1 Introduction

To date, gaining reproducible information on the relationship between the TnC isoform composition and other biochemical (eg. MHC isoform composition) and/or physiological characteristics (eg. Sr^{2+} -activation characteristics) of a single muscle fibre has been limited by the difficulties associated with the identification of the TnC isoform bands on gels of low molecular weight (< 42 kDa) muscle proteins from single fibre segments. Indeed, as illustrated by other studies (Babu *et al.*, 1987; Gulati *et al.*, 1988) and discussed in detail here, there is a relatively high risk of misidentification of other protein species for TnC isoforms in single muscle fibres if protein bands are identified solely on the basis of relative electrophoretic migration. TnC isoform bands have the potential to co-migrate with neighbouring protein species of known or unknown identity. Evidence supporting this point comes from the earlier studies of Gulati *et al.* (1988), who showed that TnC-f co-migrated with MLC2 in hamster trabeculae, and Babu *et al.* (1987) and Metzger (1996) who reported the co-migration of both TnC-f and TnC-s isoform bands with MLC2 in rabbit trabeculae and soleus (SOL) muscle fibres respectively.

Based on reports that the electrophoretic mobilities of TnC in urea gels (Head and Perry, 1974) and calmodulin in SDS gels (Burgess *et al.*, 1980) increase or decrease in the presence or absence of calcium respectively, it has become common practice to add CaCl_2 or EGTA to electrophoretic samples in order to identify Ca^{2+} -binding proteins (eg. Head *et al.*, 1977; Grab *et al.*, 1979; Babu *et al.*, 1987; Gulati *et al.*, 1988; Xu and Hitchcock-

DeGregori, 1988; Babu *et al.*, 1992; Rhyner *et al.*, 1992; Tanokura *et al.*, 1992). Using this technique, a given TnC isoform would be identified as the band that migrated further in the presence of Ca^{2+} than in the absence of Ca^{2+} (presence of EGTA). It is worth pointing out that when used as such for identifying TnC isoforms in single muscle fibres this technique suffers from two major limitations. Firstly, it does not necessarily eliminate the co-migration problems discussed in the previous paragraph (see for example the study of Gulati *et al.*, 1988). Secondly, it requires the sample to be run in two separate electrophoretic lanes (one with Ca^{2+} , the other with EGTA); this can be a problem if the size of the fibre is very small (as is the case for fibres from small animals) and/or if one wishes to analyse the same fibre for other myofibrillar protein isoforms using a different gel system (eg. MHC analysis).

Described in this chapter is a simple, rapid and inexpensive strategy for unequivocal identification of TnC isoforms in single muscle fibres using SDS-PAGE. This strategy involves the application of a novel method for identifying TnC isoform bands on SDS gels based on the previously reported influence of Ca^{2+} on the migration of Ca^{2+} -binding proteins in SDS gels (Burgess *et al.*, 1980).

4.2 Methods

Details regarding animal handling, muscle dissection, single fibre preparation and TnC analysis by Glycine-SDS-PAGE are given in the appropriate sections of Chapter 2.

4.2.1 Identification of TnC isoform bands in single muscle fibres using EGTA

The EGTA-based method for identification of TnC isoforms in single fibres was developed within the scope of the study described in this thesis. Details of the final protocol are as follows. Single fibre samples (10 μ l) containing \sim 4 nl fibre volume were run on 16% glycine PA gels as described in Chapter 2. The samples were loaded in such a way that each single fibre sample was adjacent to a lane to which was applied a small volume (5 μ l) of solubilisation buffer (see section 2.3 for composition) containing 50 nmoles EGTA (10 mM; see Fig. 4.1). In this way TnC bands could be identified by a characteristic upward bend caused by the diffusion of EGTA from the adjacent lane as seen in the electrophoretogram in Fig 4.1.

4.3 Results and discussion

4.3.1 Effect of EGTA on the electrophoretic mobility of TnC in SDS gels

The reported effect of EGTA on the electrophoretic migration of calcium binding proteins in SDS gels (Burgess *et al.*, 1980) was found to hold true for both the fast and slow isoforms of TnC purified from the rat (as described in Chapter 3), and for the commercially purified rabbit TnC-f and human TnC-s samples. In Fig. 4.2 is an electrophoretogram showing the effect of different concentrations of EGTA on the migration of rat extensor digitorum longus (EDL) TnC-f. Each sample lane contains \sim 0.03 μ g TnC-f, and every second TnC-f sample also contains either 2, 4, 6 or 8 mM EGTA as indicated above the lane. Importantly, Fig. 4.2 shows that (i) the addition of 2-8 mM EGTA to a sample of TnC caused a reduction in the migration of the band to the same degree, regardless of the EGTA concentration, (ii) during electrophoresis the EGTA

diffused outward, causing a characteristic upward curvature of the TnC bands in adjacent lanes, and (iii) the higher the concentration of EGTA in the adjacent lane the greater the proportion of the band's length which curves. This consistently reproducible feature was further exploited to enable positive identification of TnC isoforms in single rat muscle fibres by running 5 μ l of solubilisation buffer containing 50 nmol EGTA (10mM) next to sample lanes, as illustrated in Figs. 4.1 and 4.3.

4.3.2 Identification of TnC isoforms in single muscle fibres of the rat

The danger of misidentifying a non-TnC band for TnC on SDS gels of rat single muscle fibres when the identification of TnC is based solely on the relative electrophoretic migration of myofibrillar proteins is well illustrated in Fig. 4.3. Shown in Fig. 4.3a is the low molecular weight protein profile of a single fibre (lane 2), which is flanked by the rat TnC marker (a mixture of fast and slow rat TnC isoforms) in lane 1, and the rat TnC marker containing 50 nmoles EGTA in lane 3. The electrophoretogram of the fibre clearly shows two protein bands that curve up from the positions of the TnC bands in lane 1 to the positions of the EGTA-shifted TnC bands in lane 3, indicating that the fibre examined on this gel contains both TnC isoforms. The identity of the two curved bands as the TnC-f and TnC-s isoforms is strongly supported by the finding that EGTA did not affect the migration of any other bands. Furthermore, one should note that all fibres used in this investigation were mechanically skinned and washed in an aqueous solution (see section 2.2, page 28), making it unlikely that either of the curved bands is CaM, a non-myofilament bound, Ca²⁺-binding, muscle protein of similar molecular weight to TnC (Grant *et al.*, 1981).

The value of the EGTA strategy for TnC identification in rat single muscle fibres is further illustrated by the data shown in Figs. 4.3b, 4.3c and 4.4. In Fig. 4.3b it can be seen that the fibre shown in lane 2 contains the fast TnC isoform, which curves from a position identical to that of the TnC-f in the TnC marker without EGTA (lane 1) to the position of the TnC-f band in the EGTA treated TnC marker (lane 3). It is important to note that the fibre shown in lane 2 also contains a band, indicated by the arrowhead, that exhibits identical electrophoretic migration to that of TnC-s in lane 1. Based on this band, it would be assumed that this fibre also contained TnC-s. However, as seen in Fig. 4.3b, the migration of this band was unaffected by the EGTA diffusion from lane 3, and therefore could not be TnC-s.

Fig. 4.3c shows an electrophoretogram of a single fibre (lane 2) which, judging by the migration of TnC-s in lane 1 and the curve of the band induced by EGTA diffusion from lane 3, expresses only TnC-s. Notably, the upward curve of the TnC-s band reveals the presence of two bands (labeled Band X₁ and Band X₂ in Fig 4.4) both of which co-migrated with TnC, but were not affected by EGTA. Based on this result, it would be inappropriate to use a gel slice containing this TnC-s band for amino acid sequencing or quantitation purposes. Note that either one or both 'X' bands appeared in ~50% of the rat single fibres examined in the studies described in this thesis, regardless of the muscle of origin.

Shown in Fig. 4.4 are electrophoretograms of the MLC1-MLC2-TnC region of three single fibres (run on separate 16% glycine PA gels), all containing the Bands X₁ and X₂.

Clearly, except for the TnC isoform bands (which can be identified based on their upward curvature toward the left side of the sample lane), all the protein bands in these electrophoretograms, including bands X₁ and X₂, migrated to the same relative positions. In contrast, the positions of TnC isoform bands unaffected by EGTA (ie. the horizontal portions of the curved bands) varied markedly (eg. TnC-f migrated close to MLC1-f in lane 1, roughly equidistant from MLC2-f and Band X₁ in lane 2, and co-migrated with Band X₁ in lane 3). It is worth noting that even in a situation where TnC-f is almost co-migrating with MLC2-f (Fig. 4.4, lane 1), the EGTA induced curvature is clear enough to allow unambiguous identification of the TnC isoform.

4.3.3 Detection of TnC isoforms in single muscle fibres by silver staining

The conclusions drawn from electrophoretic analyses of TnC isoform composition in single muscle fibres when the protein bands are visualised by silver staining depend upon (i) the sensitivity of TnC to the stain, (ii) the amount of TnC present in the single fibre segments, and (iii) the maximum level of staining intensity which is compatible with optimal resolution of all protein bands of interest on the gel. As seen in Fig. 4.5 (upper panel), the smallest amount of purified TnC detectable by the Hoefer silver staining protocol used (see section 2.4.5) was 0.5 ng for both TnC-f and TnC-s.

Using a visual comparison of the intensities of the TnC bands in several 4 nl segments of pure fibres with those of known amounts of purified TnC isoforms it was estimated that a single fibre segment of about 4 nl (see for example Fig 4.5, lower panel) contains 8-10 ng TnC. It is worth noting that this value is similar to that calculated (8 ng / 4 nl fibre) from

the TnC content of rabbit skeletal muscle (93 pmole/mg wet weight) reported earlier by Yates and Greaser (1983) using amino acid analysis of myofibrillar proteins separated by SDS-PAGE. Based on these results, and as shown by the data presented in Fig 4.5 (lower panel, right lane), one would predict that in a mixed TnC-f/TnC-s sample containing 10 ng total protein (such as a 4 nl fibre segment containing both TnC-f and TnC-s), one should be able to detect both TnC isoform bands as long as neither of them was less than 5% (0.5/10 ng) of the total. A direct implication of this finding is that if the electrophoretogram of a 4 nl fibre segment displays only one TnC isoform band, then the relative proportion of that isoform in the fibre should be at least 95% of the total.

In conclusion, as shown by the results of this study, the misidentification of TnC bands in single fibres due to co-migration of TnC with other protein species can be avoided by allowing the diffusion of EGTA from a lane adjacent to the single fibre sample to produce a characteristic upward curve of TnC bands only. The notable advantage of this method is that, unlike previously reported methods using Ca^{2+} /EGTA to identify TnC bands, it requires sample for one electrophoretic well only. Thus a combined TnC and MHC electrophoretic analysis can be successfully performed on fibres as small as 5.6 nl volume - a feature of substantial benefit in studies involving the identification of MHC and TnC isoforms in very small fibres from atrophied muscles or from small animals (such as the fibres analysed in the studies described in Chapters 5 and 6). The EGTA diffusion strategy also has the potential to be of great benefit in studies involving TnC extraction/reconstitution experiments, in which SDS-PAGE is commonly used to assess the success of the extraction/replacement protocols. Furthermore, since the method allows

the TnC-f band to be visualised without being shifted fully into the position of MLC2-f, it allows for accurate quantitation of MLC isoforms whenever required.

Chapter 5: MHC and TnC isoform composition of single skeletal muscle fibres of the rat

5.1 Introduction

As discussed in detail in Chapter 1 (see section 1.4), the polymorphic nature of the MHC and TnC proteins (see sections 1.4.1.1 and 1.4.1.6 respectively) coupled with compelling evidence that the functions of each one is influenced by the actions of the other (see section 1.3.2, pp 14-16) suggests that mammalian skeletal muscle fibres may contain specific combinations of MHC and TnC isoforms.

To date there has been no large-scale systematic study on the types of MHC and TnC isoform combinations that occur in single fibres of mammalian skeletal muscle. This is due in part to the lack of an experimental strategy that allows the determination of the MHC *and* TnC isoform content of the same single fibre (for this point, see also the Introduction to Chapter 4). Within the scope of the work described in this chapter, electrophoretic analyses of MHC and TnC isoforms were performed on a large number of pure and hybrid single fibres from non-transforming muscles using the Alanine-SDS-PAGE method for reproducibly separating MHC isoforms (see Chapter 2 for methodological details), and the method for unequivocal identification of TnC isoforms on SDS glycine gels described in Chapter 4. The fibres were dissected from the sternomastoid (SM, predominantly fast-twitch) and soleus (SOL, predominantly slow-twitch) muscles of the adult rat.

5.2 Materials and methods

5.2.1 Animals, muscles and single fibre preparation

SOL and SM muscles were excised from male Sprague-Dawley rats (aged 13-14 wks) and immediately placed under paraffin oil. Single fibres were randomly isolated and prepared as described in Chapter 2.

5.2.2 Electrophoretic analyses of myofibrillar protein isoforms in single fibres

MHC isoforms were separated using Alanine-SDS-PAGE as described in Chapter 2. TnC isoforms were identified in single fibres run on 16% glycine PA gels (see Chapter 2) according to the method described in Chapter 4.

5.3 Results

5.3.1 Classification of MHC isoform based fibre-types

In this study 245 single fibres were examined; 218 from the SM muscle and 27 from the SOL. The pool of SM fibres comprised thirteen MHC isoform based-fibre types (listed in Table 5.1), while the population of soleus fibres was composed of only three of the fibre types listed in Table 5.1 (type **I**, 21 fibres; type **IIA + I**, 5 fibres; type **IIA + IID + I**, 1 fibre). In Fig. 5.1 are shown representative electrophoretograms of fibres classified as ‘pure’ types (**IIB**, **IID**, **IIA** and **I**), which contained only one MHC isoform (Fig. 5.1, upper panel), fibres classified as ‘fast-fast hybrids’, which contained various combinations of fast MHC isoforms (Fig. 5.1, middle panel), and ‘fast-slow hybrids’ containing both the slow MHC **I** isoform and one or several fast MHC isoforms (Fig. 5.1, lower panel). In agreement with other reports (reviewed by Stephenson, 2001), some of

the MHC isoform combinations found in this study did not follow the 'nearest neighbour rule' formulated by Pette and Staron (1991).

Table 5.1. TnC isoform composition of the pure and hybrid MHC-based fibre types obtained from soleus and sternomastoid muscles of adult rat. The values listed represent the number (proportion) of fibres of a given fibre type containing the indicated TnC isoform(s).

MHC isoforms present	TnC isoforms present		
	TnC-f	TnC-f + TnC-s	TnC-s
<i>Pure Fibres</i>			
IIa (n=4)	4 (100%)	0	0
IIb (n=68)	68 (100%)	0	0
IIc (n=10)	10 (100%)	0	0
I (n=22)	0	0	22 (100%)
<i>Fast-Fast Hybrid Fibres</i>			
IIa + IIb (n=4)	4 (100%)	0	0
IIa + IIc (n=15)	15 (100%)	0	0
IIb + IIc (n=77)	77 (100%)	0	0
IIa + IIb + IIc (n=13)	13 (100%)	0	0
<i>Fast-Slow Hybrid Fibres</i>			
IIa + I (n=11)	3 (27%)	5 (46%)	3 (27%)
IIc + I (n=3)	0	3 (100%)	0
IIa + IIc + I (n=9)	2 (22%)	7 (78%)	0
IIb + IIc + I (n=4)	2 (50%)	2 (50%)	0
IIa + IIb + IIc + I (n=5)	3 (60%)	2 (40%)	0

5.3.2 TnC isoforms detected in pure and hybrid fibres

As listed in Table 5.1, and shown by the examples in Fig. 5.2, all pure slow type I fibres (n=22, Fig. 5.2a) displayed only TnC-s, and all pure fast (n=82, Fig. 5.2b) and fast-fast hybrid fibres (n=109, Fig. 5.2c), displayed only TnC-f. Clearly, in each of these fibres the

type of TnC isoform present 'matched' that of the MHC isoform(s). In contrast, fibres classified as fast-slow hybrids (n=32, Fig. 5.2d-f) were found to display either TnC-f only, TnC-s only, or both TnC isoforms depending, largely, upon the proportion of fast and slow MHC isoforms present (as illustrated by Figs. 5.2 and 5.3). For example, in the fibres shown in Fig. 5.2d-f, displaying TnC-f (Fig. 5.2d), TnC-s (Fig. 5.2e), and both TnC-f and TnC-s (Fig. 5.2f), the proportions of MHC isoforms were 89% fast / 11% slow, 7% fast / 93% slow and 58% fast / 42% slow, respectively.

Further insight into the relationship between the relative proportion of fast and slow MHC isoforms and the TnC isoform composition in adult rat skeletal muscle fibres is provided by the graphical representation of the fast-slow hybrid fibre analysis shown in Fig. 5.3. In this diagram each fibre is represented by a circle, the proportion of fast and slow MHC isoforms contained in the fibre is indicated by the relative position of the circle on the horizontal scale, and the type of TnC isoform(s) detected in the fibre is represented by the colour of the circle.

As seen in Fig. 5.3, the 12 fast-slow hybrid fibres in which the proportions of the fast and slow MHC isoform types were greater than about 30% displayed both TnC-f and TnC-s. Since the types of TnC isoforms present in these fibres matched those of the MHC isoforms, they are hereafter referred to as 'matched fibres'. The population of fast-slow hybrids in which one of the MHC isoform types was less than about 30% included two groups of fibres; one comprising fibres that displayed two MHC and two TnC isoform types (i.e. matched fibres), and a second containing fibres that displayed a single TnC

isoform type, which was matched with one of the MHC isoform types present and mis-matched with the other. In these latter fibres, hereafter referred to as 'mis-matched fibres', which originated from either the SOL or the SM muscle, the TnC isoform was always matched with (of the same type as) the dominant (greater than about 70%) MHC isoform type, and was mis-matched with (of the opposite type as) the less abundant MHC isoform type. The population of fast-slow hybrids containing less than ~ 30% fast MHC isoforms included three type **IIA + I** fibres (all mis-matched) and three type **IID + I** fibres (all matched). The subgroup of fibres containing less than ~ 30% slow MHC isoform was composed of three type **IIA + I** fibres (all mis-matched), five type **IIA + IID + I** fibres (3 matched and 2 mis-matched), three type **IIB + IID + I** fibres (1 matched and 2 mis-matched) and four type **IIA + IIB + IID + I** fibres (1 matched and 3 mis-matched).

5.4 Discussion

The major finding of this study is that, in SM and SOL muscles of adult rat, fibres containing exclusively fast MHC isoforms (one or several) displayed only TnC-f, fibres containing exclusively the slow MHC isoform displayed only TnC-s and fibres containing both fast and slow MHC isoforms displayed either both TnC isoforms or one TnC isoform matching the most abundant MHC isoform type. These data are consistent with the idea that MHC and TnC isoforms co-exist in specific combinations in fibres from non-transforming mammalian skeletal muscle. The strength of this conclusion comes from the large number (245) of single fibres examined, the breadth of the fibre types included in the study (13 out of 15 theoretical possibilities) and from the reproducibility

and effectiveness of the microelectrophoretic methods used for analysing MHC and TnC isoform composition in single fibre segments.

These data are in contrast to those of Danieli-Betto *et al.* (1990) and Geiger *et al.* (1999), who reported cases of mis-matched MHC and TnC isoforms in both pure fast-twitch (TnC-f and TnC-s co-existing with MHC IIa, Danieli-Betto *et al.*, 1990) and pure slow-twitch (TnC-s and TnC-f or TnC-f alone co-existing with MHC I, Danieli-Betto *et al.*, 1990; Geiger *et al.*, 1999) single fibres of the adult rat. The discrepancy between the results of this study and those of Danieli-Betto *et al.* (1990) and Geiger *et al.* (1999) may be explained if one considers that in the latter studies TnC bands on SDS gels were identified only on the basis of electrophoretic migration, without reference to appropriate markers (such as purified rat TnC isoforms). The value of this strategy is limited considering that TnC isoform bands have the potential to co-migrate with neighbouring protein species of known or unknown identity, as discussed in Chapter 4. Therefore, it is likely that the discrepancy between the results presented here and those of previous studies (Danieli-Betto *et al.*, 1990; Geiger *et al.*, 1999) with regard to MHC and TnC isoform composition in single rat muscle fibres could be the result of misidentification of TnC isoform bands in the latter.

Based on the number of MHC and TnC isoforms known to exist in skeletal muscles of adult rat (4 and 2, respectively) and assuming that these isoforms could combine in a non-restricted manner, one would expect that analyses of MHC and TnC isoform composition of a large pool of single fibres from rat skeletal muscles would produce 15 combinations of MHC isoforms and 45 combinations of MHC and TnC isoforms (all of which appear

in Table 5.2). In this study 245 single fibres were examined, randomly isolated from SOL and SM muscles of 9 adult rats. In this population of single fibres were found 13 combinations (~87% of theoretical possibilities) of MHC isoforms (one of which, IIa + IIb, had not been detected before in non-transforming mammalian muscle), but only 18 MHC and TnC isoform combinations (~40% of theoretical possibilities; see Table 5.2 for details). This finding is consistent with the idea that the combinations of MHC and TnC isoforms follow a specific pattern in fibres from non-transforming mammalian skeletal muscle.

Table 5.2. Theoretically possible MHC-TnC isoform combinations

The MHC-TnC isoform combinations detected in this study in a pool of 245 single fibres from non-transforming rat skeletal muscle represent only a small proportion of the theoretically possible combinations between 4 MHC and 2 TnC isoforms. Symbols used for combinations: +, theoretically possible and detected; 0, theoretically possible, but not detected.

MHC isoform	TnC isoform		
	TnC-f	TnC-f & TnC-s	TnC-s
<u>Pure Slow</u>			
I	0	0	+
<u>Pure Fast</u>			
IIa	+	0	0
IId	+	0	0
IIb	+	0	0
<u>Fast - Fast Hybrid</u>			
IIa + IIb	+	0	0
IIa + IId	+	0	0
IIb + IId	+	0	0
IIa + IIb + IId	+	0	0
<u>Slow - Fast Hybrid</u>			
IIa + I	+	+	+
IIb + I	0	0	0
IId + I	0	+	0
IIa + IIb + I	0	0	0
IIa + IId + I	+	+	0
IIb + IId + I	+	+	0
IIa + IId + IIb + I	+	+	0

Chapter 6: Sr²⁺-activation characteristics and TnC isoform composition of single fibres of the rat diaphragm muscle

6.1 Introduction

Strontium ion (Sr²⁺) does not play a direct role in vertebrate skeletal muscle contractility *in vivo*, yet has been used frequently in the laboratory as an activator of contractile processes in reconstituted or ‘synthetic’ actomyosin, myosin B or ‘natural’ actomyosin, actomyosin threads, myofibrils, glycerinated muscle and mechanically skinned muscle fibres. The main reason for its use is that, as first reported by Ebashi *et al.* (1968), cardiac/skeletal slow-twitch type and skeletal fast-twitch type muscle preparations differ markedly with respect to their sensitivity to Sr²⁺ of contractile activation. Based on this finding, Ebashi & colleagues (1968) designed a series of elegant experiments which demonstrated that the regulatory effects of Ca²⁺, the physiological activator of muscle contraction, on contractile processes are mediated by Tn via its divalent cation-binding subunit TnC. Since this pioneering work of Ebashi, Sr²⁺ has been employed both by physiologists and biochemists as a tool for gaining further insights into the process of regulation of muscle contraction by divalent cations.

Fibre-type differences with respect to Sr²⁺-activation properties have been used (eg. Cordonnier *et al.*, 1985; Fink *et al.*, 1986; Wilson and Stephenson, 1990) as a physiological criterion for identifying slow- and fast-twitch fibres in studies of mammalian muscle contractility using single fibre preparations. Thus, Sr²⁺ also has the potential to become a valuable tool in studies concerned with the functional diversity and

plasticity of skeletal muscle fibres. This is particularly the case if the identity of the structure(s) responsible for the inter-fibre type differences in Sr^{2+} -sensitivity of contractile processes was precisely known. Here it is worth pointing out that, based on current knowledge, the Sr^{2+} -sensitivity-based method of fibre-typing does not appear to be fully correlated with the more widely used methods of fibre-typing based on electrophoretically defined MHC isoform composition (Bortolotto *et al.*, 2000), which means that with some types of fibres one has to determine both Sr^{2+} -activation characteristics *and* MHC isoform composition in order to obtain more complete functional and structural information.

In an earlier study, Yamamoto (1984) showed that the sensitivity to Sr^{2+} of actomyosin ATPase regulated by a Tn complex containing skeletal TnI and TnT and cardiac TnC (TnC-s) was higher than that of the enzyme regulated by another Tn complex containing cardiac TnI and TnT and skeletal fast-twitch TnC. This finding prompted Yamamoto and others (for review see Ohtsuki *et al.*, 1986) to conclude that the difference in sensitivity to Sr^{2+} of contractile processes in cardiac and skeletal muscle preparations is 'determined *solely* by the [molecular] species of TnC.' This idea is consistent with the results obtained from TnC extraction/reconstitution experiments by Morimoto and Ohtsuki (1987) with rabbit skeletal muscle myofibrils, Babu *et al.* (1987) with myocardial trabeculae of Syrian hamster, Hoar *et al.* (1988) with rat cardiac fibres and Sweeney *et al.* (1990) with rabbit soleus fibres. In the study by Sweeney *et al.* (1990), for example, the endogenous TnC was replaced with recombinant cardiac, native fast-twitch skeletal or mutated fast-twitch skeletal TnC species.

Not all studies using reconstituted functional actomyosin systems support Yamamoto's conclusion regarding the contribution of the TnC molecular structure to the muscle type-

specific relationship between $[Sr^{2+}]$ and contractile activation parameters. Thus, Kerrick *et al.* (1980) reported that purified skeletal acto-heavy meromyosin (HMM) systems regulated by the native troponin-tropomyosin (Tn-Tm) complex from either skeletal or cardiac muscle display the same $[Sr^{2+}]$ -dependence of ATPase activation. Later, Kerrick *et al.* (1985) also found that the relationship between isometric force and $[Sr^{2+}]$ for fast-twitch skinned muscle fibres was essentially the same before removal of endogenous TnC isoform and after its replacement with either cardiac or fast-twitch skeletal species. Based on these data, Kerick and colleagues (1985) argued that protein-protein interactions associated with the activation process, which strongly affect TnC affinity for Sr^{2+} , rather than the molecular type of TnC, determine the difference in sensitivity to Sr^{2+} of contractile events in cardiac and fast-twitch skeletal muscle preparations.

A close examination of the papers listed above reveals two kinds of methodological problems that may account for the conflicting data produced by the aforementioned studies. One kind relates to the inherent shortcomings of the TnC extraction/replacement strategy, well detailed in a review by Moss (1992), and the other to the effectiveness of the protocols used for the separation, visualization and identification of TnC isoform bands on electrophoretograms of TnC-extracted and TnC-reconstituted fibres. The present study proposed to revisit the issue of the factors determining the fibre type differences with respect to sensitivity to Sr^{2+} of contractile activation processes using an experimental strategy that avoids the two kinds of problems. This strategy involves the use of pure and hybrid diaphragm fibres that contain different naturally occurring combinations of myofibrillar protein isoforms (Bortolotto *et al.*, 2000), in conjunction

with the electrophoretic method for the unequivocal identification of TnC isoforms in single fibre segments described in Chapter 4.

6.2 Materials and methods

6.2.1 Animals and muscles

The diaphragm muscles used in this study were prepared for single fibre dissection from male Sprague Dawley rats (aged 13 weeks) as described in Chapter 2.

6.2.2 Preparation of single fibres

Skinned single fibres were prepared as described in Chapter 2. Each skinned fibre segment was mounted at slack length between a force-sensitive transducer (Sensoror 801, Horten, Norway) and a pair of fine Barcroft forceps on the apparatus for mechanical measurements.

6.2.3 Preparation of solutions used for force activation experiments

The solutions used to activate the skinned fibre preparations, designed to mimic the *in vivo* environment of the myofibrils (Stephenson and Williams, 1980), were prepared from the stock solutions listed in Table 6.1 by Aida Yousef (Muscle Research Laboratory, LaTrobe University).

Table 6.1. Composition of stock solutions used to make force activation solutions

Component	Relaxing Solution	Ca ²⁺ Maximally Activating Solution	Sr ²⁺ Maximally Activating Solution
	Final concentration of components (mM)		
HEPES	90	90	90
K ⁺	117	117	117
Na ⁺	36	36	36
Mg _{total}	10.3	8.1	8.5
EGTA _{total}	50	50	50
Ca ²⁺ _{total}	-	48.5	-
Sr ²⁺ _{total}	-	-	40
ATP _{total}	8	8	8
Creatine Phosphate	10	10	10
NaN ₃	1	1	1

A set of eleven strongly buffered (with 50 mM total EGTA) Sr²⁺-activation solutions (pSr range of 3.6 to >9, where pSr = -log₁₀[Sr²⁺]) and a set of ten strongly buffered (with 50 mM EGTA) Ca²⁺-activation solutions (pCa range of 4.3 to >9, where pCa = -log₁₀[Ca²⁺]) were prepared by combining differing volume ratios of the *Relaxing Solution* and the *Ca²⁺ Maximally Activating Solution* or the *Sr²⁺ Maximally Activating Solution* respectively. In addition to the 50 mM Sr²⁺-EGTA or Ca²⁺-EGTA buffer, all solutions contained (in mM) 117 K⁺, 37 Na⁺, 1 Mg²⁺ (free), 90 HEPES (pH 7.10 ± 0.01), 8 total ATP, 10 creatine phosphate, 1 N₃⁻. The pH, osmolality and ionic strength of all solutions at RT were 7.10 ± 0.01, 295 ± 5 mosmol/kg and 234 ± 2 mM, respectively.

The pSr or pCa values for each activating solution were calculated based upon (i) the volume of the Relaxing Solution, (ii) the respective volumes of the Sr²⁺ or Ca²⁺ Maximally Activating Solutions, (iii) the precisely known concentration of excess EGTA

([EGTA]_{excess}), determined by titration of the stock solutions described in Table 6.1, and (iv) the apparent affinity constants for Sr²⁺ and Ca²⁺ binding to EGTA (the values used in this study, ie. $1.53 \times 10^4 \text{ M}^{-1}$ and $4.78 \times 10^6 \text{ M}^{-1}$ respectively, were those measured earlier for the same conditions, Stephenson and Williams, 1980; West and Stephenson, 1993). The pSr values of the Sr²⁺-activating solutions were >9, 6.5, 6.3, 6.0, 5.6, 5.3, 5.0, 4.8, 4.5, 4.0 and 3.6. The pCa values of the Ca²⁺-activating solutions were >9, 6.7, 6.5, 6.2, 6.02, 5.82, 5.59, 5.36, 5.18, and 5.0.

6.2.4 Protocol for isometric force activation experiments

Note that the experimental procedures described in this section were performed in collaboration with D.G. Stephenson (Muscle Research Laboratory, LaTrobe University) and R. Blazev (Muscle Cell Biochemistry Laboratory, Victoria University). The apparatus used for the force activation experiments consisted of several components including (i) a micromanipulator (Prior, UK), to which were connected a pair of fine forceps and a stainless steel pin attached to the force transducer, (ii) a microscope (Olympus, magnification range 6.7-40) to aid in mounting the fibre between the forceps and the pin, and (iii) a tray holding a series of 2.5 ml Perspex wells, which could be moved horizontally (to position any of the wells beneath the mounted fibre), as well as vertically (via a laboratory jack), to place/remove the fibre into/out of the wells.

The isometric force activation characteristics of individual fibres were determined at RT from the steady-state isometric force responses developed by the fibre segments in the strongly Sr²⁺- and Ca²⁺- buffered solutions. All these experiments were carried out with fibre segments at slack length, where the average sarcomere length is about 2.65 μm

(Bortolotto *et al.*, 2000). Each preparation was initially equilibrated for two minutes in a 'relaxing solution' (pCa , $pSr > 9$) and then was activated in a solution of pSr 5.3. Based on the size of the force response developed in this solution, fibres could be distinguished into three categories; fibres with fast-twitch (no active force), fibres with slow-twitch (almost maximal active force) and fibres with intermediate (intermediate active force) activation characteristics (e.g. Fink *et al.*, 1986; Wilson and Stephenson, 1990; Bortolotto *et al.*, 2000; Woolley *et al.*, 2002). All fibres that developed forces greater than 0.0025 mN, indicative of a slow-twitch activation component (Fink *et al.*, 1986; Wilson and Stephenson, 1990; Bortolotto *et al.*, 2000; Woolley *et al.*, 2002), were sequentially activated in the Ca^{2+} - and Sr^{2+} -activating solutions as shown under the trace in Fig. 6.1a for a representative fibre. Of the fibres that did not develop force in the pSr 5.3 solution, five randomly selected fibres (used as reference for fast-twitch activation characteristics) were sequentially activated in the Ca^{2+} and Sr^{2+} solutions as shown in Fig. 6.1a, but the majority were sequentially activated only in the Sr^{2+} solutions. This protocol was consistent with the main thrust of this investigation of the relationship between myofibrillar protein isoform composition and fibre type differences in Sr^{2+} -activation characteristics. The fibre remained in each solution until maximum force was achieved. At the end of the activation protocol, each fibre segment was placed in SDS-PAGE solubilizing buffer ($\sim 1 \mu l$ per 0.4 nl fibre volume; see section 2.3 for composition) for electrophoretic analyses of myofibrillar protein isoform composition (see section 6.2.6).

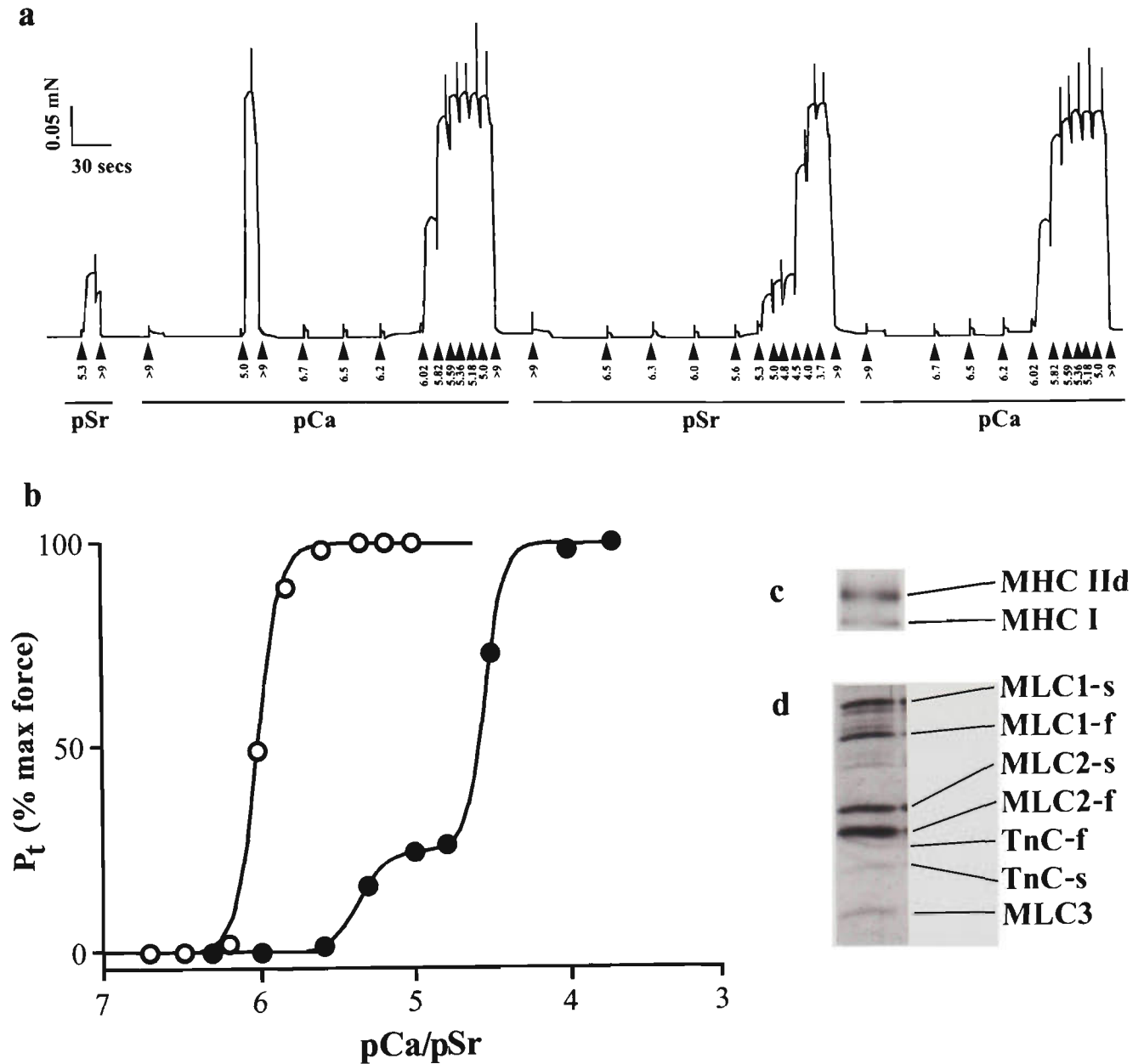


Fig. 6.1. Sample of complete data collected for a single muscle fibre. The data shown were collected for one of the fibers from Group 4 (see Table 6.1). (a): Continuous chart recording of force responses produced by placing the fiber into strongly Ca^{2+} - and Sr^{2+} -buffered solutions (pCa or pSr values indicated under arrowheads). The arrowheads indicate the moment when the fibre was transferred to a solution of given pSr or pCa. Note the small artifacts caused by the transfer of the preparation between solutions. (b): P_t -pCa (open circles) and P_t -pSr (closed circles) curves generated from the trace shown in A using Eq. 1 and Eq. 2 (see methods) respectively. The descriptors of the P_t -pSr and P_t -pCa curves are as follows; $\text{pSr}_{50/1} = 5.37$, $\text{pSr}_{50/2} = 4.54$, $n_{\text{Sr}1} = 4.63$, $n_{\text{Sr}2} = 3.66$, $n_{\text{Ca}} = 5.308$, $\text{SrF}_{\text{max}}/\text{CSA} = 107 \text{ kN/m}^2$, $\text{CaF}_{\text{max}}/\text{CSA} = 107 \text{ kN/m}^2$. (c): Electrophoretogram showing the MHC isoform composition of the fibre, see chapter 2. (d): Electrophoretogram showing some of the low molecular weight ($< \sim 30 \text{ kDa}$) protein isoforms detected in the fibre. Note that the TnC isoform bands can be readily identified by a characteristic upward curvature caused by the diffusion of EGTA applied to adjacent left lane as described in Chapter 4.

6.2.5 Determination of Sr^{2+} - and Ca^{2+} - activation characteristics of single fibre segments

For each fibre segment, the relationship between isometric force and $[\text{Sr}^{2+}]$ or $[\text{Ca}^{2+}]$ was determined by plotting the steady-state force responses developed by the fibre at different $[\text{Sr}^{2+}]$ or $[\text{Ca}^{2+}]$, expressed as percent of the maximum Sr^{2+} -activated force (SrF_{max}) or Ca^{2+} -activated force (CaF_{max}) respectively (P_t , % max. force), against the pSr or pCa values of the solutions in which the fibre was activated. Note that the force responses were measured relative to the baseline obtained when the fibre was incubated in the 'relaxing solution' (pCa, pSr > 9). To correct for the slight deterioration in force production associated with the repeated activation of skinned fibre preparations (see Fig. 6.1a), a simple interpolation protocol was used to estimate the values of SrF_{max} (or CaF_{max}) corresponding to the force responses obtained in a particular pSr (or pCa) solution; prior to calculation of (P_t), the measured height of each force response was multiplied by the following correction factor:

$$(\mathbf{M}_i - \mathbf{M}_f) / \mathbf{N}$$

where \mathbf{M}_i and \mathbf{M}_f are the *initially measured* and *finally measured* maximum force responses respectively, and \mathbf{N} is the total number of force responses measured, including the two maximums.

The P_t -pSr and P_t -pCa data points were then best fitted by theoretical Hill curves using the *nonlinear regression analysis* protocols provided by GraphPad Prism software. In this

study, a proportion of the P_t -pSr curves and all P_t -pCa curves could be fitted to the data points with a correlation coefficient, $r^2 \geq 0.9990$ using a simple Hill equation:

$$P_t = 100\% / [1 + 10^{n_H (x - x_{50})}] \quad (\text{Eq. 1})$$

where n_H is the associated Hill coefficient, x is pSr or pCa and x_{50} is the pSr or pCa value where 50% of SrF_{\max} (pSr₅₀) or CaF_{\max} (pCa₅₀) was reached. When the P_t -pSr curves could not be fitted by the simple Hill equation with a correlation coefficient

$r^2 \geq 0.9990$, then the data points were fitted by a ‘composite’ Hill curve (consisting of the sum of two Hill curves; see also (Bortolotto *et al.*, 2000):

$$P_t = w_1 / [1 + 10^{n_{\text{Sr}1} (\text{pSr} - \text{pSr}_{50/1})}] + w_2 / [1 + 10^{n_{\text{Sr}2} (\text{pSr} - \text{pSr}_{50/2})}] \quad (\text{Eq. 2})$$

where w_1 and w_2 are normalized weighting factors ($w_1 + w_2 = 1$) referring to the slow (w_1) and fast (w_2) Sr^{2+} -sensitivity components, $n_{\text{Sr}1}$, $n_{\text{Sr}2}$ are the corresponding Hill coefficients and $\text{pSr}_{50/1}$, $\text{pSr}_{50/2}$ are the corresponding pSr₅₀ values for the two Hill curves. The above composite Hill curves fitted all P_t -pSr data point sets with a correlation coefficient $r^2 \geq 0.9990$. In Fig. 6.1b are shown P_t -pCa and P_t -pSr curves that have been fitted to the data points obtained from Fig. 6.1a using Eq. 1 and Eq. 2, respectively.

The following Sr^{2+} - and, where applicable, Ca^{2+} -activation parameters were determined for the individual skinned fibre segments: (i) maximum Sr^{2+} - or Ca^{2+} -activated force per cross sectional area ($\text{SrF}_{\max}/\text{CSA}$; $\text{CaF}_{\max}/\text{CSA}$; kN/m^2), (ii) pSr₅₀ or pCa₅₀ (sensitivity to $\text{Sr}^{2+}/\text{Ca}^{2+}$) if the data points were well fitted by a simple Hill equation or pSr_{50/1} and pSr_{50/2} if the data points were well fitted by the ‘composite’ Hill equation and (iii) n_{Sr} or n_{Ca} (minimum number of cooperating Sr^{2+} or Ca^{2+} -binding sites) if the data points were well fitted by a simple Hill equation or $n_{\text{Sr}1}$ and $n_{\text{Sr}2}$ if the data points were well fitted by the

'composite' Hill equation. SrF_{max}/CSA and CaF_{max}/CSA were determined from the amplitude of the force responses developed by the mechanically skinned fibre segment in the maximally Sr^{2+} - or Ca^{2+} -activating solutions at the end of the first pSr (or pCa) staircase run (Fig. 6.1a) and from its estimated cross-sectional area measured in paraffin oil before exposure to aqueous solutions.

6.2.6 Electrophoretic analyses of myofibrillar protein isoform composition

The Alanine-SDS-PAGE protocol was used to separate MHC isoforms in the single fibre segments as described in Chapter 2, while the TnC isoform composition was unambiguously identified electrophoretically on Glycine-SDS gels (see Chapter 2) using the method described in Chapter 4. In Fig. 6.1d is displayed the electrophoretogram of the low molecular weight (< 30 kDa) protein isoforms (note curvature in the TnC bands induced by the diffusion of EGTA from the adjacent left lane) for the fibre segment used to obtain the force responses shown in Fig. 6.1a. Since it was not possible to perform a full densitometric analysis of the curved TnC bands, the following procedure was adopted to quantify the percentage of the two TnC isoforms present in the preparation, (i) if only one curved band was visible on the gel then only one TnC species was ascribed to that fibre segment, (ii) if one curved band was clearly more intense than the other, then a 75%:25% ratio for the two TnC isoforms expressed was given and (iii) if the curved bands displayed similar intensities (like in Fig. 6.1d), then a 50%:50% ratio for the two TnC isoforms was given. Note that the limit of detection of any of the two TnC isoform bands was 5% of the total TnC present in the fibre segments used in this study (see Chapter 4).

6.2.6.1 Analysis of low molecular weight myofibrillar proteins (other than TnC) on SDS-PA gels

The isoforms of MLCs and TnI were resolved and visualized as illustrated in Figs. 6.2 and 6.3. The identity of the protein bands was established on the basis of their apparent electrophoretic mobility using as reference (i) low molecular weight markers, (ii) purified rat skeletal muscle myosin for MLC bands, (iii) relevant data reported in the literature for TnI isoforms (Simpson *et al.*, 2002), and (iv) typically pure fast-twitch and pure slow-twitch fibres from the extensor digitorum longus and soleus muscles of the rat. Note that the apparent molecular weight of the rat TnI isoforms as determined from the 16% gels in this study (~26 kDa for the slow skeletal and ~25 kDa for the fast skeletal isoforms) were close to those previously reported on 12% gels (~25 kDa for the slow skeletal and ~24 kDa for the fast skeletal isoforms, Simpson *et al.*, 2002). Tm and TnT isoforms were visualized and identified not individually, but as a group of bands (Tm + TnT; see Fig 6.3) located in the molecular weight range ~ 29-39 kDa, as predicted from the data of Muroya *et al.* (2003) and Mortola and Naso (1995).

6.2.7 Statistics

Results are expressed as mean \pm SEM. Two-tailed Student's t-test and ANOVA followed by Bonferroni post test were used, as appropriate, to determine the statistical significance of differences between fibre types with respect to contractile parameters.

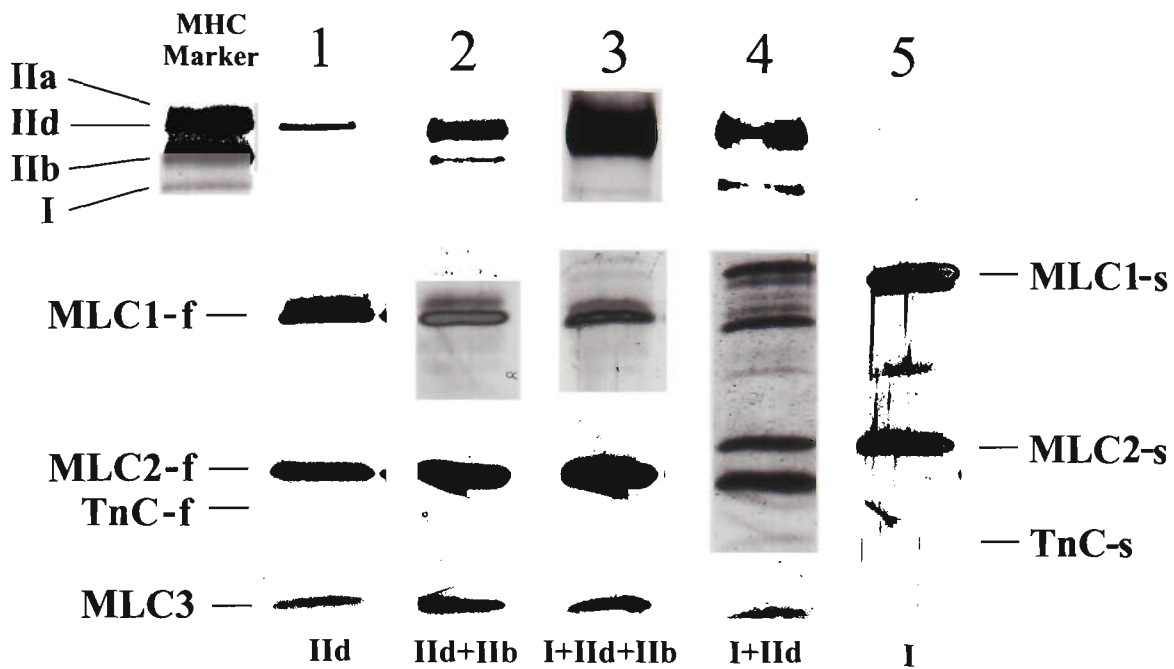


Fig. 6.2. Representative electrophoretograms showing the MHC and TnC isoforms detected in the single muscle fibers examined in this study. The fibers were classified according to their MHC and TnC isoform composition into one of five groups as follows; Lane 1: Group 1 fibers displayed one fast MHC isoform and TnC-f only; Lane 2: Group 2 fibers displayed two or more fast MHC isoforms and TnC-f only; Lane 3: Group 3 fibers displayed both fast and slow MHC isoforms but TnC-f only; Lane 4: Group 4 fibers displayed both fast and slow MHC isoforms and both TnC-f and TnC-s; Lane 5: Group 5 consisted of one fiber which contained the slow MHC and TnC-s only. The identity of the MHC isoforms present in the fibers illustrated in this Figure is shown under each lane.

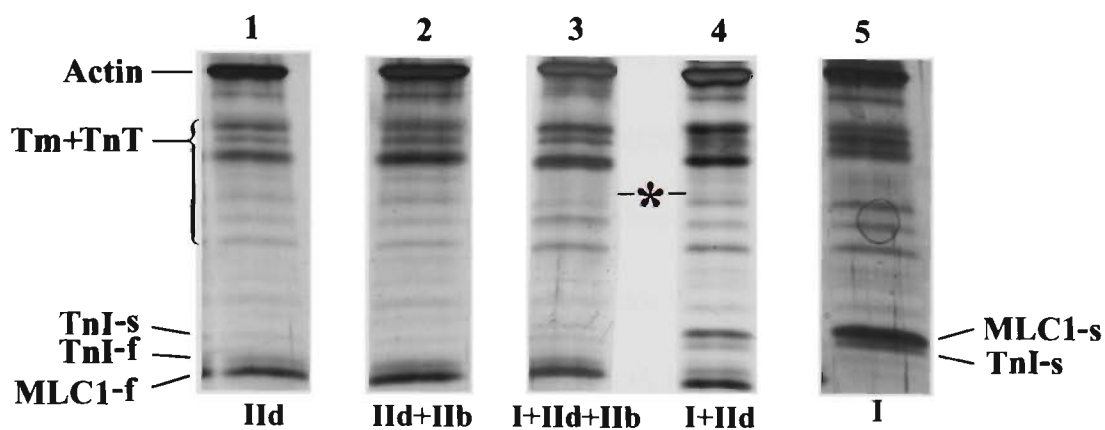


Fig. 6.3. Representative electrophoretograms showing typical regulatory protein isoform composition for each group. Lane 1: Group 1 fibre; Lane 2: Group 2 fibre; Lane 3: Group 3 fibre; Lane 4: Group 4 fibre; Lane 5: the slow Group 5 fibre. See Methods section for details of protein band identification. Note that Tm and TnT isoforms were visualized and identified not individually, but rather as a group of bands (Tm+TnT) located in the molecular weight range 29-39 kDa. The minor band indicated by the asterisk was detected in fibres from groups 3 and 4, but not in fibres from groups 1 and 2. The identity of the MHC isoforms present in the fibres illustrated in this figure is shown under each lane.

6.3 Results

In this study the contractile activation characteristics and myofibrillar protein isoform composition were determined in the same single fibre segments of rat diaphragm muscle. A representative set of data obtained from one of the 59 fibre segments examined is presented in Fig. 6.1a-d. The isometric force responses developed by the fibre segment in strongly Ca^{2+} - and Sr^{2+} -buffered solutions are presented in Fig. 6.1a. The amplitudes of these force responses were subsequently used to generate the P_r -pCa and P_r -pSr curves shown in Fig. 6.1b. At the end of the activation protocol, the fibre segment was placed in SDS-PAGE solubilising buffer for electrophoretic analyses of myofibrillar protein isoform composition. In Fig. 6.1c and 6.1d are shown the electrophoretograms of the MHC and some low molecular weight ($< \sim 30$ kDa) myofibrillar protein isoforms respectively. Note the EGTA-induced curvature of the TnC isoform bands, with TnC-s appearing higher than TnC-f on the electrophoretogram.

6.3.1 Myofibrillar protein isoform combinations in single fibres of rat diaphragm

Fibres were classified into five groups according to their electrophoretically determined MHC and TnC isoform composition (see Table 6.2): Group 1 ($n=41$), composed of fast-twitch fibres displaying a single fast MHC isoform and only TnC-f; Group 2 ($n=8$), composed of hybrid fast-twitch fibres displaying more than one (in this case two) fast MHC isoforms and only TnC-f; Group 3 ($n=4$), composed of hybrid fast- and slow-twitch fibres displaying fast and slow MHC isoforms but only TnC-f; Group 4 ($n=5$), composed of hybrid fast- and slow-twitch fibres displaying fast and slow MHC isoforms and both TnC-f and TnC-s and Group 5 ($n=1$) composed of one pure slow-twitch fibre displaying

Table 6.2. MLC, TnI, TnT+Tm isoform composition and Sr²⁺ activation characteristics of fibres classified by MHC and TnC isoform composition. Values are mean \pm SEM, the proportions of slow and fast MHC and TnC isoforms for relevant fibres are given in parentheses in the respective columns and the proportions for the slow and fast Sr²⁺-sensitivity components (w_1/w_2) of the force-pSr curve for relevant fibres are given in parentheses in the pSr₅₀ column.

Fibre group	MHC (%slow/% fast)	TnC (approx. % slow/%fast)	MLC1	MLC2	MLC3	TnI	TnT+Tm	SrF _{max} /CSA	pSr ₅₀ or pSr _{50T} /pSr _{50Z} (w_1/w_2)
1 (n=41)	IIId (n=40)	f	f	f	f	s+f	f	274 \pm 13 (n=40) 349	4.51 \pm 0.01 (n=40) 4.51
2 (n=8)	IIId+IIb	f	f	f	f	s+f	f	225 \pm 18 (n=8) 81	4.50 \pm 0.03 (n=8) 4.50
3 (n=4)	I+IIId+IIb (20/80)	f	s+f	s+f	f	s+f	f		
	I+IIa (18/82)	f	s+f	s+f	f	s+f	f	364	4.41
	I+IIId (5/95)	f	s+f	s+f	f	s+f	f	402	4.59
	I+IIId+IIb (6/94)	f	s+f	s+f	f	s+f	f	315	4.52
4 (n=5)	I+IIId (40/60)	s+f (25/75)	s+f	s+f	f	s+f	f	185	5.31/4.31 (31/69)
	I+IIId (33/67)	s+f (50/50)	s+f	s+f	f	s+f	f	169	5.38/4.27 (36/64)
	I+IIId (24/76)	s+f (25/75)	s+f	s+f	f	s+f	f	187	5.00/4.33 (28/72)
	I+IIId (38/62)	s+f (25/75)	s+f	s+f	f	s+f	f	107	5.37/4.54 (25/75)
	I+IIa+IIId (50/50)	s+f (50/50)	s+f	s+f	f	s+f	f	132	5.44/4.51 (65/35)
5 (n=1)	I	s	s	s	-	s	s	112	5.35

only slow MHC (MHCI) and TnC-s. Seven of the fibres examined in this study contained 'atypical' (Pette et al., 1999) MHC isoform combinations (I + IId + IIb - 2 fibres; I + IId - 5 fibres). Such deviations from the 'nearest neighbor rule', while rare in non-transforming muscles, were also found in rat sternomastoid muscle fibres in the study described in Chapter 5, and by Wu et al. (1998) in dog thyroarytenoid muscle fibres. Note that, in agreement with the results of the study described in Chapter 5, no fibres displaying two TnC isoforms and only one MHC isoform type were found in this study. The relative proportions of slow and fast MHC isoform types in fibres from Groups 3 and 4 were determined by densitometric analysis (see Chapter 2) and are indicated in parentheses in column 2.

Representative electrophoretograms showing the MHC, MLC and TnC isoform compositions of a fibre from each group are presented in Fig. 6.2, with the gel regions containing the other low molecular weight myofibrillar proteins from the same fibres shown in Fig. 6.3. The majority of fibres in Group 1 were of type **IID** and there was only one type **IIA** fibre. All fibres in Group 2 were type **IID+IIB** fibres. All the fibres in Groups 1 and 2 (lanes 1 and 2) appeared to contain only fast MLC isoforms and both fast and slow TnI isoforms. All fibres belonging to these two groups displayed the same pattern of Tm+TnT bands. The fibres in Groups 3 and 4 (lanes 3 and 4) appeared to contain both fast and slow MLC and TnI isoforms. The patterns of Tm+TnT bands detected in fibres from these two groups were very similar, but different from those of the fibres in groups 1 and 2 (note the minor band indicated by an asterisk in Fig. 3, which can be seen in lanes 3 and 4 but not in lanes 1 and 2). The type I fibre from Group 5 (lanes 5) displayed only slow MLC and TnI isoforms, and a Tm+TnT pattern that differed from

that of the other groups, particularly in the region of the three slowest migrating bands. When both TnC isoforms were detected in one fibre (as it was the case for Group 4 fibres, see Fig. 6.2, lane 4), their relative abundance was estimated visually by comparing the staining intensity of the TnC bands. As shown in Chapter 4, the presence of a population of TnC isoforms (fast or slow) could be routinely detected if it amounted to $\geq 5\%$ of the total TnC normally present in the fibre.

3.6.2 Sr^{2+} -activation characteristics of single fibres of rat diaphragm

Shown in Fig. 6.4 are representative Sr^{2+} -activation curves (P_t -pSr) for all five groups of fibres investigated. The sensitivity to Sr^{2+} was indicated by the pSr₅₀ descriptor (see Eq. 1 in section 6.2.5) if the data were fitted by a simple Hill curve, as it was the case for all fibres in Group 1 (Fig. 6.4a), Group 2 (Fig. 6.4b), Group 3 (Fig. 6.4c) and Group 5 (Fig. 6.4d). If the data points were fitted by a composite Hill curve, as it was the case for all fibres in Group 4 (Fig. 6.4d), then the sensitivity to Sr^{2+} was indicated by two pSr descriptors, pSr_{50/1} and pSr_{50/2} (see Eq. 2 in section 6.2.5). In the latter case, the fraction of the two functional components (w_1 and w_2) were also apportioned (characterized by pSr_{50/1} and pSr_{50/2} respectively). The values for pSr₅₀ or pSr_{50/1}/pSr_{50/2} and the proportions of w_1 and w_2 are summarized in the last column of Table 6.2.

Note that all fibres expressing only fast MHC isoforms (Groups 1 and 2) had pSr₅₀ values within a tight range around 4.50, characteristic of typical fast-twitch fibres (see Bortolotto *et al.*, 2000), even though all appeared to contain both fast and slow TnI isoforms. Also, fibres in Group 3 that expressed a combination of fast and slow MHC and MLC isoforms had pSr₅₀ values close to 4.50. Taken together these data indicate that a value of pSr₅₀

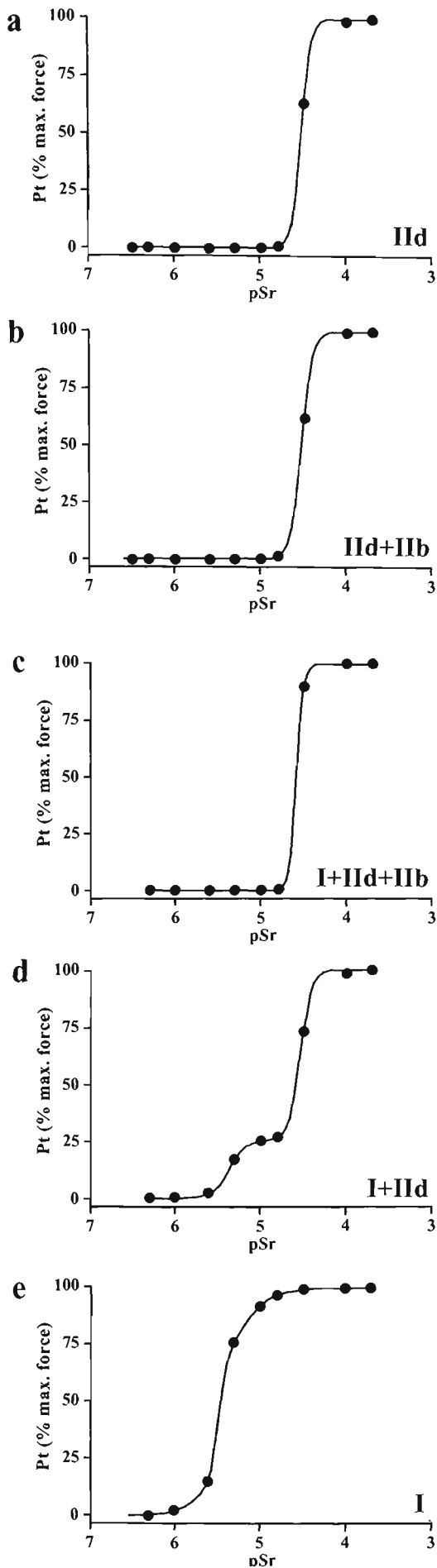


Fig. 6.4. Representative P_i -pSr curves of one fibre from each of the five groups, A: Group 1 (pure fast), $pSr_{50}=4.55$, $n_{Sr}=6.51$, $r^2=1.000$. B: Group 2 (fast-fast hybrid), $pSr_{50}=4.54$, $n_{Sr}=8.91$, $r^2=0.9998$.

C: Group 3 (fast-slow hybrid containing only TnC-f), $pSr_{50}=4.59$, $n_{Sr}=10.81$, $r^2=1.000$.

D: Group 4 (fast-slow hybrid containing both TnC-f and TnC-s), $pSr_{50/1}=5.37$, $pSr_{50/2}=4.54$, $n_{Sr1}=3.79$, $n_{Sr2}=3.39$. Note that the data points for Group 4 fibres could not be fitted to Eq. 1 (see Methods) with $r^2>0.9990$, however using Eq. 2 (see Methods) the curve fit the data points of this representative fibre with $r^2=0.9998$.

E: Group 5 (pure slow) $pSr_{50}=5.35$, $n_{Sr}=3.67$, $r^2=0.9998$. The solid lines are the Hill curves fitted through the experimental data points.

The identity of the MHC isoforms present in the fibres illustrated in this figure is shown on the respective diagram.

close to 4.50 was not tightly correlated with the MHC, MLC or TnI isoform composition of the fibres.

It had previously been shown that the sensitivity to Sr^{2+} of typically slow-twitch fibres is characterized by pSr_{50} values that are 0.7-0.9 log units greater than those of fast-twitch fibres (Bortolotto *et al.*, 2000). Consistent with these data, the pSr_{50} value determined for the only typical slow twitch-fibre detected among the 59 diaphragm fibres examined in this study was 5.35. (Note that all myofibrillar protein isoforms in this fibre appear to be of the slow type). This value is very close to the average value for pSr_{50} (5.36 ± 0.10) of a group of four pure type I rat diaphragm fibres comprising the fibre presented in Table 6.2, a fibre described in the study of Bortolotto *et al.* (2000) and two other fibres originating from different strains of rats (Zucker obese and Zucker lean; unpublished data).

A further look at the results obtained for Groups 3 and 4 indicates that the only difference between these two fibre groups, with respect to the myofibrillar protein isoform composition, relates to the TnC isoforms, with fibres in Group 3 expressing only TnC-f and fibres in Group 4 expressing both TnC-f and TnC-s. The presence of both TnC isoforms in Group 4 fibres was tightly associated with the occurrence of 'composite Sr^{2+} -activation curves' characterized by the $\text{pSr}_{50/1}$ and $\text{pSr}_{50/2}$ descriptors with the values of the $\text{pSr}_{50/1}$ being close to the pSr_{50} value of the fibre that expressed only the TnC-s (Group 5) and the values of the $\text{pSr}_{50/2}$ being in the vicinity of the pSr_{50} value typical of fibres that expressed only TnC-f (Groups 1-3). Thus, the data in Table 6.2 unequivocally show that the lower sensitivity to Sr^{2+} ($\text{pSr} \sim 4.5$) is directly correlated with the presence of TnC-f

isoform while the higher sensitivity to Sr^{2+} ($p\text{Sr} \sim 5.4$) is directly correlated with the presence of TnC-s isoform. Indeed, the relative abundance of the slow and fast TnC isoforms detected in Group 4 fibres (column 3) is well reflected in the proportion of the 'slow-type' and 'fast-type' Sr^{2+} -sensitivity components (w_1/w_2 ; last column in Table 6.2) in the 'composite Sr^{2+} -activation curves' of the fibres. This is shown in Fig. 6.5 where the relative proportion of 'slow type' Sr^{2+} -sensitivity component (w_1 , functional descriptor of TnC isoform, y-axis) for all fibres was plotted against the estimated proportion of TnC-s isoform (biochemical descriptor of TnC isoform, x-axis) detected in the respective fibres.

The line of best fit in Fig. 6.5 passes in very close proximity to the origin on the graph axes, has a slope of 1.01 ± 0.02 and displays a very high correlation coefficient ($r^2=0.97$), suggesting that both the functional and biochemical parameters describe the same population of TnC in the fibre. This population of TnC is most likely that which is assembled in the myofilaments, since (i) only TnC fully assembled in the myofilaments would render the contractile response sensitive to divalent cations, and (ii) only TnC tightly associated with, or most likely fully assembled in, the myofilament structure (ie. 'unwashable' TnC) would be detectable by electrophoretic analysis of skinned fibre segments that had been exposed to aqueous solutions for ~ 10 min prior to incubation in the SDS-PAGE solubilizing buffer. Note that under these conditions one could routinely detect the presence of a functional slow TnC isoform when its functional contribution was above 5%, as demonstrated by the finding that theoretical composite curves with a slow type component ($w_1 \geq 0.04$) could not be fitted by a simple Hill equation (Eq. 1) with $r^2 \geq 0.9990$ and therefore required fitting with Eq. 2.

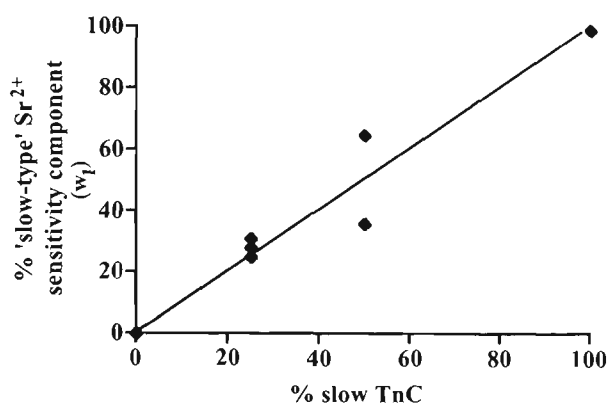


Fig. 6.5. Graph showing the relationship between the estimated amount of TnC-s in single pure and hybrid fibre segments ($n=59$) and the proportion of the 'slow-type' (w_1) Sr^{2+} -sensitivity component of the force-pSr curve produced by the fibres.

With respect to SrF_{max}/CSA there were no statistically significant differences (ANOVA $p > 0.05$), between fibres in Group 1 ($274 \pm 13 \text{ kNm}^{-2}$), Group 2 ($225 \pm 18 \text{ kNm}^{-2}$) and Group 3 ($290 \pm 72 \text{ kNm}^{-2}$). However, fibres in Group 4 produced significantly lower maximum Sr^{2+} -activated specific forces ($156 \pm 15 \text{ kNm}^{-2}$) than fibres in Group 1 (ANOVA, $p < 0.05$), as did the fibre in Group 5 (112 kNm^{-2}). The Hill coefficients for the force-pSr curves were 10.68 ± 1.50 (Group 1, $n=33$), 6.50 ± 0.32 (Group 2; $n=8$), 8.50 ± 1.59 (Group 3, $n=4$), 5.56 ± 2.11 (fast component) and 3.76 ± 0.21 (slow component) (Group 4, $n=5$) and 3.69 (Group 5, $n=1$). A two tailed Student's t-test found that the n_{Sr} values for Group 1, Group 2, Group 3 and the fast-type Sr^{2+} -sensitivity component of Group 4 fibres were not significantly different from one another, but all were significantly higher than the n_{Sr} values for both the slow-type Sr^{2+} -sensitivity component of Group 4 fibres and the pure slow fibre in Group 5 ($p < 0.05$).

3.6.3.1 Other contractile activation characteristics

Regarding the descriptors of force-pCa curves, the pCa_{50} (5.68 ± 0.04 , $n=5$) and Hill coefficient values (4.79 ± 0.46 , $n=5$) for fibres containing both TnC-f and TnC-s isoforms (Group 4) were significantly smaller ($p < 0.05$; Student's two tailed t-test) than the corresponding pCa_{50} (5.78 ± 0.02 , $n=5$) and Hill coefficient values (6.14 ± 0.49 , $n=5$) for fibres containing only TnC-f (eg. fibres from Group 1). The only pure slow-twitch fibre in Group 5 had a pCa_{50} value of 5.68 and a Hill coefficient of 3.72. For all fibres that were also maximally activated in Ca^{2+} solutions (five Group 1 fibres, all Group 4 fibres and one Group 5 fibre; see Methods), the ratio SrF_{max}/CaF_{max} was close to 1.00 (0.95 ± 0.01 , $n=5$ for Group 1; 0.96 ± 0.03 , $n=5$ for Group 4 and 1.05 for the fibre in Group 5).

6.4 Discussion

This study has unequivocally shown that in isometrically contracting fibres of the rat diaphragm muscle, the presence of the fast TnC isoform confers a much lower sensitivity to Sr^{2+} (by a factor of about 7) than the presence of the slow TnC isoform. Thus, (i) all fibres that displayed only TnC-f (Groups 1-3) presented a consistent pSr_{50} value of about 4.5 ($[\text{Sr}^{2+}] = 3.15 \times 10^{-5} \text{ M}$) regardless of the MHC, MLC, TnI, and Tm+TnT isoform composition, (ii) the fibre in Group 5 that displayed only the TnC-slow isoform, as well as three other pure type I rat diaphragm fibres (see Results) had an average pSr_{50} value of 5.36 ($[\text{Sr}^{2+}] = 4.37 \times 10^{-6} \text{ M}$) and (iii) all fibres that displayed both TnC isoforms (Group 4) produced composite force- pSr activation curves made up of two functional components, one characterized by high sensitivity to Sr^{2+} ($\text{pSr}_{50/1}$ value around 5.36) and the other by low sensitivity to Sr^{2+} ($\text{pSr}_{50/2}$ values around 4.5). Moreover, the proportion of one of the two functional components (the slow component, w_1) derived from fitting the composite curves to the data points was directly proportional to the relative proportion of the respective TnC isoform (TnC-s) detected electrophoretically in the individual fibres (Table 6.2 and Fig. 6.5).

As mentioned in section 6.1, previous TnC isoform substitution studies have led to conflicting conclusions with respect to the role of TnC in determining sensitivity to Sr^{2+} of contractile activation processes. It is highly likely that the disagreement between the various groups concerning the major determinant of Sr^{2+} -sensitivity differences in mammalian skeletal muscle is due to the inherent problems of the extraction-

reconstitution experiments and to the inadequacy of the protocols used to resolve, visualize and identify the TnC isoforms in TnC extracted/reconstituted fibres. In the present study, single skeletal muscle fibres displaying a wide range of *naturally occurring* combinations of myofibrillar protein isoforms were used, thus avoiding the inherent drawbacks of the extraction/reconstitution experiments. Furthermore, the method used for electrophoretic identification of TnC isoforms (see Chapter 4) *also* allowed densitometric MHC isoform analysis *and* Sr^{2+} -activation measurements to be performed on the same single fibre segments. The results obtained lead to the clear-cut conclusion that skeletal muscle fibre-type differences in sensitivity to Sr^{2+} of contractile activation processes are determined primarily by the difference in TnC isoform composition.

The results of this study provide us with further insight into the functional and molecular expression of TnC isoforms in relation to the molecular expression of MHC isoform type. In Fig. 6.6 are plotted the percentage of 'slow-type' Sr^{2+} -sensitivity component (w_1 , the functional indicator of slow TnC isoform; circles, left y-axis) and the proportion of the slow TnC isoform, estimated visually (asterisks, right y-axis), against the proportion of the slow-type MHC isoform, determined densitometrically (x-axis) using data points collected from all 59 single fibre segments examined in this study. The sigmoidal curve shown in Fig. 6.6 highlights the trend followed by the experimental data. Several conclusions can be drawn from this graph. First, the data show that the levels of TnC isoform expression of a fibre, as measured by either functional or electrophoretic means, display a similar relationship to the MHC isoform type composition of the fibre. This further supports the earlier argument (see section 6.3.2, p. 106) that the functional and biochemical analyses performed in this study define the same population of TnC, *viz.* the

TnC assembled in the myofilaments. Second, the profile of the sigmoidal curve shown in Fig. 6.6 (which reflects the absence of fibres containing both TnC isoforms in combination with only one MHC isoform type), suggests that the assembly of TnC in the myofilaments does not occur prior to that of the MHC protein. Furthermore, from the inflection points of the curve shown in Fig. 6.6 one can deduce that a TnC isoform (in this case TnC-s) is assembled in myofibrils, thus becoming functional, only when the proportion of the matching MHC isoform type (in this case the slow MHC I) reaches values higher than about 20%.

Based on the relationships between sensitivity to Sr^{2+} , TnC isoform and MHC isoform type composition established from the graph in Fig. 6.6, one can predict that MHC hybrid fibres that display slow to fast MHC isoform ratios in the range 0.2 to 0.8 are also likely to display hybrid TnC profiles and 'composite' Sr^{2+} -activation curves. Furthermore, these relationships provide the basis for predicting two of the above three parameters when the third is determined experimentally in pure and hybrid fibres. Here it is important to stress that from data on TnC isoform expression obtained by either the functional or the biochemical protocols described in this study, one is able to predict only the *type* of MHC present, but not the number or identity of the individual MHC isoforms.

The mechanism responsible for the higher Sr^{2+} -sensitivity of the contractile apparatus in fibres expressing the slow TnC isoform than in fibres expressing the fast TnC isoform is most likely related to differences with respect to the affinity for Sr^{2+} of the two TnC isoforms. A corollary of this is that the affinity of the regulatory site II for Sr^{2+} (but not Ca^{2+}) is much greater if the regulatory site I is inactive (as is the case for the slow TnC

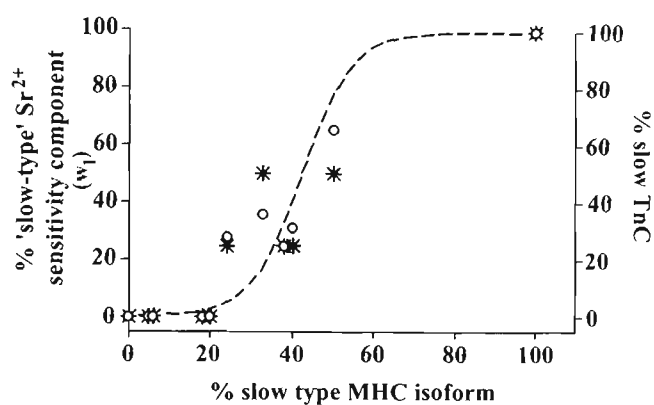


Fig. 6.6. Graph showing the relationship between the proportion of TnC-s, estimated electrophoretically (indicated by asterisks, right y-axis), the proportion of the 'slow-type' Sr²⁺ sensitivity component (w_1) of the force-pSr curve (indicated by circles, left y-axis) and the proportion of slow MHC isoform present in each fibre (x-axis). The sigmoidal curve indicating the trend followed by the data was generated using the non-linear regression (variable slope) option provided by Graphpad Prism.

isoform) than when site I is functional (as is the case with the TnC fast isoform). This idea is consistent with the findings reported by others (eg. Sweeney *et al.*, 1990; Pearlstone *et al.*, 2000). The loss of site I in TnC-s is also most likely to be responsible for the significantly smaller Hill coefficient associated with the slow P_r -pSr curves or slow force components.

It is worth noting then that within a given fibre, the affinities of the Ca^{2+} (and likely Sr^{2+}) binding sites for divalent cations are also affected by the incorporation of TnC in the troponin complex, the incorporation of the troponin complex into the thin filament structure (Zot *et al.* 1986) and by the interactions between myosin and actin filaments (Bremel and Weber, 1972; Morris *et al.*, 2001). One should also keep in mind that there are many other factors that can alter the sensitivity of the contractile apparatus for Ca^{2+} and Sr^{2+} without altering the binding properties of TnC for the activator (Gordon *et al.*, 2000). Therefore, in absolute terms, the sensitivity to Sr^{2+} and Ca^{2+} of the contractile activation process in an individual fibre is ultimately dependent not only on the molecular species of TnC, but also on the complex interactions between TnC and other molecular entities. Indeed, the only typical slow-twitch fibre in group 5, expressing only TnC-s, appeared to be less rather than more sensitive to Ca^{2+} than any of the fast-twitch fibres in Group 1, a result contrary to previous observations from this laboratory using similar activating solutions (eg. Bortolotto *et al.*, 2000), but consistent with another study on diaphragm muscle (Eddinger and Moss, 1987). Moreover, all composite fibres in Group 4, which expressed both TnC isoforms, displayed a significantly reduced sensitivity to Ca^{2+} compared with the fast-twitch fibres in Group 1. This result suggests that an increased apparent sensitivity to Sr^{2+} conferred by the expression of the TnC slow isoform

is not also translated into an equivalent increase in Ca^{2+} -sensitivity. If so, the conformational changes induced by Sr^{2+} binding to the TnC isoforms in the Ca^{2+} -regulatory system may be different from those induced by the binding of Ca^{2+} to the same isoforms. This is not surprising considering that in some skeletal muscle fibres, Sr^{2+} is unable to induce the full activation of the contractile apparatus (Stephenson and Williams, 1980; West and Stephenson, 1993).

Notwithstanding the contribution of the various interactions between TnC and other myofibrillar molecular entities to the precise sensitivity of the contractile apparatus to activating divalent cations, the very marked difference between the affinities of the TnC-s and TnC-f isoforms for Sr^{2+} (but not for Ca^{2+}) is translated into clear cut differences in the relative sensitivities to Sr^{2+} (but not to Ca^{2+}) of the contractile apparatus, irrespective of the other interactions between myofibrillar components.

The composite fibres in Group 4, expressing both fast and slow TnC isoforms, also produced significantly lower maximal Sr^{2+} - and Ca^{2+} -activated specific force responses compared with the other fibres in Groups 1-3 that expressed only the TnC-fast isoform. The $\text{SrF}_{\text{max}}/\text{CSA}$ and $\text{CaF}_{\text{max}}/\text{CSA}$ values in the composite fibres in Group 4 were however similar to the respective values of two slow (type I MHC) diaphragm fibres (one in Group 5 of this study, and one in an earlier study on diaphragm muscle from this laboratory; Bortolotto *et al.*, 2000). Therefore, the reduced force level produced in these fibres cannot be simply ascribed to the co-existence of the two TnC isoforms. Regarding the steepness of the P_r -pCa curves, the Group 4 fibres displayed Hill coefficients that were intermediate between the Hill coefficients associated with the pure fast fibres (Group 1) and the two

slow diaphragm fibres mentioned above, suggesting that these fibres would be active over a broader range of $[Ca^{2+}]$ than the most abundant group of fibres (**IID**) commonly detected in the rat diaphragm muscle.

In conclusion, the results obtained in this study with pure and hybrid rat diaphragm muscle fibres show clearly that differences with respect to Sr^{2+} -dependence of contractile activation processes between MHC-based fibre types are determined by the molecular species of TnC protein present in the fibres, with the presence of TnC-slow isoform conferring on average a ~ 7 fold greater sensitivity to Sr^{2+} than the TnC-fast isoform. These results also have direct practical importance because they validate the use of differential sensitivities to Sr^{2+} to distinguish between fibres containing different proportions of fast and slow TnC isoforms and provide the basis for predicting either sensitivity to Sr^{2+} , TnC isoform composition or MHC isoform type composition of pure and hybrid fibres when only one of these parameters is determined experimentally.

Concluding remarks

The investigations presented in this thesis have produced several notable methodological and conceptual contributions to the area concerned with the polymorphism of TnC isoforms in rat (mammalian) skeletal muscle. These include:

- (1) Evidence that Potter's purification procedure for troponin subunits (1982) can be used with slight modifications to successfully purify rat skeletal muscle TnC isoforms from small amounts of tissue.
- (2) The tryptic peptide maps produced by the rat TnC-f and TnC-s isoforms are different to one another, but are the same as those produced by the commercially purified rabbit skeletal TnC-f and human cardiac TnC-s isoforms, respectively.
- (3) Compelling evidence of the potential methodological artefacts associated with determination of TnC isoforms in single fibres based only on the relative electrophoretic mobility of the TnC isoform bands.
- (4) A simple, rapid and inexpensive method for definitive determination of TnC isoform composition in electrophoretically fibre-typed (based on MHC isoform composition) single muscle fibres. The method was validated using the purified rat TnC isoforms.
- (5) Evidence that MHC and TnC isoforms exist in specific combinations in non-transforming rat skeletal muscle fibres, such that all fibres that contain only one MHC isoform (slow or fast) contain only the matching TnC isoform, and all fibres that

contain multiple fast MHC isoforms contain only the fast TnC isoform. Fibres expressing both slow and fast MHC isoforms display either both TnC isoforms, or only one TnC isoform of a type dependent on the relative proportion of fast/slow MHC present.

(6) Compelling evidence that fibre-type related differences in Sr^{2+} -activation are primarily determined by TnC isoform composition.

(7) Evidence that differences with respect to Sr^{2+} -dependence of contractile activation processes between MHC-based fibre types are determined by the molecular species of TnC protein present in the fibres, with the presence of TnC-s isoform conferring a higher sensitivity to Sr^{2+} than the TnC-f isoform. These results have direct practical importance because they validate the use of differential sensitivities to Sr^{2+} to distinguish between fibres containing different proportions of fast and slow TnC isoforms and provide the basis for predicting either sensitivity to Sr^{2+} , TnC isoform composition or MHC isoform type composition of pure and hybrid fibres when only one of these parameters is determined experimentally.

Bibliography

Adhikari BB and Wang K. Interplay of troponin- and myosin-based pathways of calcium activation in skeletal and cardiac muscle: the use of W7 as an inhibitor of thin filament activation. *Biophys. J.* 86: 359-70, 2004.

Akella AB, Su H, Sonnenblick EH, Rao VG, and Gulati J. The cardiac troponin C isoform and the length dependence of Ca^{2+} sensitivity of tension in myocardium. *J. Mol. Cell Cardiol.* 29: 381-389, 1997.

Babu A, Pemrick S, and Gulati J. Ca^{2+} activation of troponin C-extracted vertebrate striated fast-twitch muscle fibres. *FEBS Lett.* 203: 20-24, 1986.

Babu A, Scordilis SP, Sonnenblick EH, and Gulati J. The control of myocardial contraction with skeletal fast muscle troponin C. *J. Biol. Chem.* 262: 5812-5822, 1987.

Babu A, Su H, Ryu Y, and Gulati J. Determination of residue specificity in the EF-hand of troponin C for Ca^{2+} coordination, by genetic engineering. *J. Biol. Chem.* 267: 15469-15474, 1992.

Berg JS, Powell BC, and Cheney RE. A millennial myosin census. *Mol. Biol. Cell.* 12: 780-794, 2001.

Bottinelli R, Canepari M, and Reggiani C. Myofibrillar ATPase activity during isometric contraction and isomyosin composition in rat single skinned muscle fibres. *J. Physiol. (Lond.)*. 481: 663-675, 1996.

Bottinelli R, Schiaffino S, and Reggiani C. Force-velocity relations and myosin heavy chain isoform compositions of skinned fibres from rat skeletal muscle. *J. Physiol.* 437: 655-672, 1991.

Bortolotto SK, Cellini M, Stephenson DG, and Stephenson GMM. MHC isoform composition and Ca^{2+} - or Sr^{2+} -activation properties of rat skeletal muscle fibres. *Am. J. Physiol. Cell Physiol.* 279: C1564-C1577, 2000.

Brandt PW and Schachat FH. Troponin C modulates the activation of thin filaments by rigor cross-bridges. *Biophys. J.* 72, 2262-2267, 1997.

Bremel RD and Weber A. Cooperation within actin filaments in vertebrate skeletal muscle. *Nature New Biol.* 238: 97-101, 1972.

Briggs MM, Klevit RE, and Schachat FH. Heterogeneity of contractile proteins. Purification and characterization of two species of troponin T from rabbit fast skeletal muscle. *J. Biol. Chem.* *J. Biol. Chem.* 259: 10369-10375, 1984.

Burgess WH, Jemiolo DK, and Kretsinger RH. Interaction of calcium and calmodulin in the presence of sodium dodecyl sulfate. *Biochim. Biophys. Acta* 632: 257-270, 1980.

Burke M and Kamalakannan V. Effect of tryptic cleavage on the stability of myosin subfragment 1. Isolation and properties of the severed heavy-chain subunit. *Biochemistry*. 24: 846-852, 1985.

Chao SH, Bu CH, and Cheung WY. Activation of troponin C by Cd^{2+} and Pb^{2+} . *Arch. Toxicol.* 64: 490-496, 1990.

Cleveland DW, Fischer SG, Kirschner MW, and Laemmli UK. Peptide mapping by limited proteolysis in sodium dodecyl sulfate and analysis by gel electrophoresis. *J. Biol. Chem.* 252: 1102-1106, 1977.

Cohen P, Klee CB, Picton C, and Shenolikar S. Calcium control of muscle phosphorylase kinase through the combined action of calmodulin and troponin. *Ann. N.Y. Acad. Sci.* 356, 151-161, 1980.

Collins JH, Greaser ML, Potter JD, and Horn MJ. Determination of the amino acid sequence of troponin C from rabbit skeletal muscle. *J. Biol. Chem.* 252: 6356-6362, 1977.

Collins JH. Myosin light chains and troponin C: structural and evolutionary relationships revealed by amino acid sequence comparisons. *J. Muscle Res. Cell Motil.* 12: 3-25, 1991.

Cordonnier C, Stevens L, Picquet F, and Mounier Y. Structure-function relationship of soleus muscle fibres from the rhesus monkey. *Pflugers Arch.* 430: 19-25, 1985.

- Cox JA, Comte M, and Stein EA. Calmodulin-free skeletal-muscle troponin C prepared in the absence of urea. *Biochem. J.* 195: 205-211, 1981.
- Cummins P and Perry SV. The subunits and biological activity of polymorphic forms of tropomyosin. *Biochem. J.* 133: 765-777, 1973.
- Danieli-Betto D, Betto R, and Midrio M. Calcium sensitivity and myofibrillar protein isoforms of rat skinned skeletal muscle fibres. *Pflugers Arch.* 417: 303-308, 1990.
- da Silva AC and Reinach FC. Calcium binding induces conformational changes in muscle regulatory proteins. *Trends. Biochem. Sci.* 16: 53-57, 1991.
- Demaille J, Dutruge E, Eisenberg E, Capony J-P, and Pechere J-F. Troponins C from reptile and fish muscles and their relation to muscular parvalbumins. *FEBS Lett.* 42: 173-178, 1974.
- Ebashi S. Third component participating in the precipitation of 'natural actomyosin'. *Nature* 200: 1010, 1963.
- Ebashi S and Ebashi F: A new protein component participating in the superprecipitation of myosin. *J. Biochem.* 55: 604-613, 1964.

Ebashi S, Kodama A, and Ebashi F. Troponin I. Preparation and physiological function. *J. Biochem. (Tokyo)*. 64: 465-477, 1968.

Eddinger TJ and Moss RL. Mechanical properties of skinned single fibres of identified types from rat diaphragm. *Am. J. Physiol. Cell Physiol.* 22: C210-C218, 1987.

Fink RH, Stephenson DG, and Williams DA. Calcium and strontium activation of single skinned muscle fibres of normal and dystrophic mice. *J. Physiol. (Lond)*. 373: 513-525, 1986.

Fuchs F and Wang YP. Force, length and Ca^{2+} -troponin C affinity in skeletal muscle. *Am. J. Physiol. Cell Physiol.* 261: C787-C792, 1991.

Galler S, Schmitt TL, and Pette D. Stretch activation, unloaded shortening velocity, and myosin heavy chain isoforms of rat skeletal muscle fibres. *J. Physiol.* 478: 513-521, 1994.

Geiger PC, Cody MJ, and Sieck GC. Force-calcium relationship depends on myosin heavy chain and troponin isoforms in rat diaphragm muscle fibres. *J. Appl. Physiol.* 87: 1894-1900, 1999.

Gomez AV, Potter JD, and Szczesna-Corday D. The role of troponins in muscle contraction. *IUBMB Life*. 54: 323-333, 2002.

Gordon AM, Homsher E, and Regnier M. Regulation of contraction in striated muscle. *Physiol. Rev.* 80: 853-924, 2000.

Grab DJ, Berzins K, Cohen RS, and Siekevitz P. Presence of calmodulin in postsynaptic densities isolated from canine cerebral cortex. *J. Biol. Chem.* 254: 8690-8696, 1979.

Grabarek A, Drabikowski W, Vinokurov L, and Lu RC. Digestion of troponin C with Trypsin in the presence of Ca^{2+} . Identification of cleavage points. *Biochim. Biophys. Acta* 671: 227-233, 1981.

Grant RJA, Shenolikar S, and Cohen P. The amino acid sequence of the δ subunit (calmodulin) of rabbit skeletal muscle phosphorylase kinase. *Eur. J. Biochem.* 113: 359-367, 1981.

Greaser ML and Gergely J. Reconstitution of Troponin activity from three protein components. *J. Biol. Chem.* 246: 4226-4233, 1971.

Greaser ML and Gergely J. Purification and properties of the components from Troponin. *J. Biol. Chem.* 248: 2125-2133, 1973.

Greene LE and Eisenberg E. Cooperative binding of myosin subfragment 1 to the actin-troponin-tropomyosin complex. *Proc. Natl. Acad. Sci. USA* 77: 2616-2620, 1980.

Gulati J, Scordilis S, and Babu A. Effect of troponin C on the cooperativity in Ca^{2+} activation of cardiac muscle. *FEBS Lett.* 236: 441-444, 1988.

Guth K and Pottter JD. Effect of rigor and cyclic cross-bridges on the structure of troponin C and on the Ca^{2+} affinity of the Ca^{2+} specific regulatory sites in skinned rabbit psoas fibres. *J. Biol. Chem.* 262: 13627-13635, 1987.

Hai H, Sano K-I, Maeda K, Maeda Y, and Miki M. Ca^{2+} - and S1-induced conformational changes of reconstituted skeletal muscle thin filaments observed by fluorescence energy transfer spectroscopy: structural evidence for three states of thin filament. *J. Biochem.* 131: 407-418, 2002.

Hannon JD, Chase BC, Martyn DA, Huntsman LL, Kushmerick MJ, and Gordon, AM. Calcium-independent activation of skeletal muscle fibers by a modified form of cardiac troponin C. *Biophys. J.* 64: 1632-1637, 1993.

Hartner K-T, Kirschbaum PJ, and Pette D. The multiplicity of troponin T isoforms. Distribution in normal rabbit muscles and effects of chronic stimulation. *Eur. J. Biochem.* 179: 31-38, 1989.

Head JF and Perry SV. The interaction of the calcium-binding protein (Troponin C) with bivalent cations and the inhibitory protein (Troponin I). *Biochem. J.* 137: 145-154, 1974.

- Head JF, Weeks RA, and Perry SV. Affinity-chromatographic isolation and some properties of troponin C from different muscle types. *Biochem. J.* 161: 465-471, 1977.
- Heeley DH, Golosinska K, and Smillie LB. The effects of troponin T fragments T1 and T2 on the binding of nonpolymerizable tropomyosin to F-actin in the presence and absence of troponin I and troponin C. *J. Biol. Chem.* 262: 9971-9978, 1987.
- Hitchcock-DeGregori SE, Lewis SF and Chou T. Tropomyosin lysine reactivities and relationship to coiled-coil structure. *Biochemistry.* 24: 3305-3314, 1985.
- Hoar PE, Potter JD, and Kerrick WGL. Skinned ventricular fibres: troponin C extraction is species-dependent and its replacement with skeletal troponin C changes Sr^{2+} activation properties. *J. Muscle Res. Cell Motil.* 9: 165-173, 1988.
- Hochachka PW. Muscles as molecular and metabolic machines, CRC Press, USA, 1994.
- Huxley HE. *Cold Spring Symp. Quant. Biol.* 37: 361-376, 1972.
- Huxley AF and Niedergerke R. Structural changes in muscle during contraction. Interference microscopy of living muscle fibres. *Nature*, 173: 971-973, 1954.
- Huxley HE and Hanson J. Changes in the cross-striations of muscle during contraction and stretch and their structural interpretation. *Nature*, 173: 973-976, 1954.

Kerrick WGL, Malencik DA, Hoar PE, Potter JD, Coby RL, Pocinwong S, and Fischer EH. Ca^{2+} and Sr^{2+} activation: Comparison of cardiac and skeletal muscle contraction models. *Pflügers Archiv*. 386: 207-213, 1980.

Kerrick WGL, Zot HG, Hoar PE, and Potter JD. Evidence that the Sr^{2+} activation properties of cardiac Troponin C are altered when substituted into skinned skeletal muscle fibers. *J. Biol. Chem*. 260: 15687-15693, 1985.

Kischel P, Bastide B, Potter JD, and Mounier Y. The role of the Ca^{2+} regulatory sites of skeletal troponin C in modulating muscle fibre reactivity to the Ca^{2+} sensitizer bepridil. *Br. J. Pharmacol*. 131: 1496-502, 2000.

Kischel P, Bastide B, Stevens L, and Mounier Y. Expression and functional behavior of troponin C in soleus muscle fibres of rat after hindlimb unloading. *J. Appl. Physiol*. 90: 1095-1101, 2001.

Li H-C and Fajer PG. Structural coupling of troponin C and actomyosin in muscle fibres. *Biochemistry*. 37: 6628-6635, 1998.

Lorenz M, Poole KJ, Popp D, Rosenbaum G, and Holmes KC. An atomic model against x-ray fiber diffraction data by the use of a directed mutation algorithm. *J. Mol. Biol*. 246: 108-119, 1995.

Maita T, Yajima E, Nagata S, Miyanishi T, Nakayama S, and Matsuda G. The primary structure of skeletal muscle myosin heavy chain: IV. Sequence of the rod, and the complete 1,938-residue sequence of the heavy chain. *J. Biochem. (Tokyo)*. 110: 75-87, 1991.

Malencik DA, Heizmann CW, and Fisher EH. Structural proteins of dogfish skeletal muscle. *Biochemistry* 14: 715-721, 1975.

Marieb EN. Human Anatomy and Physiology (5th Edition), Benjamin/Cummings Publishing Company Addison Wesley Longman, USA, 2001.

Martyn DA, Freitag CJ, Xu D, and Gordon AM. Ca^{2+} and cross-bridge-induced changes in troponin C in skinned skeletal muscle fibers: effects of force inhibition. *Biophys. J.* 76: 1480-1493, 1999.

McKillop DF and Geeves MA. Regulation of the interaction between actin and myosin subfragment 1: evidence for three states of the thin filament. *Biophys. J.* 65: 693-701, 1993.

Metzger JM. Effects of troponin C isoforms on pH sensitivity of contraction in mammalian fast and slow skeletal muscle fibres. *J. Physiol.* 492: 163-172, 1996.

Moraczewska J. Structural determinants of cooperativity in acto-myosin interactions. *Acta Biochim. Pol.* 49: 805-812, 2002.

Morimoto S. The effect of Mg^{2+} on the Ca^{2+} binding to troponin C in rabbit fast skeletal myofibrils. *Biochim. Biophys. Acta.* 1073: 336-340, 1991.

Morimoto S. Effect of myosin cross-bridge interaction with actin on the Ca^{2+} -binding properties of troponin C in fast skeletal myofibrils. *J. Biochem. (Tokyo)*. 109: 120-6, 1991.

Morimoto S and Ohtsuki I. Ca^{2+} - and Sr^{2+} -sensitivity of the ATPase activity of rabbit skeletal myofibrils: Effect of the complete substitution of troponin C with cardiac troponin C, calmodulin, and parvalbumins. *J. Biochem. (Tokyo)*. 101: 291-301, 1987.

Morris CA, Tobacman LS, and Homsher E. Modulation of contractile activation in skeletal muscle by a calcium-insensitive troponin C mutant. *J. Biol. Chem.* 276: 20245-20251, 2001.

Mortola JP and Naso L. Electrophoretic analysis of contractile proteins of the diaphragm in chronically hypoxic rats. *Am. J. Physiol.* 269: L371-L376, 1995.

Moss RL. Ca^{2+} regulation of mechanical properties of striated muscle. Mechanistic studies using extraction and replacement of regulatory proteins. *Circ. Res.* 70: 865-884, 1992.

Moss ML, Diffie GM, and Greaser ML. Contractile properties of skeletal muscle fibers in relation to myofibrillar protein isoforms. *Rev. Physiol. Biochem. Pharmacol.* 126: 1-63, 1995.

Moss ML, Lauer MR, Giulian GG, and Greaser ML. Alter Ca^{2+} dependence of tension development in skinned skeletal muscle fibers following modification of troponin by partial substitution with cardiac troponin C. *J. Biol. Chem.* 261: 6096-6099, 1986.

Muroya S, Nakajima I and Chikuni K. Amino acid sequences of multiple fast and slow troponin T isoforms expressed in adult bovine skeletal muscles. *J. Anim. Sci.* 81: 1185-1192, 2003.

Nelson DL and Cox MM. *Lehninger: Principles of Biochemistry* - 3rd edition, Worth Publishers, New York, 2000.

Nieznanska H, Nieznanski K, and Stepkowski D. The effects of the interaction of myosin essential light chain isoforms with actin in skeletal muscles. *Acta Biochim. Pol.* 49: 709-719, 2002.

Ogut O and Jin J-P. Developmentally regulated alternative RNA splicing-generated pectoral muscle-specific troponin T isoforms and role of the NH_2 -terminal hypervariable region in the tolerance to acidosis. *J. Biol. Chem.* 273: 27858-27866, 1998.

Ohtsuki I, Maruyama K, and Ebashi S. Regulatory and cytoskeletal proteins of vertebrate skeletal muscle. *Adv. Protein Chem.* 38: 1-67, 1986.

Pearlstone JR, Chandra M, Sorenson MM, and Smillie LB. Biological function and site II Ca^{2+} -induced opening of the regulatory domain of skeletal Troponin C are impaired by invariant site I or II Glu mutations. *J. Biol. Chem.* 275: 35106-35115, 2000.

Pearson AM and Young RB. Muscle and meat biochemistry. Academic Press, San Diego, 1989.

133Periasamy M, Strehler EE, Garfinkel LI, Gubits RM, Ruiz-Opazo N, and Nadal-Ginard B. Fast skeletal muscle myosin light chains 1 and 3 are produced from a single gene by a combined process of differential RNA transcription and splicing. *J. Biol. Chem.* 259: 13595-13604, 1984.

Perry SV and Cole HA. Phosphorylation of troponin and the effects of interactions between the components of the complex. *Biochem. J.* 141: 733-743, 1974.

Pette D, Peuker H, and Staron RS. The impact of biochemical methods for single muscle fibre analysis. *Acta Physiol. Scand.* 166: 261-277, 1999.

Pette D and Staron RS. Cellular molecular diversities of mammalian skeletal muscle fibers. *Rev. Physiol. Biochem. Pharmacol.* 116: 1-76, 1990.

- Pette D and Staron RS. Transitions of muscle fiber phenotypic profiles. *Histochem. Cell. Biol.* 115: 359-372, 2001.
- Potter JD. Preparation of troponin and its subunits. *Methods Enzymol.* 85(Pt. B): 241-263, 1982.
- Potter JD and Gergely J. Troponin, tropomyosin, and actin interactions in the Ca²⁺ regulation of muscle contraction. *Biochemistry.* 13: 2697-2703, 1974.
- Potter JD and Gergely J. The calcium and magnesium binding sites on troponin and their role in the regulation of myofibrillar adenosine triphosphate. *J. Biol. Chem.* 250: 4628-4633, 1975.
- Reggiani C and Kronnie T. Microarrays and 2D gels: new tools for postgenomic muscle biology. *Basic Appl. Myol.* 14: 7-12, 2004.
- Robertson SP, Johnson JD, and Potter JD. The time-course of Ca²⁺ exchange with calmodulin, troponin, parvalbumin, and myosin in response to transient increases in Ca²⁺. *Biophys. J.* 34: 559-569, 1981.
- Romero-Herrera AE, Castillo O, and Lehmann H. Human skeletal muscle proteins. *J. Mol. Evol.* 8: 251-270, 1976.

Rhyner JA, Koller M, Durussel-Gerber I, Cox, JA, and Strehler EE. Characterization of the human calmodulin-like protein expressed in *Escherichia coli*. *Biochemistry* 31: 12826-12832, 1992.

Schachat FH, Bronson DD, and McDonald OB. Heterogeneity of contractile proteins. A continuum of troponin-tropomyosin expression in mammalian skeletal muscle. *J. Biol. Chem.* 260: 1108-1113, 1985.

Schiaffino S and Reggiani C. Molecular diversity of myofibrillar proteins: Gene regulation and functional significance. *Physiol. Rev.* 76: 371-423, 1996.

Shiraishi F, Kambara M, and Ohtsuki I. Replacement of troponin components in myofibrils. *J. Biochem. (Tokyo)*. 111: 61-65, 1992.

Sia SK, Li MX, Spyropoulos L, Gagne SM, Liu W, Putkey JA, and Sykes BD. Structure of cardiac muscle troponin C unexpectedly reveals a closed regulatory domain. *J. Biol. Chem.* 272: 18216-18221, 1997.

Simpson JA, Labugger R, Hesketh GG, D'Arsigny C, O'Donnell D, Matsumoto N, Collier CP, Iscoe S, and Van Eyk JE. Differential detection of skeletal Troponin I isoforms in serum of a patient with Rhabdomyolysis: Markers of muscle injury? *Clin. Chem.* 48: 1112-1114, 2002.

Squire JM and Morris EP. A new look at thin filament regulation in vertebrate skeletal muscle. *FASEB. J.* 12: 761-771, 1998.

Stephenson GMMS. Hybrid skeletal muscle fibres: A rare or common phenomenon? *Clin. Exp. Pharmacol. Physiol.* 28: 692-702, 2001.

Stephenson GM and Stephenson DG. Endogenous MLC2 phosphorylation and Ca(2+)-activated force in mechanically skinned skeletal muscle fibres of the rat. *Pflugers Arch.* 424: 30-38, 1993.

Stephenson DG and Williams DA. Activation of skinned arthropod muscle fibres by Ca²⁺ and Sr²⁺. *J. Muscle Res. Cell Motil.* 1: 73-87, 1980.

Stevens L, Bastide B, Kischel P, Pette D, and Mounier Y. Time-dependent changes of troponin subunit isoforms in unloaded rat soleus muscle. *Am. J. Physiol. Cell Physiol.* 282: C1025-C1030, 2002.

Stienen GJM, Bottinelli R, and Reggiani C. Myofibrillar ATPase activity in skinned human skeletal muscle fibres: fibre type and temperature dependence. *J. Physiol. (Lond.)* 493: 299-307, 1996.

Swartz DR, Moss RL, and Greaser ML. Characteristics of troponin C binding to the myofibrillar thin filament: extraction of troponin C is not random along the length of the thin filament. *Biophys. J.* 73: 293-305, 1997.

- Sweeney HL, Brito RMM, Rosevear PR, and Putkey JA. The low affinity Ca^{2+} binding sites in cardiac/slow skeletal muscle troponin C perform distinct functions: Site I alone cannot trigger contraction. *Proc. Natl. Acad. Sci. USA*. 87: 9538-9542, 1990.
- Tanokura M, Imaizumi M, Yamada K, Shiraishi F, and Ohtsuki I. Preparation and characterization of troponin C from bullfrog skeletal muscle. *J. Biochem. (Tokyo)*. 112:800-803, 1992.
- Tobacman LS. Structure and regulation of cardiac and skeletal muscle thin filaments in *Molecular Control Mechanisms in Striated Muscle Contraction* (Solaro RJ and Moss ML, eds) Vol. 1, pp. 143-162, Kluwer Academic Publishers, Dordrecht, 2002.
- Uyemura DG, Brown SS, Spudich JA. Biochemical and structural characterization of actin from *Dictyostelium discoideum*. *J. Biol. Chem.* 253: 9088-9096, 1978.
- Van Eerd J-P and Takahashi K. Determination of the complete amino sequence of bovine cardiac troponin C. *Biochemistry* 15: 1171-1180, 1976.
- West JM and Stephenson DG. Ca^{2+} and Sr^{2+} activation properties of skinned muscle fibres with different regulatory systems from crustacea and rat. *J. Physiol. (Lond)*. 462: 579-596, 1993.

Wilkinson JM. The amino acid sequence of troponin C from chicken skeletal muscle. *FEBS Lett.* 70: 254-256, 1976.

Wilkinson JM. Troponin C from rabbit slow skeletal and cardiac muscle is the product of a single gene. *Eur. J. Biochem.* 103: 179-188, 1980.

Wilson GJ and Stephenson DG. Calcium and strontium activation characteristics of skeletal muscle fibres from the small marsupial *Sminthopsis macroura*. *J. Muscle Res. Cell Motil.* 11: 12-24, 1990.

Woolley PA, Patterson MF, Stephenson GM, and Stephenson DG. The ilio-marsupialis muscle in the dasyurid marsupial *Sminthopsis douglasi*: form, function and fiber-type profiles in females with and without suckling young. *J. Exp. Biol.* 205: 3775-3781, 2002.

Wu YZ, Baker MJ, Crumley RL, Blanks RH, and Caiozzo VJ. A new concept in laryngeal muscle: Multiple myosin isoforms types in single muscle fibres of the lateral cricoarytenoid. *Otolaryngeal. Head. Neck. Surg.* 188: 86-94, 1998.

Xu GQ and Hitchcock-DeGregori SE. Synthesis of a troponin C cDNA and expression of wild-type and mutant proteins in *Escherichia coli*. *J. Biol. Chem.* 263: 13962-13969, 1988.

Yamamoto K. Sensitivity of actomyosin ATPase to calcium and strontium ions. Effect of hybrid troponins. *J. Biochem. (Tokyo)*. 93: 1061-1069, 1984.

Yates L and Greaser M. Troponin subunit stoichiometry and content in rabbit skeletal muscle and myofibrils. *J. Biol. Chem.* 258: 5770-5774, 1983.

Zot HG, Guth K, and Potter JD. Fast skeletal muscle skinned fibres and myofibrils reconstituted with N-terminal fluorescent analogues of troponin C. *J. Biol. Chem.* 261: 15883-15890, 1986.

Zot HG and Potter JD. A structural role for the Ca^{2+} - Mg^{2+} sites on troponin C in the regulation of muscle contraction. Preparation and properties of troponin C depleted myofibrils. *J. Biol. Chem.* 257: 7678-7683, 1982.